REPORT NO.
UCB/EERC-83/18
JULY 1983

EARTHQUAKE ENGINEERING RESEARCH CENTER

INTERACTIVE COMPUTER ANALYSIS METHODS FOR PREDICTING THE INELASTIC CYCLIC BEHAVIOUR OF STRUCTURAL SECTIONS

by

S. A. KABA
S. A. MAHIN

Report to the National Science Foundation

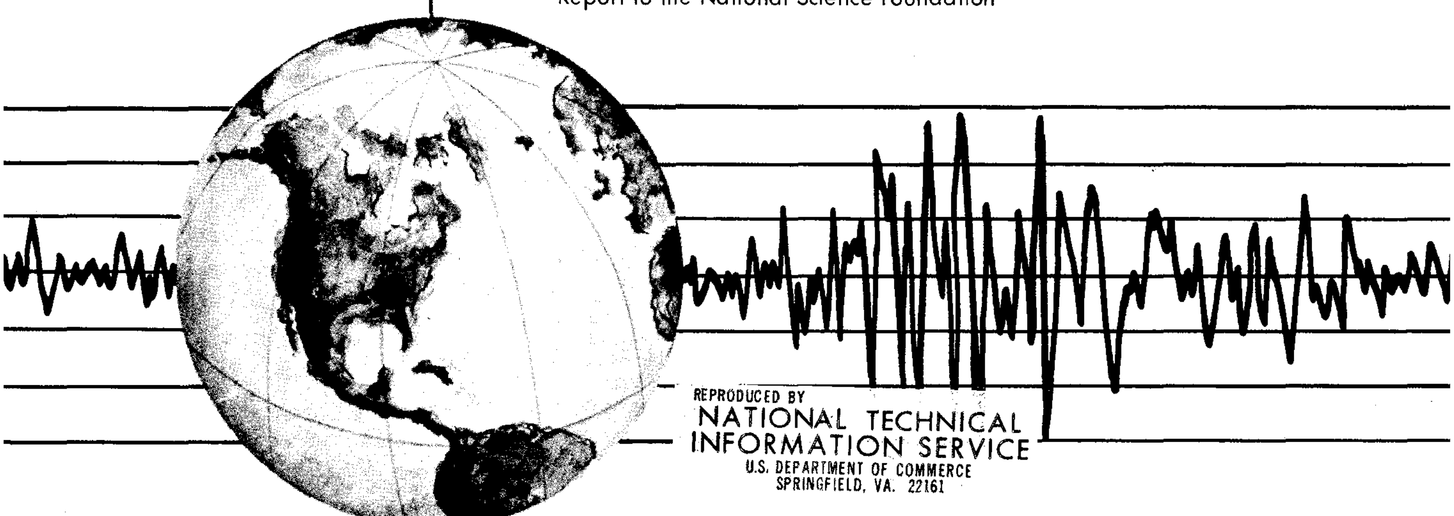

COLLEGE OF ENGINEERING

UNIVERSITY OF CALIFORNIA · Berkeley, California

For sale by the National Technical Information Service, U.S. Department of Commerce, Springfield, Virginia 22161.

See back of report for up to date listing of EERC reports.

50272-101

REPORT DOCUMENTATION PAGE	1. REPORT NO. NSF/CEE-83031	2.	3. Recipient's Accession No. PB84 192012

4. Title and Subtitle Interactive Computer Analysis Methods for Predicting the Inelastic Cyclic Behaviour of Structural Sections	5. Report Date July 1983 6.
7. Author(s) S. A. Kaba and S. A. Mahin	8. Performing Organization Rept. No. UCB/EERC-83/18
9. Performing Organization Name and Address Earthquake Engineering Research Center University of California 1301 South 46th Street Richmond, Calif. 94804	10. Project/Task/Work Unit No. 11. Contract(C) or Grant(G) No. (C) (G) CEE81-07217
12. Sponsoring Organization Name and Address National Science Foundation 1800 "G" Street, N.W. Washington, D.C. 20550	13. Type of Report & Period Covered 14.

15. Supplementary Notes

16. Abstract (Limit: 200 words)

An interactive analysis program suited for micro-computers has been developed to analyze structural steel, reinforced concrete, and prestressed concrete sections subjected to axial load and uniaxial bending moments. The program currently includes bilinear, cubic, and Ramberg-Osgood steel models and a concrete model that can mimic ones suggested by other researchers. Additional material models are relatively easy to implement.

The report discusses the theoretical background for the program, the solution strategies used and their limitations, and the types of analyses for which the program is suited. Using various options in the program conventional moment-curvature and axial load-moment interaction curves can be conveniently developed. In addition, complicated loading histories such as non-proportional application of axial load and moment including unloading and reversal may be considered. The program is interactive in nature permitting the user to rapidly redo a particular load increment, a complete load excursion starting from specified initial conditions, or to impose additional loading on the current state of the section. Input of section geometry and materials is also interactive and a user can modify parameters related to these items and reanalyze the section during the same or subsequent analysis sessions.

17. Document Analysis a. Descriptors

b. Identifiers/Open-Ended Terms

c. COSATI Field/Group

18. Availability Statement:	19. Security Class (This Report)	21. No. of Pages
Release Unlimited		113
	20. Security Class (This Page)	22. Price

(See ANSI-Z39.18) See Instructions on Reverse OPTIONAL FORM 272 (4-77) (Formerly NTIS-35) Department of Commerce

Interactive Computer Analysis Methods For Predicting the Inelastic Cyclic Behaviour of Structural Sections

by

Said A. Kaba

and

Stephen A. Mahin

A report on research sponsored by

the National Science Foundation

Report No. UCB/EERC-83/18

Earthquake Engineering Research Center

College of Engineering

University of California

Berkeley, California

July 1983

ABSTRACT

An interactive analysis program suited for micro-computers has been developed to analyze structural steel, reinforced concrete, and prestressed concrete sections subjected to axial load and uniaxial bending moments. The sections considered must have an axis of symmetry and the neutral axis must remain perpendicular to this axis. However, relatively general loading conditions including load reversal, may be considered. Plane sections are assumed to remain plane during deformation. However, initial stresses and strains may be specified to account for prestressing, residual stresses, and sequential construction. The program currently includes bilinear, cubic, and Ramberg-Osgood steel models and a concrete model that can mimic ones suggested by Kent, Scott, Hognestad, Vallenas, Sheikh and Uzumeri, and others. Additional material models, however, are relatively easy to implement.

The report discusses the theoretical background for the program, the solution strategies used and their limitations, and the types of analyses for which the program is suited. Using various options in the program conventional moment-curvature and axial load-moment interaction curves can be conveniently developed. In addition, complicated loading histories such as non-proportional application of axial load and moment including unloading and reversal may be considered. The program is interactive in nature permitting the user to rapidly redo a particular load increment, a complete load excursion starting from specified initial conditions, or to impose additional loading on the current state of the section. Input of section geometry and materials is also interactive and a user can modify parameters related to these items and reanalyze the section during the same or subsequent analysis sessions. Files are developed to store section and material properties as well as analysis results.

ACKNOWLEDGEMENTS

The work described in this report was conducted under the sponsorship of the National Science Foundation. This financial support is gratefully acknowledged.

The assistance of graduate student Christos Zeris in developing the program, especially the Ramberg-Osgood model is particularly appreciated.

The program was developed and the examples run using the facilities of the Microcomputer Research Laboratory of the Structural Engineering and Structural Mechanics division of the University of California's Department of Civil Engineering. The report and many of the figures were prepared using facilities of the Berkeley Campus Computer Center.

The fine efforts of the technical illustrators in preparing this report are appreciated.

TABLE OF CONTENTS

I INTRODUCTION

1.1 Introductory Remarks

The inelastic behaviour of structural sections, especially reinforced concrete sections, depends on many parameters including the material properties, the section geometry, and the history of moment and/or axial load to which the section is subjected. Investigation of the importance and influence of these and other parameters on section behaviour depends on the availability of a versatile computer program. For maximum flexibility, such a program should be capable of handling a section of general geometric shape, incorporate realistic material properties, and consider arbitrary loading conditions and histories. For convenience, the user should also be able to easily and selectively obtain conventional axial load-moment interaction diagrams and moment-curvature plots corresponding to specified loading conditions and histories.

While various closed form analytical solutions are possible for monotonic loading conditions when the cross section and material properties are relatively simple, computer programs based on such idealizations are typically too restrictive in their applications. General three-dimensional finite element computer programs can be used to compute section response but this is generally inconvenient and uneconomical. An alternate approach is to use a fiber or laminar model. The fiber model idealizes a section by breaking it into a number of discrete layers (or fibers). The uniaxial stress-strain history of each of these fibers is then used in the analyses along with kinematic and equilibrium requirements to obtain the mechanical behaviour of the section. A number of computer programs have been written based on the fiber model [1,2,3,4], but these have a number of significant limitations or are not generally available.

1.2 The Fiber Model for Reinforced Concrete

Reinforced concrete section behaviour is complicated and quite hard to quantify satisfactorily. The difficulty arises from the many phenomena and parameters which have to be considered. The phenomena which affect the response of reinforced concrete structural elements include cracking and crushing of concrete as well as yielding, strain hardening, slipping and buckling of the reinforcing steel. Furthermore, when load and displacement reversals are taken into consideration such phenomena as pinching of the hysteresis loops due to shear, bond deterioration, Bauschinger effects and other causes become important. The fiber model is the simplest, theoretically consistent, general method of analysis that can account for these phenomena.

Due to its versatility, the fiber model has been widely used to study the influence of material and cross-section properties and loading variations on the response of reinforced concrete structures [3,5,6,7,8,9]. Cross-section properties that have been studied include section dimensions, steel ratios, and transverse confinement resulting from rectangular ties or circular spirals. Variations in loading can affect the stiffness and strength of the member especially when reversals occur. Furthermore, the axial load acting on a section influences the flexural stiffness, the moment capacity, the ductility, and the overall moment-curvature properties of a section.

In a broad and comprehensive study using fiber models, Mark [10] studied the moment-curvature relations, member deflections, and finally the response of a single-bay, one-story, reinforced concrete frame subjected to seismic base motions. Some of the observations drawn from this investigation were:

(1) The fiber model can adequately represent the main aspects of the behaviour of a reinforced concrete cross-section.

(2) Since the model explicitly considers the coupling of axial load and bending, both the "pinching" effect as well as changes in moment capacity associated with axial force can be

reproduced.

(3) Satisfactory agreement was found between analytical and experimental results, although none of the stress-strain analytic models considered were able to reproduce the moment-curvature relationship exactly.

(4) Moment-curvature relations under cyclic loading depend strongly on the assumed steel stress-strain relationship. The elasto-plastic steel model was found to provide better agreement with experimental results than might be expected from such a simple formulation.

Mark, however, uses an incremental tangent stiffness approach without equilibrium checks and corrections at every step. Hence the method is sensitive to increment size and subject to error propagation. RCCOLA [1] and CYCMC [2] are two available computer programs which do not rely on the incremental stiffness approach. Both programs divide the section into layers and use an iterative solution to ensure equilibrium at every step within a specified convergence tolerance.

The last two programs differ in that CYCMC was written for rectangular or T-sections with two layers of reinforcement only, while RCCOLA accepts a general section - admitting one axis of symmetry. The main difference, however, lies in the assumptions regarding the cyclic stress-strain material properties. RCCOLA assigns to a given strain a stress value from the primary curve irrespective of the current loading stage (i.e. loading, unloading, or load reversal all lie on the same primary envelope curve). CYCMC, however, applies hysteresis rules to the primary stress-strain curves to define the cyclic behaviour. Furthermore, both programs can only accept a constant axial load while the curvature to which the section is subjected varies.

All of the programs mentioned so far use the assumptions that plane sections remain plane and materials can be adequately described in terms of their uniaxial behaviour. Bazant and Bhat [3] use triaxial material properties and thick beam bending theory including transverse shear. To describe the triaxial behaviour, they use a constitutive relation for concrete called Endochronic Theory. However, Bazant and Bhat's study only investigated the moment-curvature relations for a simple beam. The effect of axial loads has not been explicitly considered. Moreover, this and other similar [4] approaches result in computational complications and require consideration of the action of the section as part of a complete member.

1.3 The Fiber Model for Structural Steel

A number of closed form solutions exist to compute the flexural behaviour of common structural steel cross sections as long as the steel material properties can be idealized as elasto-perfectly plastic [11]. However, computations where such solutions do not exist, especially where moment-curvature information is required, are at best tedious. Although moment-curvature relationships may not always be needed, this information is essential where deflections are to be computed. In addition, flexural properties for built-up sections, for sections subjected to axial load, and for sections subjected to load or deformation reversal may be difficult to compute by hand. Moreover, the assumption of ideal material properties may not be realistic. Residual stresses can substantially affect the initial proportional limit and the moment-curvature relation. Bauschinger effects can similarly affect behaviour when reversals occur. Because of the difficulty of hand solutions in such cases, a variety of fiber models have been used in the analysis of structural steel sections [5,7]. This permits consideration of complex built-up or composite sections as well as complex loading paths.

1.4 Limitations of the Fiber Model

Although the fiber model is versatile and capable of handling a wide variety of problems, its assumptions and the resulting limitations must be clearly kept in mind. These are:

(1) Plane sections may not always remain plane due to such factors as shearing deformations or, in reinforced and prestressed concrete sections, shear cracks and bond slip.

(2) Shearing deformations and their effects on section behaviour are not taken into consideration.

(3) Cross-sections may change at large deformations due to Poisson effects, local buckling, and so on. The fiber model can only account for section variation in as much as the phenomenon can be included in the uniaxial material properties.

(4) Inelastic material behaviour may not be well-known in all cases. This is especially true at large strain levels and when significant deformation reversals may occur. Although many analytical material models have been developed, their limitations must be kept in mind.

(5) Uniaxial material properties are not adequate in certain cases (due to the effects of shear, transverse confinement, etc.) and hence the need for triaxial material properties may arise.

(6) Once cracked, concrete is usually assumed incapable of carrying tensile stresses. This disregards the ability of the concrete between the cracks to carry some tensile stresses. This results from bond-transferred stresses, a phenomenon known as tension stiffening. There are, however, ways of simulating this effect using fiber models by modifying the concrete or steel material models [12].

1.5 Interactive Computing

Because of the nonlinear nature of material properties an iterative solution strategy is usually required to compute sectional behaviour. While computer programs are ideal for performing these computations, the usual non-interactive (batch) mode of analysis has a number of limitations:

(1) There might be sudden changes in material characteristics due in the case of reinforced or prestressed concrete to the opening or closing of cracks or crushing of concrete, as well as the fracture or buckling of the reinforced steel. Such abrupt changes make it difficult to select *a priori* suitable values for iteration control parameters and for load or deformation increments. Consequently, solutions are often uneconomical due to over-conservativeness in setting these values; or worse, the computations might converge to an incorrect solution. In addition,

the initially specified sequence of loads or deformations may not have sufficient points located in the range where significant changes in material properties occur; consequently batch analyses must be rerun using adjusted load histories until the desired behavioural characteristics are identified. It is therefore desirable to be able to inspect analysis results as the solution progresses so that possible problems may be detected and corrected before continuing the analysis.

(2) When performing section computations one is often interested in rapidly assessing the effect of different loading histories, design details, or material properties on mechanical response. The batch mode of analysis usually entails considerable delay in obtaining and comparing results. This is due to the need for a number of reruns, each involving minor changes in the input. Consequently, such studies, although technically desirable, may not be undertaken because of the inconvenience inherent in the non-interactive mode of analysis. A solution method where one can rapidly inspect results, modify data or load histories and reanalyze the section would be more suitable for this type of problem and would encourage more detailed studies of section behaviour.

(3) Batch processing of a program is often viewed as impractical or too costly by many engineering design firms if an in-house computer or terminal is not available. As a result, there is a tendency to persist in using simplistic and approximate hand solution methods. Mini- and micro-computers are increasingly gaining acceptance in design offices as well as in research institutions. These computers are relatively inexpensive and are ideal for interactive computing. Moreover, the computational capabilities of these computers are consistent with those needed for section analysis using the fiber model.

1.6 Objectives and Scope

Due to the limitations of the programs and methods mentioned above and the ever increasing need to assess the nonlinear behavioural characteristics of complex structural cross-sections, it is desirable to develop a general purpose program for the analysis of reinforced concrete, prestressed concrete, and structural steel sections. Such a program should have the following capabilities:

(1) General cross-sections should be possible to enable consideration of complex shapes (built-up members, composite sections, etc.), but input should be relatively simple for standard shapes.

(2) Complex loading conditions, including reversals, should be permitted.

(3) Due to the nature of the problem it is desirable to make the calculations interactive permitting the user to revise or reject calculations during the analyses.

(4) Material properties should be versatile but it should be easy to modify existing models or add new ones.

(5) Initial steel strains or stresses should be considered, thus the program should have the capability of considering bonded prestressed concrete sections or residual stresses in structural steel sections.

The objectives of this report are: (1) to describe the theoretical basis of a program developed to achieve these capabilities; (2) to assess the advantages and limitations of interactive computing using micro-computers as applied to the analysis of inelastic section behaviour; and (3) to briefly explore some of the effects that various assumptions and parameters have on the mechanical behaviour of steel, reinforced concrete, and prestressed concrete sections.

Chapter 2 describes a new program (UNCOLA) devised to analyze structural sections. This computer program can be used to evaluate the general flexural characteristics of cross-sections subjected to axial forces and/or uniaxial bending moments. Though envisioned primarily for analysis of reinforced concrete sections, structural steel sections may be considered as well. The program has been specifically designed for interactive use on a microcomputer. Sections must have an axis of symmetry and the neutral axis must remain perpendicular to this axis. Material properties are specified in terms of stress-strain curves obtained for monotonic loading. Cyclic behaviour can then be derived from the monotonic envelope using appropriate unloading and load reversal rules.

Chapter 3 discusses the influence of material properties and section idealization on the behaviour of reinforced concrete sections. The capacity of the program to produce moment-axial load interaction diagrams as well as moment-curvature plots is illustrated. Furthermore, the use of the program to study the effects of various material parameters is briefly discussed. Chapter 3 also illustrates the use of the program in studying the behaviour of a section subjected to various loading paths and histories.

Chapter 4 discusses two cases of initial stress: (1) a steel section with simplified residual stress distributions is analyzed and the results compared to an analysis of the same section assumed free of residual stresses; and (2) moment-curvature relations for prestressed concrete sections are obtained by using the initial stress option. Finally, Chapter 5 offers some comments on the advantages and disadvantages of microcomputers and interactive computing as applied to section analysis. Conclusions and recommendations for additional work are also presented in this chapter.

II UNCOLA: UNIAXIAL COLUMN ANALYSIS PROGRAM

2.1 Introduction

A computer program (UNCOLA) has been written to implement fiber model computations for section mechanical characteristics. It can process a cross-section of general geometry and relatively arbitrary material properties subjected to variable load conditions and history. As indicated previously, only uniaxial bending is considered, i.e. the section must be symmetric about one axis and the neutral axis must remain perpendicular to this axis of symmetry. Solving for the mechanical characteristics of a section using the fiber model starts by defining the section in terms of layers to which geometric and material data are assigned. Assuming plane sections remain plane, the strain in the various layers of concrete and/or steel can be calculated given the strain profile. Once the strains of the various layers are determined, the stresses can be extracted from the specified stress-strain relationships and, by proper summations, the axial load and bending moment can be calculated, as shown in Fig. 2.1.

The constraints on the section geometry that can be considered, the analysis methods used and the ways of specifying material properties are described in this chapter.

2.2 Solution Strategies

Two general classes of analyses can be performed using the program. In the the first, which does not involve any iterations, a strain profile is specified by the user and the program calculates the axial load and bending moment corresponding to the prescribed material properties. Thus, by specifying the strain at a given location and then calculating the axial load and bending moment for a set of neutral axis positions, conventional interaction diagrams can be easily produced. Another operation that does not involve iterating for a solution is specifying one or more uniform (constant) strain profiles for which the program calculates the corresponding axial loads.

The second class of analyses involves iterating on the strain profile until the calculated axial load converges to a specified value. An iterative approach is used in the program since it is believed that this method is more versatile and more accurate for this type of problem than the incremental tangent stiffness approach [12]. Section 2.6 discusses the iterative method in detail. Several options are possible in the program using iteration. One option is for the user to specify the strain at a given location and the axial load for which the accompanying bending moment is desired. This permits the evaluation of the cracking moment, the moments at first yield of tension or compression reinforcement and so on for that axial load. In addition the program will consider an option where the axial load varies during steps permitting analysis of complex loading conditions.

The last option permits the axial load and section curvature to be specified and the program computes the corresponding bending moment. Plotting moment-curvature relations for a cross section subjected to a constant axial load can be easily achieved by specifying a sequence of curvatures. The program automates such computations if the initial curvature, the number and magnitude of constant curvature increments, and the applied axial load are specified.

As will be discussed in subsequent sections the program accepts a sequence of these options so that relatively complex load histories can be considered. For example, axial loading can be applied to a section followed by bending under constant or varying axial load. Alternatively, at any point in the analysis, the control parameters and material history data can be reinitialized to consider a different loading condition or history starting from zero initial conditions.

2.3 Section Geometry

The program can handle a section of general geometric shape (but admitting one axis of symmetry). The section is divided into groups of concrete and steel layers. For computational efficiency adjacent layers having the same material properties and the same area may be considered as a single group. Different groups, however, can be assigned different areas and material properties. Coordinates of all layers are given or specified with respect to the *bottom of the section.* Program limits on the number of layers and groups may be found in Appendix D.

To simplify input of concrete layer data a number of generation options are available for rectangular or circular sections, see Fig. 2.2. When a portion of a section can be modelled as a group (i.e. contiguous layers with same depth, width, and material properties) a group generation feature can be used. By specifying the coordinate of the bottom of the first layer (BC) and the coordinate of the top of the last layer (TC) in the group, the program calculates the coordinates of the various layers in the group. Note that the last layer is the farthest from the bottom of the section. The area of a typical layer in the group is given by:

$$A = b \cdot d \tag{1}$$

where b = width of layer in a group

d = (TC - BC) / Number of layers in the group

and the coordinate of the center of the 'i'th layer of the group relative to the bottom of the section is given by:

$$y_{ci} = BC + (i - \tfrac{1}{2})\, d \tag{2}$$

For example, to describe the section shown in Fig. 2.3, it can be divided into four groups of layers (three for the cover and one for the confined core). Two different types of concrete might be assigned (one for the confined portion and another for the unconfined portion). Note, however, that the area of reinforcing steel bars is not automatically subtracted from the area of the concrete layer which contains these bars. To account for this, additional concrete layers may be defined having the same location as the steel reinforcement but with a negative area equal in magnitude to the area of the reinforcing steel bars.

For the sections shown in Fig. 2.2 it is possible to subdivide them as illustrated by simply specifying the relevant radii and the number of layers desired. The program then automatically calculates the coordinates of the centroids and the exact areas of the various layers. It should be mentioned that in this case the various layers have the same height and their centroid is assumed to be at the mid-height of the layer.

Steel distribution is specified in a similar manner. Layers belonging to the same group should have the same area and the distance between all adjacent layers in the group should be the same.

Another convenient program feature is the possibility of dividing the section into layers of different depths. Such a procedure can reduce the amount of calculations with no observable loss of accuracy. This is due to the fact that the contribution of some of the layers to the load and moment capacity is known to be minimal or because stresses are judged to be nearly constant over part of the section. Furthermore, it is also possible to analyze a plain concrete section or a plain steel section.

2.4 Strain Profile

Since plane sections are assumed to remain plane, the strain at any position in the section can be easily calculated. When the strain at a given location and the curvature are given, the strain at any point in the section is given by:

$$\epsilon=\epsilon_c+(y-y_c)\phi \tag{3}$$

where ϵ_c = the given strain;

y = distance to the point at which the strain (ϵ) is sought;

y_c = distance to the point at which the strain is ϵ_c;

ϕ = curvature; and

where all distances are referred to at the bottom of the section.

However, when the neutral axis position is known along with the curvature, the strain at any point in the section is given by:

$$\epsilon=(y-y_{na})\phi \quad (4)$$

where y_{na} = distance to the neutral axis;

Alternatively, when the user specifies the strain at a particular location and the neutral axis position, Equation 3 can be used by first calculating the curvature [$\phi = \epsilon_c/(y_c - y_{na})$].

2.5 Available Material Models

Using the subroutines attached to the program it is possible to specify a concrete model that follows the Hognestad [13,14], Sheikh and Uzumeri [15], Park and Kent [16], Scott *et al* [17],or the Vallenas *et al* [18] models. Note that it is possible to specify different types of concrete in the same section in order to model confined as well as unconfined portions or to consider portions that might have been cast at different times. The steel behaviour can be described by a bilinear formulation, a Ramberg-Osgood model, or a cubic formulation. These various models are described in the following two sections. It might be worth mentioning, however, that the user can easily write additional subroutines to describe material behaviour models. Guidelines for adding such subroutines are to be found in Appendix C.

2.5(a) Concrete Models

The concrete model currently incorporated in the program is derived from one suggested by Sheikh and Uzumeri [15]. The various parameters shown in Fig. 2.4 are required to describe the concrete behaviour using this model. By appropriate choice of parameter values, the stress-strain curve can degenerate into the model suggested by Hognestad [13,14], Park and Kent [16], or Vallenas *et al* [18]. The various possibilities are shown in Fig. 2.5.

The model proposed by Kent [16], shown in Fig. 2.5, uses a parabola to define compressive stresses corresponding to strains less then ϵ_0 (the strain at which the stress attains $f'c$):

$$f_c = f_c' \frac{\epsilon}{\epsilon_0} \left(2 - \frac{\epsilon}{\epsilon_0} \right) \tag{5}$$

This initial portion is assumed independent of the confinement. Beyond ϵ_0 the descending portion of the stress-strain relationship is assumed linear with a slope equal to $- Z \cdot f'c$ where Z is a function of ϵ_0, $f'c$, and the tie size and spacing. Hence, the rate of decrease of stress with increasing strain, increases with larger tie spacing or smaller tie size.

Vallenas *et al* [18], after experimentally measuring the stresses in concrete confined by rectangular hoops noted that the maximum compressive strength (f'_c) increases with confinement. Hence a factor 'k' which is a function of the amount of confinement and longitudinal steel is applied to f'_c. The initial phase is described by a slightly more elaborate function than the parabolic segment of Kent's model:

$$f_c = \frac{E_c \epsilon - f_c' \left(\frac{\epsilon}{\epsilon_0} \right)^2}{1 + \left[\frac{E_c \epsilon_0}{f_c'} - 2 \right] \left(\frac{\epsilon}{\epsilon_0} \right)} \tag{6}$$

As mentioned by Vallenas *et al* [18] this formulation satisfies the conditions of zero slope at maximum stress, and the user specified slope E_c at zero strain and stress. When the default value of $2 \cdot f_c^{'} / \epsilon_0$ is used for E_c, the equation degenerates into the usual parabolic formulation used by Kent (Equation 5). The initial phase is again followed by a descending linear portion which extends to $0.3kf'_c$ and remains constant beyond that as shown in Fig. 2.5.

Sheikh and Uzumeri [19] proposed a model that takes into consideration the total confinement. Thus the arrangement of longitudinal steel in addition to the amounts of confinement and longitudinal steel are considered. The model differs from the previous models in that a horizontal portion (see Fig. 2.5), where the stress is held constant at maximum strength, follows the initial parabolic phase and precedes the linear descending portion.

The effect of concrete spalling can be included by specifying a crushing strain. The concrete is assumed to be incapable of resisting any stress when strains exceed this value. In addition, it is possible to include brittle tensile behaviour by specifying a non-zero rupture stress. The tensile portion of the curve is linear and has a slope equal to E_c with a default value of $2 \cdot f_c^{'} / \epsilon_0$.

The user has the option of specifying monotonic or cyclic concrete behaviour. For monotonic conditions the stress corresponding to the monotonic stress-strain envelope curve is always used for the strain in the layer under consideration even if unloading occurs. Even in cases of monotonic loading this is not necessarily always correct and is only slightly computationally advantageous. For cyclic conditions unloading always proceeds at a slope of E_c, with a default value of $2 \cdot f_c^{'} / \epsilon_0$ (see Fig. 2.6). Reloading follows this same path until the envelope curve is again reached. This idealization is not strictly correct but Ma, *et al* [2] found that it is sufficiently accurate for reinforced concrete though it may be less so for prestressed concrete [20].

When cyclic behaviour is specified along with a tensile rupture stress, the concrete can be in tension until it cracks. From then on it is assumed incapable of carrying tension. Furthermore, as shown in Fig. 2.6 it will only resist compression once the crack closes again. When cyclic behaviour is specified the concrete is assumed incapable of carrying any stresses once it has crushed (i.e. when the strain in a layer exceeds the crushing strain ϵ_{cr}).

2.5(b) Steel Models

The steel models currently incorporated in the program can be referred to as: the bilinear model, the cubic model, and the Ramberg-Osgood model. For the bilinear steel model, the only required input values are the initial and final slopes, as well as the yield stress. When cyclic behaviour is specified, unloading and reloading proceed at a slope of E_s as shown in Fig. 2.7. Note that the elasto-perfectly plastic model is a special case of the bilinear model and can be used by simply setting the second slope (E_{sh}) equal to zero.

A more refined steel model is referred to as the cubic formulation since it uses third degree polynomials to model strain hardening as well as load reversals. The required input parameters are shown in Fig. 2.8. This model's simplified behaviour is based on the primary loading envelope and no additional data is needed to define reversals.

The strain hardening portion of the primary loading envelope is defined by a cubic function derived using the input values ϵ_{sh}, f_y, E_{sh}, $\epsilon_{\max}$ and $f_{\max}$ (defined in Fig 2.8). To have a smooth cubic function, E_{sh} should satisfy:

$$1.5 \cdot \frac{f_{\max}-f_y}{\epsilon_{\max}-\epsilon_{sh}} \leqslant E_{sh} \leqslant 3 \cdot \frac{f_{\max}-f_y}{\epsilon_{\max}-\epsilon_{sh}} \qquad (7)$$

When Equation 7 is violated by the input parameters, $\epsilon_{\max}$ is automatically shifted (by as little as possible to satisfy the equation) and a message is printed to this effect.

When cyclic material properties are specified, unloading proceeds elastically until stress reverses; then a cubic function is used to approximate the steel behaviour. Note that these cubic segments are defined by a shifted origin, the slope at the origin, and a final point at which the slope is zero. To ensure a smooth cubic curve, the final point is automatically shifted as shown in Fig. 2.9(a). Whenever this occurs a message is printed. However, to avoid cluttering the output this message is not printed when automatic curvature generation is used. Moreover, for this model the absolute value of the stress does not exceed $f_{\max}$; this constraint, in conjunction with the relatively quick way the cubic polynomial can reach this maximum stress, results in the unrealistically long flat portion between points A and B shown in Fig. 2.9(b). Whenever large strain cycles occur, such flat portions dominate; hence, it might be more appropriate in such cases to use the Ramberg-Osgood model.

The input for the Ramberg-Osgood [21,22,23] model is the same as for the cubic model (i.e.: E_s, f_y, ϵ_{sh}, E_{sh}, $\epsilon_{\max}$, and $f_{\max}$). In addition, however, the empirical values of the parameters determined by Kent and Park [22,23] to define stress reversals are incorporated into the program. The model behaves in a manner similar to the cubic model in the loading portion. When the stress reverses, a Ramberg-Osgood function is used instead of a cubic polynomial (see Fig. 2.10).

For a Ramberg-Osgood model an iterative solution is required to evaluate the stress corresponding to a given strain. The modified Regula Falsi [24] method is used in the program with a convergence tolerance of 0.001 f_y set on the stress. Due to this additional iteration requirement, using the Ramberg-Osgood steel formulation may delay the output slightly - depending on the number of steel layers, type of analysis involved and other factors.

For the cubic model, unloading proceeds at a slope given by,

$$E_u = E_s \cdot (\epsilon_y \,/\, \epsilon_m)^{\alpha} \tag{8}$$

Where ϵ_m is the maximum strain attained in the loading direction and α is set by the user. Elastic unloading can be specified by setting $\alpha = 0$ (see Fig. 2.11). Note that if the strain has not exceeded the yield strain, unloading proceeds at a slope of E_s irrespective of the value of α. The Ramberg-Osgood model as used in [22,23] specified elastic unloading. Setting $\alpha = 0$ might therefore be appropriate when using this model. The user, however, may decide to assign an unloading slope which is a function of maximum strain as in equation (8) by assigning a finite value to α.

2.5(c) Detection of Buckling in Longitudinal Reinforcement

It is also possible to check for buckling of reinforcement when the Ramberg-Osgood steel formulation is used. Checking is done using the Euler buckling formula, as in [18,25]:

$$f_{cr} = (\pi \cdot d_b \;/\; k \cdot s)^2 \cdot E_t \;/\; 16 \tag{9}$$

Where:	d_b	=	reinforcing bar diameter
	s	=	tie or stirrup spacing

k is an effective length coefficient which is a function of the 'support conditions' at the points of contact between ties and main reinforcement. If the main reinforcement is prevented from rotation at these contact points, k is equal to 0.5. If, on the other hand, the main reinforcement is free to rotate at the contact points, then k is equal to 1.0. Neither of these conditions is exactly true in practice [18] and the product ($k \cdot s$ = effective spacing) is left for the user to specify.

E_t is the tangential steel modulus given by the slope of the steel stress-strain curve. The slope is found by exact differentiation when necessary. For a strain corresponding to a stress on an initial flat yield plateau, E_t is taken as [11]:

$$\frac{1}{E_t} = \frac{k}{E_{sh}} + \frac{1-k}{E_s} \tag{10}$$

where	E_s	=	initial elastic modulus
	E_{sh}	=	slope at onset of strain hardening
	k	=	$(\epsilon - \epsilon_y) \;/\; (\epsilon_{sh} - \epsilon_y)$
	ϵ	=	current strain
	ϵ_y	=	yield strain
	ϵ_{sh}	=	strain at onset of strain hardening

It is assumed that the concrete cover provides sufficient restraint to prevent buckling of the longitudinal steel and hence buckling can only occur after the adjacent concrete spalls (the concrete strain exceeds the crushing strain). The steel is assumed to have no direct effect on spalling. Whenever a steel layer is to be checked for buckling, the user should supply the identification number of the adjacent concrete layer. In the program, whenever the adjacent concrete cover spalls, the current steel stress is checked against the buckling stress. Should the buckling stress be the lower of the two then a message is printed giving the number of the steel layer which buckled and the corresponding buckling stress (f_{cr}). The analysis may be continued. However, this would be based on the stress obtained from the material properties disregarding buckling.

Buckling is not checked for the bilinear steel model as Equation 9 can be checked directly and the value of E_t is not believed to be sufficiently accurate for the cubic model - due to possible shifts - to justify implementation of this option.

2.5(d) Initial Steel Strains or Stresses

The user can specify an initial strain or stress in the various steel layers. It is therefore possible to analyze a bonded prestressed concrete section, a structural steel section with residual stresses, or a composite section. This section describes the steel behaviour and the adopted analysis procedure.

In the analysis, strains at the centroids of the various steel layers are calculated from the section geometry, the curvature, and position of the neutral axis assuming plane sections remain plane. Consequently, any initial strain must be added to the calculated strain for the steel layer:

$$\epsilon_{sp} = \epsilon_s + \epsilon_0 \tag{11}$$

where

ϵ_{sp} = total strain in the steel

ϵ_s = strain at steel level calculated from the section curvature

ϵ_0 = initial steel strain

The concrete is assumed to be initially without any stress or strain. Hence the strains in the concrete fibers are those given by Equation 4. Once the strains in the various fibers are defined, the stresses are calculated from the material models and proper summation of the stresses give the axial load and moment acting on the section as before.

Residual stresses in a structural steel section are handled in exactly the same manner. Initial stresses for the various steel layers are specified from which the corresponding "initial strains" are calculated. Hence the stress-strain state of the various layers is known and the analysis can proceed.

2.6 Analysis Methods

Four types of problems may be solved depending on the values of the control variables specified by the user (see Table 1). In each case it is possible to specify cyclic or non-cyclic material behaviour. The possible analyses have been divided into those which involve iterating for equilibrium and those which do not. It is possible during the execution of the program to move from one type of analysis to another. Hence it is possible to move from one state to another along different paths. The possible analyses are described in the next two sub-sections.

Table 1 - Analysis Control Variables

ICNTR	INTR	ANALYSIS TYPE
1	0	Given strain at a point and N.A. position
	1	Given uniform strain over the section.
2		Given strain at a given location and axial load.
3		Given curvature and axial load.
4		Automated version of ICNTR = 3 case for constant load.

2.6(a) Non-iterative analyses (ICNTR = 1)

When the input consists of a specified strain profile (either as a uniform strain distribution (ICNTR = 1 and INTR = 1) or the strain at a given location along with the neutral axis positions (ICNTR = 1 and INTR = 0)), no iterations are involved in calculating axial load and bending moment. The stresses are obtained from the strain profile using the suitable material stress-strain relations. The axial load (P) and moment (M) are then obtained by proper summations over the layers:

$$P = \sum_{i=1}^{NS} \sigma_{si} \cdot A_{si} + \sum_{j=1}^{NC} \sigma_{cj} \cdot A_{cj} \tag{12}$$

$$M = \sum_{i=1}^{NS} \sigma_{si} \cdot A_{si} \cdot (y_{si} - y_p) + \sum_{j=1}^{NC} \sigma_{cj} \cdot A_{cj} \cdot (y_{cj} - y_p) \qquad (13)$$

Where,

NS	=	total number of steel layers
NC	=	total number of concrete layers
A_{si}	=	area of steel layer i
σ_{si}	=	stress in steel layer i
y_{si}	=	distance to steel layer i from bottom of section
A_{cj}	=	area of concrete layer j
σ_{cj}	=	stress in concrete layer j
y_{cj}	=	distance to concrete layer j from bottom of section
y_p	=	distance from bottom of section to the axis around which moment is desired - usually the plastic centroid.

A more efficient double summation procedure is actually implemented in the program to take advantage of the fact that many layers often have the same area (i.e. are in the same group).

2.6(b) Analyses involving iterations

When the axial load is specified along with curvature (ICNTR = 3) or with the strain at a given location (ICNTR = 2), the solution proceeds by iterating on the neutral axis position until the axial load is reached within a user-specified tolerance. When analyzing for cyclic behaviour, the neutral axis position can fluctuate dramatically; hence the following strategy is adopted. Lower and upper bounds (YNAL and YNAU) are set on the possible position of the neutral axis. The corresponding pair of axial loads (XPL and XPU) are then calculated, since the strain profile is completely defined. The bounds are expanded (by an amount set by the user) until the required axial load (AXIAL) is bracketed by XPL and XPU, at which point the iteration procedure starts. Such a technique avoids having to start with unnecessarily large bounds and hence cuts the number of iterations needed for convergence.

Fig. 2.12 is a schematic representation of the iterative procedure adopted. Linear interpolation is used to set the modified neutral axis position (YNAM) using the following expression:

$$\mathrm{YNAM} = \mathrm{YNAL} + (\mathrm{YNAU} - \mathrm{YNAL}) \cdot (\mathrm{AXIAL} - \mathrm{XPL}) \,/\, (\mathrm{XPU} - \mathrm{XPL}) \qquad (14)$$

The axial load corresponding to the modified position is then calculated (XPM). If it does not fall within the convergence tolerance, a reduced interval that brackets the solution is defined (either YNAL-YNAM or YNAM-YNAU) and another iteration is performed. Once convergence is achieved the corresponding moment is calculated and the results are printed. This iteration procedure is basically the Regula Falsi method [24,26]. Under certain conditions, it has a faster rate of convergence than the bisection method; and, unlike the secant method, the Regula Falsi method is guaranteed to converge. The option of using the bisection method, however, is also available to the user. For this method, the expression giving the modified neutral axis position (YNAM) is:

$$\mathrm{YNAM} = 0.5 \cdot (\mathrm{YNAL}+\mathrm{YNAU}) \qquad (15)$$

Note that when a small curvature is specified, the number of necessary bound expansions may be relatively large. Moreover, when the absolute value of the curvature is smaller than a set limit (0.000002/H, where H is the depth of the section) the section is assumed to be subjected to a uniform strain which is then solved for using a similar iterative procedure on the value of the uniform strain instead of on the position of the neutral axis.

When moment-curvature plots under a constant axial load are desired a fourth option (ICNTR = 4) is convenient. In this case the axial load, the initial curvature, and the number and size of the curvature increments are specified and the program automatically generates moment-curvature (or moment-ductility) plots.

2.6(c) Convergence and Updating of Results

For the iterative solutions (ICNTR=2,3,or 4) the user sets a convergence tolerance on the axial load and the number of allowed bound expansions and iterations. If no solution is found within the set number of bound expansions, it could be due to one of the following reasons:

(1) No solution is possible, given the section properties and/or the loading history (e.g. too large an axial load, etc.).

(2) Initial pair of bounds on the position of the neutral axis were too large. For example when a tensile strain is assigned to point A in Fig. 2.13 and a given compressive axial load is sought. In such a case a tensile axial force will be associated with the initial as well as any expanded bounds, for a sufficiently large DELTAH. Iteration on the position of the neutral axis should therefore start with a smaller set of bounds. The user can achieve this in such cases by specifying a smaller bound expansion increment DELTAH.

(3) Number of bound expansions is insufficient (e.g. when a very small curvature is specified). In this case it is possible for the user to increase the number of bound expansions.

If the solution does not converge once bounds on the neutral axis location are determined, it could be due to setting too small a convergence tolerance or number of iterations. This can usually be remedied by increasing the number of iterations. Lack of convergence may also be due to numerical problems, abrupt changes in material properties, or specifying too large a curvature increment. This could be remedied by diminishing the size of the increment, changing the iteration method, varying the rate of bound expansion or using another section discretization . When convergence is not achieved within the set number of iterations, the program provides the latest results and the user is then asked for instructions.

Once the iteration converges, the program checks with the user on whether the results should be stored or not. In case cyclic material behaviour is specified, the program also consults the user on whether the values of the various variables and indices should be updated or not. By not updating, the conditions at the end of the previous step are preserved and the user may change the size or direction of the last step. For example (using ICNTR=3), if the user decides that in going from A to C in Fig. 2.14 too large a step was used (the bars buckled or the concrete cracked, etc.), the analysis can back up to stage A (by not updating) and move to B instead.

By judicious use of the freedom to update or not, the user can describe the moment-curvature history of a section subjected to constant eccentricities, i.e. bending moments which are proportional to the applied axial load. Note, however, that when using automatic curvature generation (ICNTR=4) along with cyclic material behaviour, the variables and indices are updated at every step once convergence is achieved.

2.6(d) Chaining a Sequence of Operations

Once a sequence of loading cases corresponding to a given value of ICNTR is over the user can choose one of the following options:

(1) Continue with the same type of analysis. In this case the variables can either be reinitialized to virgin conditions (setting INDEP = 0) or conditions at the end of the last case can be preserved (INDEP = 1). For example, using automatic curvature generation (ICNTR = 4), once the final specified curvature is reached, it is possible to reverse the sign of the curvature increment and repeat the process starting with the final value of the previous analysis. Hence, curves as the one shown in Fig. 2.15 can be generated using three operations only. Note that when going from operation 1 to operation 2 (and from 2 to 3) the variable controlling

updating of material history data (INDEP) should be set equal to 1 so that the conditions at the end of one operation are used as the initial conditions prevailing at the start of the next operation. When variables are reinitialized to virgin conditions it is possible to reanalyze a section under a different axial load or different curvature history.

(2) Move to another type of operation, in which case it is also possible to preserve the conditions at the end of the previous operation. Hence, quite complex loading histories can be considered. For example the section may be subjected to a sequence of axial loads (with no bending) followed by a sequence of bending moments at constant axial load.

(3) Modify the section and/or material properties and resume the analysis. This is often more convenient than entering all of the section and material data anew - e.g. in the case of studying the effects of detailing or material alternatives.

(4) List output files, plot and inspect the output of previous operations, or rename and thus preserve output or data files before moving on to a new set of analyses.

(5) Produce a compact summary containing description of the section for easy reference.

(6) By using the analysis output file, calculate the strain history at any level (for example at the center of the section) and plot it against the moment history.

2.7 Concluding Remarks

The computer program described in this chapter is a convenient tool for the analysis of reinforced concrete, prestressed concrete, and structural steel sections. The various solution strategies and options increase the capabilities of the program. Flexibility is further enhanced by the interactive nature of the program. The following two chapters illustrate the use of the program to assess the sensitivity of section behaviour to material modelling, loading history, and section idealization. Further notes on the use and modification of the program can be found in the appendices.

III Behaviour of Reinforced Concrete Sections

3.1 Introduction

As indicated previously, the inelastic flexural behaviour of a section depends on the section's geometry, the properties of the materials involved, and the loading history. In addition, the calculated behaviour of the section depends on the way in which the materials and section are idealized and the solution technique employed. The purpose of this chapter is to investigate the effects of some of these factors on the behaviour of reinforced concrete sections and to identify the capabilities and limitations of the program described in the previous chapter.

A particular cross section for which experimental data is available has been selected for detailed investigation. Comparison of the analytical results with the experimental data will give an indication of the accuracy of the method. Moreover, the program can be used to develop insights as to the reasons for some of the observed behaviour and to extrapolate to cases where experimental data are not available. Various analytical results are presented to identify the effects of material modelling assumptions, section discretization methods, solution strategies and loading histories.

3.2 Example Section

A simple reinforced concrete section has been selected as the basis of most of the examples in this chapter. Experimental data is available for this section [22] and it has been used in other analytical studies [10]. The cross section, shown in Fig. 3.1, has equal areas of tension and compression reinforcement. The longitudinal reinforcement consists of two No. 4 bars on both top and bottom. The transverse reinforcement consists of No. 2 bars at 2-in. on center. The longitudinal steel has a yield stress of 48.4 Ksi and the concrete has a compressive strength of 6.95 Ksi. A concrete tensile strength of 0.95 Ksi was experimentally determined and is equal to 11.4 $\sqrt{f'c}$. For purposes of later comparisons $P_{\max}$ (given by $A_c \cdot f'c + A_s \cdot f_y$) is equal to 301 Kips.

Experimentally determined moment-curvature plots for this section are presented in Fig. 3.2. Small curvature cycles were initially applied followed by larger excursions eventually reaching curvature limits of -.00156 and .00189 rad/in. The figure shows significant stiffness deterioration. As noted by Kent [22], under reversed loading after yielding the section is often cracked over its entire depth in the working stress range and the behaviour is completely governed by the action of the steel couple. This accounts in part for the significant reduction of stiffness observed in this range. There is an increase of stiffness when under increased loading the crack closes on the compression face and the concrete starts to participate again -- such points are marked by the letter C on the curve.

This same section was modelled using UNCOLA and subjected to the curvature history measured experimentally. The material models used are shown in Fig. 3.3. The basic concrete model with tensile contribution of concrete is used and the Ramberg-Osgood steel model is employed for the steel. Both models account for cyclic strain reversals. The section is discretized into 30 concrete layers as shown in Fig. 3.4. Twelve of the layers represent the confined concrete core and the rest represent the unconfined cover.

The results of the analysis are given in Fig. 3.5. Comparison of the experimentally and analytically determined moment-curvature relations (see Figs. 3.2 and 3.5) indicates generally excellent agreement.

3.3 Influence of Concrete Properties on Section Behaviour

To analyze a given section it is desirable to experimentally determine the material properties involved and develop a model that describes these properties as accurately as possible. In most cases, however, such experimental data is unavailable or very limited. For example, the only available parameters are often the concrete compressive strength f'_c, the steel yield stress f_y, and the steel Modulus of elasticity E_s. Moreover, the material models currently implemented in UNCOLA are incapable of exactly matching experimental results. Thus it is important to assess the sensitivity of computed section behaviour to variations in material properties and to the way in which these properties are modelled. The influence of concrete modelling assumptions on section behaviour will be examined in this section. Reinforcing steel modelling will be treated in the next section.

Since the concrete compressive strength of the example beam was experimentally determined from cylinders, this experimental value is used in most of the examples. However, the effects of the concrete tensile capacity, spalling, and confinement, as well as of of different modelling methods will be examined in greater detail.

3.3(a) Effect of Concrete Tensile Capacity

Many of the available computer programs assume concrete incapable of carrying any tension. As can be seen in Fig. 3.6, this assumption is justified if one is concerned with ultimate behaviour or cyclic response. In this figure the rupture stress f_r is alternatively set equal to zero or 0.95 Ksi (the experimentally determined value [22]). Once this value is exceeded, the concrete is assumed cracked and henceforth incapable of carrying any tension.

However, response under service loading can be significantly affected by the tensile capacity. To illustrate these effects computed moment-curvature relationships under service conditions are shown in Fig. 3.7. Table 2 summarizes some of these results. When the axial load is zero, the initial stiffness of the section is substantially increased by considering the concrete tensile capacity. Once cracking starts the stiffness rapidly returns to that predicted by the model with no concrete tensile strength. As one would expect the effect of the concrete tensile strength becomes less significant when the section is subjected to axial compression.

P/P_{max}	f_r = 0.0 ksi				f_r = 0.95 ksi			
	ϕ_{cr}, in^{-1}	M_{cr}, k-in	ϕ_y, in^{-1}	M_y, k-in	ϕ_{cr}, in^{-1}	M_{cr}, k-in	ϕ_y, in^{-1}	M_y, k-in
0	.0	.0	.000351	113.0	.0000464	56.3	.000356	115.0
1/9	.00004	46.9	.000453	205.2	.0000865	100.5	.000453	205.4
2/9	.00008	89.3	.000551	281.9	.00013	142.5	.000551	282.3

TABLE 2. Cracking and Yield Data for Two Valves of Concrete Rupture Stress (f_r)

One can also note that the cracking and yield moments increase with an increase of the compressive axial load. Axial load-bending moment interaction diagrams as in Fig. 3.8 are often used to show such variations. In this case monotonic material properties are assumed to simplify the computations (as often done in design). A given strain is specified in a particular layer and the program calculates the axial load and bending moment corresponding to a series of neutral axis positions. As discussed in Section 2.6(a) this solution strategy is usually adequate for this purpose. Since cracking and steel yielding may be used as design criteria it is possible to include them on the diagrams. In Fig. 3.8 the the cracking interaction diagram assumes a rupture stress of 0.95 Ksi.

There is considerable uncertainty in the tensile capacity of concrete. The experimentally obtained value of $11.4\sqrt{f'_c(psi)}$ is significantly higher the commonly assumed value of $7.5\sqrt{f'_c(psi)}$ [27]. Experiments indicate that expressing the rupture stress as a function of the square root of concrete compressive strength may not be satisfactory. Warwaruk [28] suggests using:

$$f_r = \frac{1000 \cdot f'_c}{4000 + f'_c} \tag{16}$$

and Kent modifies this equation to better fit his experimental values [22]:

$$f_r = \frac{1400 \cdot f'_c}{4000 + f'_c} \tag{17}$$

UNCOLA can be used to assess the consequences of such uncertainties in predicting the tensile capacity. In addition, initial shrinkage and other stresses are not accounted for by the program and would also affect the cracking load and the initial stiffness.

Moment-curvature plots shown so far really give the average of the average of the curvature along the length of the beam between two cracks. Since the concrete between two cracks is intact, it can help the longitudinal reinforcement carry the tensile force assuming bonding stresses exist between the concrete and the reinforcement. This phenomenon, usually referred to as tension stiffening, has been ignored in the analyses presented above. Methods for taking tension stiffening into consideration are given in [12]. By suitably modifying the concrete or steel material models, some of the suggested approaches can be conveniently implemented in conjunction with the fiber model. The concrete model available in UNCOLA makes it especially simple to modify the concrete stress-strain behaviour in order to account for tension stiffening.

The results of an analysis carried out using the stepped concrete model suggested in [12] are given in Fig. 3.9. Also given in the same figure are the results of analyses assuming brittle rupture and no concrete tensile capacity. Comparing the plots shown in Fig. 3.9 it is evident that tension stiffening can appreciably affect section behaviour under service loading. Tension stiffening results in a significantly higher post-cracking bending stiffness. Hence, ignoring tension stiffening can result in significantly overestimating deflections of beams and slabs under service loads.

The model suggested in [12] is intended only for monotonic loading. Recent research [29] has indicated that an equivalent concrete model in tension used in conjunction with the fiber model can partially account for the bond slip in the vicinity of a crack and its effect on moment-curvature relationships under load reversals.

3.3(b) Effect of Concrete Compressive Strength

The use of high strength concrete is becoming increasingly popular. Adequate studies, however, on the influence of the concrete strength on inelastic section behaviour have yet to be carried out. UNCOLA can be used to obtain an idea of how section behaviour is affected by the concrete strength. The section chosen is the one described in Section 3.2 except that it is assumed to be unconfined The Ramberg-Osgood model (Fig. 3.3) is used to describe the steel behaviour. The unconfined concrete model suggested by Kent [22] is used to represent the concrete behaviour throughout the section. The stress-strain curves corresponding to f'_c of 3, 5, and 7 Ksi are given in Fig. 3.10. Lee [30] suggests that the strain at which the concrete stress peaks is also a function of the compressive strength. Kent [22], however, suggests that there is no firm correlation and that only the linear descending branch of the stress-strain curve is significantly affected. Kent's suggestion of a strain of .002 at peak strength is adopted along with his formula for calculating the slope of the descending branch. As shown in Fig. 3.10 the slope increases with an increase in the concrete strength.

Using the material models described in the preceding paragraph and shown in Fig. 3.10, the cross-section is subjected to a uniformly increasing curvature. Fig. 3.11 gives the resulting moment-curvature plots for axial loads of 0.0 and 33.5 Kips ($=P_{max}/9$). The curves stop when the extreme compressive concrete strain reaches 0.004. For comparison, the points where the maximum strain is 0.003 are marked by an "x" on the figure. Note that higher strength concrete results in larger section ductility (defined here by the ratio of the ultimate to yield curvature) since the ultimate curvature increases while the yield curvature decreases. Note also that there is only a slight rise in the moment capacity of the section for a higher strength concrete, especially for zero axial load.

3.3(c) Effect of Confinement

Confinement affects the shape of the effective uniaxial concrete stress-strain relationship. The parameters needed to define the models suggested by Kent [22], Vallenas et al [18], and Sheikh and Uzumeri [19] were calculated for the example section described in Section 3.2 and using the experimental data from Kent [22]. The resulting stress-strain diagrams are given in Fig. 3.12. Note that these are assumed to represent the behaviour of the confined portion of the section bound by the centerline of the ties. For this particular section, applying Equation 13 in Sheikh and Uzumeri's paper [19] indicates that there is no flat portion at the maximum compressive stress as described in Section 2.5(a). Note, however, that the Vallenas model as well as that of Sheikh and Uzumeri predict an increase in the maximum compressive strength and in the strain at which this peak strength occurs (ϵ_0).

The behaviour of the unconfined portions of the section is not explicitly described in [18] and [19]. Hence, Kent's model (Fig. 3.12(d)) is used except that Sheikh and Uzumeri [19] advocate a reduction of 15% in the maximum compressive capacity (i.e. use of $0.85f'_c$). Vallenas et al [18] and Sheikh and Uzumeri [19] suggest a sudden drop in the unconfined concrete capacity when spalling occurs.To assess this effect, the strain beyond which the unconfined concrete is assumed incapable of carrying any load is alternatively set at .003 and .006 for the Vallenas model.

Moment-curvature plots corresponding to the above-mentioned concrete models are given in Fig. 3.13. Because spalling is expected to have little effect on the moment-curvature relationships of doubly reinforced beams with low percentages of steel [1], an axial load ($2/9P_{\max}$) was applied to the section to better assess this effect. This load increases the contribution of the concrete to the moment capacity and reduces the ductility of the section. Thus, differences in the models are expected to have a more pronounced effect. In the initial phases of the plots in Fig. 3.13 (up to a curvature of around 0.0007) all models give similar results with the plot corresponding to the Sheikh and Uzumeri models being lowest because the strength of the unconfined concrete is assumed limited to $0.85f'_c$. Beyond this initial phase, Kent's model leads to higher moment values because the strain at which the concrete stress peaks is lower. Thus, the moment and axial load can be developed through higher curvatures without the cover spalling. All curves evince a drop in the moment capacity at curvatures ranging from 0.0007 for the Vallenas model with the crushing strain set at the lower bound of 0.003 to 0.0009 for the Kent model. All the models result in the same moment capacity at large curvatures again indicating the relative insensitivity of the response to the concrete model used.

3.4 Influence of Steel Properties on Section Behaviour

The properties of the reinforcing steel have a significant effect on the inelastic behaviour of reinforced concrete members. The following section investigates the influence of the steel material properties. Since the yield stress and Young's modulus have been experimentally determined they are taken as the typical case. However, the steel model used to represent the stress-strain behaviour is varied. The effect of this variation on the cyclic moment-curvature relation is investigated.

3.4(a) Influence of Steel Strength

One of the important parameters that affect reinforced concrete section behaviour is the steel yield stress (f_y). The actual yield stress is often significantly higher than the specified design yield stress. For the example cross-section described in Section 3.2 the actual yield stress (experimentally determined by Kent [22]) is 48.4 Ksi while the reinforcement is actually specified Grade 40. To illustrate the influence of the steel yield stress, two analyses are carried out using the example section. The first analysis assumes an elasto-perfectly plastic steel stress-strain curve with a yield stress of 40 Ksi. The second analysis uses the experimental stress-strain curve, with a yield stress of 48.4 Ksi, to describe the steel behaviour.

Fig. 3.14 gives the interaction diagrams corresponding to the two steel models with the maximum concrete compressive strain set at 0.003. As expected, the moment capacity of the section increases with an increase in steel yield stress for all values of the axial load. This observation is also shown in Fig. 3.15 which gives the moment-curvature plots corresponding to the two steel models. Section ductility, however, decreases with an increase in the steel yield stress. The drop in ductility is due both to a drop in the ultimate curvature as well as a rise in the yield curvature. These two factors are both evident in Fig. 3.15. It should be noted that for the cases considered here the steel did not enter the strain hardening range which would have resulted in further discrepancies between the two models.

3.4(b) Influence of Steel Modelling

Because of the large influence of the steel on section behaviour, it is important to use a steel model which reflects the relevant physical phenomena such as strain hardening, buckling, and the Bauschinger effect. The plots described so far have generally been based on the Ramberg-Osgood steel formulation. As discused in Chapter 2, two other models are available in the program: the bilinear and the cubic models. Fig. 3.16 shows the effect of the steel model chosen on the moment-curvature relation. The parameters used in defining the monotonic envelope curve for the cubic steel model are identical to those used in conjunction with the Ramberg-Osgood model. The bilinear model parameters are chosen to model an elasto-perfectly plastic steel with a yield stress of 48.4 *Ksi*.

Note from Fig. 3.16 that the choice of the steel model does not affect the initial loading phase since the steel strain does not exceed the hardening strain ϵ_{sh}. The steel model, however, has a marked influence on the unloading phase as well as on successive cycles. The Ramberg-Osgood and cubic models lead to a curvilinear moment-curvature diagram due to the Bauschinger effect while the bilinear model leads to a multilinear diagram with slight curvilinearities resulting from the concrete action. As discussed in Section 2.5(b), the cubic steel model results in higher stresses (and hence larger bending moments) upon reversal than the Ramberg-Osgood model - compare points C and R in Fig. 3.16. All models, however, show the basic double-sided pinching of the moment-curvature plot associated with the compressive load as will be explained in Section 3.6. Note that the steel model used is very influential in determining the overall section behaviour, especially in the working stress moment regions. Some intervals of the moment-curvature diagram are in fact nothing more than the action of a steel couple since the whole section is cracked in these intervals. In these examples a curvature history was imposed. If a moment history were stipulated, the discrepancies between the two models would be even greater due to the differences in the ways that the Bauschinger effect and hardening are accounted for in the models.

3.5 Influence of the Amount of Compression Steel

The influence of the amount of compression steel on the hysteresis loops is shown in Fig. 3.17. An unsymmetrical steel distribution (with a $\frac{\rho'}{\rho}$ ratio of 0.5) results in different moment capacities in the two bending directions. In addition, it causes pinching on one side of the hysteresis loops. The loading history considered results in tension yielding of the bottom layer of reinforcement (point B on Fig. 3.17). Upon unloading and moment reversal, the top layer eventually yields in tension but because of its smaller size the moment is less than that resulting from the initial loading (compare points C and D).

When reloading in the original direction again, the top layer cannot develop sufficient stress to permit tensile yielding of the bottom layer. Consequently, the top layer must first yield in compression allowing the crack on the top part of the section to close before the bottom layer can yield in tension. This compression yielding of the top bar results in a step plateau (or pinching) of the moment-curvature diagram (point D') prior to developing the full moment capacity (point E).

Note that pinching only occurs in one direction since upon unloading and moment reversal, the top layer yields in tension but its small size prevents the bottom bar from yielding in compression and the crack on the bottom part of the section from closing. This is illustrated in Figs. 3.17(b) and 3.17(c) where it is shown that while the top layer yields in tension and compression, the larger bottom layer only yields in tension. Note that both bars tend to become progressively longer during cycling resulting in a net elongation of the section.

Comparing the curves in Fig. 3.18 corresponding to different axial loads for a $\frac{\rho'}{\rho}$ ratio of 0.5 and 1.0, it is evident that the ductility is also influenced by this ratio. Note that for this section the strength and ductility for low axial loads are somewhat independent of the $\frac{\rho'}{\rho}$ ratio; while for larger loads, both strength and ductility decrease with decreasing $\frac{\rho'}{\rho}$ ratios. The decrease in ductility is due to a higher yield curvature as well as a lower ultimate curvature (here defined as the curvature at which the maximum concrete strain reaches 0.004). This section does not show a significant loss of ductility for a lower $\frac{\rho'}{\rho}$ ratio because ρ is relatively low and because the concrete is partially confined - compare with the ductility versus $\frac{\rho'}{\rho}$ curves given in [23] where there is a dramatic drop of ductility for higher ρ ratios. Note, however, that in [23] the concrete is assumed unconfined throughout the section. Note also that a lower ρ' ratio means lower moment capacity in the other direction and more severe pinching of hysteresis loops of the type indicated in Fig. 3.17. Hence it is desirable to have high $\frac{\rho'}{\rho}$ ratios when cyclic loading is expected.

3.6 Influence of Loading Path and History on Section Behaviour

Section behaviour is a function not only of the maximum magnitude but also of the overall history of the loading. For example the section can be subjected to pure axial straining followed by bending around the plastic centroid, or the curvature could be varied in such a way that the section is subjected to constant eccentricity, that is the moment to axial load ratio is held constant. The section can also be subjected to a cyclic curvature history in which the cycle amplitudes gradually increase or in which the final amplitudes are imposed initially. This section illustrates the influence of various loading histories on section behaviour.

3.6(a) Cyclic vs. Non-cyclic Material Models

If the loading history itself is cyclic then it is essential to use cyclic material models. As an illustration, Fig. 3.19 shows the moment-curvature relation for the same section subjected to a constant axial load of 33.5 Kips ($=P_{max}/9$) while the curvature increases from 0.0 to .0012 then decreases to -.0012 and finally increases back to .0012. The figure shows two plots one assuming cyclic and the other non-cyclic material behaviour. Note that when monotonic material behaviour is assumed, there is one-to-one correspondence of curvature to moment values irrespective of whether the section is being loaded or unloaded. Hence the hysteresis loops degenerate into a line and the section evinces no energy dissipation.

3.6(b) Effect of Axial Load

Fig. 3.20 shows the same section subjected to various axial loads but undergoing the same curvature history in all cases. When the axial force is tensile, the concrete affects the behaviour during the first loading and unloading; beyond that the section reduces to a steel couple. It is interesting to note that the section stiffens during its initial "elastic" loading. Since a tensile load is applied first the section is cracked and as the moment is applied the crack closes on one side increasing the effective stiffness of the section until yielding of the tensile steel occurs. In the plot corresponding to zero axial load, the portions corresponding to initial loading and unloading are stiffer due to the concrete action. In subsequent loading or unloading portions the concrete is incapable of carrying any tension because it has already cracked. Hence, there is a drop in stiffness as well as moment capacity compared to the corresponding values in the initial loading.

As the load increases, so does the pinching effect which results in the squeezing in of the hysteresis loops upon unloading or reloading. Because of the compressive load acting on the symmetrically reinforced section, the crack on the compression side must close so that the concrete fibers can participate again, before the steel on the tension side can yield. This compression yielding results in a lower yield plateau and the closing of the crack causes a sudden increase in the section stiffness thereby producing the pinched hysteresis loops. Note also that moment capacity also increases with the compressive axial load - up to a point as Figs. 3.8 and 3.20 have shown.

3.6(c) Effect of Loading Path and Idealization

The effect of progressively increasing the amplitude of the curvature cycles as opposed to achieving maximum amplitude in a single cycle is shown in Fig. 3.21. Note that progressive increases in cycle amplitude defines a symmetric moment-curvature envelope with significantly larger upper and lower bounds than those reached in the case of a single large cycle. This is due to the kinematic and isotropic hardening of the steel as indicated in Figs. 3.22 and 3.23.

Moment-curvature and moment-axial load plots corresponding to two loading histories are shown in Fig. 3.24. The first plots correspond to loading at a constant eccentricity (moment to axial load ratio), the second to applying a constant axial load followed by application of a monotonically increasing moment. Although the paths are different, the two plots converge to the same final point. Fig. 3.25 shows the curves corresponding to similar loading histories for a higher axial load. In this case, for the same final curvature value the bending moments are no longer the same. This is another indication that section behaviour becomes more dependent on loading path at higher axial loads.

3.7 Some Aspects of Section Idealization

The previous sections investigated the importance of material properties on section behaviour, mainly as related to their effect on the moment-curvature relationship. This section will illustrate the influence of the analysis technique on the computed behaviour. In particular the effect of section discretization will be investigated by comparing analyses of the same section discretized in a number of ways. In addition, the influence of ignoring possible stress reversals in the material model as often done in programs for monotonic loading will be examined.

3.7(a) Section Geometry Idealization

It is sometimes thought that the accuracy of a given analysis is somehow proportional to the number of layers used in the discretization of the concrete portion. Fig. 3.26 shows the same section subjected to the same loading cycle but with different numbers of discretizing layers. Note that there is no appreciable difference in the results for the cases considered. For a section subjected to cyclic bending, the layers at either extreme of the section are the ones that contribute most to the moment capacity. Moreover, under cyclic loading the section may be completely cracked during much of its loading history. Since the program allows layers of variable depths, it is therefore advisable to concentrate a large number of layers near the ends. Note, however, that these layers are liable to crack or spall (especially since the extreme portions are usually unconfined) and hence lose their stress carrying capacity. Hence the nature and magnitude of the loading can also influence the optimum section discretization. Some observations on section discretization are also given in [31]. Note, however, that this study is only concerned with reinforced concrete sections subjected to pure flexure.

Another aspect regarding the idealization is which portion of the section is to be considered the confined concrete portion. Fig. 3.27 shows the moment-curvature plot of the same section considering the confined concrete area as (1) 6.5 x 3.25 and (2) 5.0 x 2.25, that is bounded by the outer tie lines and inner reinforcement lines, respectively. Note that the difference is negligible except when the curvature reaches a magnitude large enough to cause spalling.

3.7(b) Cyclic Material Behaviour

Many programs [1] for determining the moment-curvature relationships for reinforced sections subjected to monotonically increasing curvatures base the material stresses on their monotonic stress-strain envelopes. However,under monotonic loading the materials at many locations can undergo significant unloading and stress reversal. In the case of beams, the neutral axis may shift upward from its initial uncracked transformed position due to cracking and inelastic concrete properties then it might drop due to the effect of the descending branch of the concrete stress-strain diagram and spalling. Finally, it might shift upward again due to possible strain hardening effects in the compression steel. This shifting of the neutral axis will result in strain reversal in the vicinity of the neutral axis. Sections under axial load that are then subjected to bending moments will also clearly have to undergo stress unloading or reversal at some locations in order to develop the moment. To assess this effect, analyses have been performed considering both cyclic and non-cyclic material properties.

Fig. 3.28 shows the monotonic moment-curvature relationship for the section described in Section 3.2 subjected to various axial loads. The figure shows twin plots for each axial load one assuming non-cyclic and the other cyclic material behaviour.Note that for low axial loads these twin plots nearly coincide indicating that the layers which unload are close to the plastic centroid of the section (around which the moment is taken) and the amount of unloading is not appreciable. For higher axial loads, however, there is significant unloading in some layers which are not close to the plastic centroid and it becomes important to model the cyclic material behaviour. In fact at high axial load it is essential to account for the history of loading as the results are highly path dependent. Methods which use the non-cyclic material stress values for an imposed strain distribution may give erroneous results which do not correspond to a physically possible state.

3.8 Effect of Load Discretization and Convergence Tolerance

Since it is up to the user to discretize the loading history into a finite number of increments and set the convergence tolerance, it is important to assess the effect that these two parameters have on the results of a section analysis. Figs. 3.29 and 3.30 show the effect of convergence tolerance and the size of the curvature increment of moment-curvature relationships. The same section described in Section 3.2 is subjected to a large axial load of 250 Kips (5/6 P_{max}). Note that the effect of the convergence tolerance is less pronounced when non-cyclic material behaviour is specified. It is worth mentioning, however, that setting a smaller convergence tolerance does not result in a significantly longer solution time because of the iteration procedure used.

The size of the curvature increment has no effect on the moment capacity when non-cyclic material behaviour is specified since the stress-strain relationship is independent of the loading history in this case. Even for cyclic material behaviour, Fig. 3.30 shows that the curvature increment size is not important when the axial loads are relatively low. The shape of the moment-curvature graph can be different because of the different number of points used for plotting but the magnitude of the moment at corresponding curvatures is nearly the same in most cases. Section behaviour, however, becomes quite sensitive to various parameters when the section is subjected to large axial loads - see Figs. 3.8, 3.18, and 3.28. In the case of the curvature increment, Fig. 3.31 gives a somewhat dramatic instance: compare the moment-curvature plots for cyclic material behaviour corresponding to increments of .000025 and .00005 rads/in.

3.9 Concluding Remarks

A computer program based on the fiber model is a useful tool for the analysis of reinforced concrete sections. It can be used to study the influence of various parameters and phenomena on section behaviour. By producing moment-axial load diagrams and moment-curvature plots, the importance and effect of cracking and crushing of concrete, moment-axial load interaction, yielding of steel, and the Bauschinger effect can be readily assessed. The examples given in this chapter have indicated the potential of the fiber model for the analysis of reinforced concrete sections where relatively general loading paths and histories need to be considered.

The examples have also indicated the sensitivity of the section behaviour to various parameters when subjected to high axial loads. Thus, at high axial loads such factors as curvature increment, convergence tolerance, as well as material modelling considerations become significant. It has also been illustrated that section behaviour, especially under cyclic loading, is highly dependent on the steel model used. Thus, it is important to use a steel model which follows as closely as possible the physical behaviour of the actual steel reinforcement. Although the Ramberg-Osgood model available in the program has proved capable of producing satisfactory results, it is desirable to implement other more recent steel models if they show better agreement with experimental analyses.

IV INITIAL STRAINS AND STRESSES

4.1 Introductory Remarks

As indicated in Section 2.5(d), the UNCOLA program is capable of considering the effects of initial stresses or strains in the steel. Two important illustrations of the effects of initial stresses on section behaviour are (1) residual stresses in steel sections, and (2) prestressed concrete sections. Section 4.2 will illustrate the former and Section 4.3 the latter.

4.2 Residual Stresses In Steel Sections

The UNCOLA program can be used as described in Chapter 3 to assess the influence of various parameters on the inelastic behaviour of structural steel sections. The program would be particularly useful where built-up sections are used or where detailed moment-curvature diagrams are required. Rather than repeat the studies conducted for concrete sections, only the particular influence of residual stresses on steel sections will be investigated here.

The idealized wide flange section (W14x78) shown in Fig. 4.1 is used in this example. Although the figure shows 20 layers, only 16 are actually used by taking advantage of the symmetric distribution of the residual stresses about the vertical axis. The elasto-perfectly plastic steel model is used along with a yield stress of 36 *Ksi*. The plastic moment for this section (given by $Z \cdot f_y$) is 4824 $K-in$, while the yield moment (given by $S \cdot f_y$) is 4356 $K-in$. Simplified residual stress distributions are shown in Fig. 4.1. Four analysis cases are considered: (1) no residual stresses; (2) peak flange residual stresses equal to $f_y/3$; (3) peak flange residual stress equal to $2f_y/3$, and (4) peak flange and web residual stress equal to $2f_y/3$. In cases 2 and 3 web residual stresses are disregarded. More complex residual stress distributions can easily be considered by the program.

The moment-curvature relations for this section are shown in Fig. 4.2. One plot shows the moment-curvature for the section assumed free of residual stresses. Other plots assume residual stresses equal to one-third and two-thirds of the yield stress in the flanges and no residual stresses in the web. Note from the figure that in spite of the section discretization being somewhat crude, the yield and plastic moment values are quite accurate for no residual stresses. Furthermore, note that, as expected, inclusion of the residual stresses does not influence the plastic moment capacity of the section. The yield moment, however, is significantly reduced and the moment-curvature curve becomes essentially trilinear. The larger the magnitude of the assumed initial residual stresses the more pronounced is the drop in the yield moment, while for large curvature values the corresponding moments are the same irrespective of the residual stresses. Similarly, as shown in Fig. 4.3, when the section is subjected to inelastic curvature cycling, the effect of residual stresses is only evident in the initial loading phase.

Fig. 4.4 compares two moment-curvature plots one corresponding to the section with residual stresses in the web and the other ignoring the initial stresses in the web. Note that the two plots almost coincide since the web does not contribute significantly to the moment capacity of the section.

4.3 Prestressed Concrete Sections

Another type of section that can be analyzed using the initial stress option is a prestressed concrete section. Moreover, the section can also have reinforcing steel along with the prestressing tendons to consider the effect of partial prestressing. The section must, however, use bonded tendons due to the assumption of plane sections remaining plane. It is also possible to consider structural steel sections with initial stress distributions corresponding to construction loads developed in composite sections using the same techniques.

The I-beam prestressed section analyzed is the same as the one considered in [32], shown in Fig. 4.5. The concrete compressive strength (f'_c) is equal to 7 ksi. The steel tendons have a yield stress equal to 240 ksi and an ultimate stress equal to 282 ksi. The steel tendons have an initial stress of 160 ksi or 66.7% of their yield stress. Concrete is modelled using the unconfined Kent [22] model and for simplicity the steel is modelled as being bilinear. This assumption is consistent with [32]. However, more realistic multi-linear models for the tendons could easily be achieved by subdividing the tendon into several fibers. Each fiber would have different stiffnesses and strengths selected so that the resultant force-strain relationship would match the desired values.

A search for the point of zero moment is first undertaken by trying different negative curvatures. The various parameters and indices are not updated after each of these trials. Once the curvature corresponding to zero moment is located the automatic curvature generation option is exercized to produce the curve shown in Fig. 4.6.

For comparison, the moment-curvature plot corresponding to a full rectangular section, shown in Fig. 4.5, is also given in Fig. 4.6. Note that the moment capacity of the two sections is the same, although the rectangular section has a concrete area which is about 75% larger than the I-section. The concrete is assumed capable of carrying tensile stresses up to a value of $7.5\sqrt{f'_c}$. Using the program, it is possible to locate the curvature at which the bottom concrete fiber starts carrying tensile stresses (point A in Fig. 4.6) and the curvature at which a crack starts propagating (point B in Fig. 4.6). Thus, the program permits detailed information regarding the behaviour of these types of sections to be obtained rapidly and for different sections to be compared with relative ease.

4.4 Concluding Remarks

Based on the examples shown in this chapter it is seen that the program has applications to steel and bonded prestressed concrete sections. The capabilities for considering initial stresses and strains are particularly useful in these cases.

V CONCLUSIONS

The fiber model used in conjunction with interactive computing is a potent and versatile tool for section analysis. The main mechanical properties describing section behaviour can be quickly assessed with reasonable accuracy. Moment-axial load interaction, cracking and crushing of concrete, and the Bauschinger effect are some of the phenomena which can be considered.

A flexible interactive program developed for micro-computers is capable of analyzing general steel, reinforced concrete, and prestressed concrete sections. The fact that the program is interactive makes it possible for the user to intervene at various stages and decide upon the type, direction, and magnitude of the next loading step after scrutinizing the results of the previous steps.

Additionally, there is the option of rejecting the last set of output and returning to the previous loading stage - by choosing not to update the various parameters and indices. This option enhances the program flexibility and makes it possible to detect certain problems and events such as spalling of concrete or buckling of steel and still be able to correct for them before carrying on with the analysis. Hence, it is possible to interactively adjust the loading history to bring out the desired mechanical behavioural characteristics.

Desirable section analyses were deemed impractical and time consuming when non-interactive batch processing was the only alternative. Given the increasing availability of micro-computers and their suitability to interactive computing, it is now possible to quickly assess the effect of various loading histories, material properties, and design details on section behaviour. It is therefore possible to perform several analyses of a section to define its mechanical response in about the same time it would take to perform simplistic and approximate hand calculations.

The fiber model can be extended in a number of ways to describe the behaviour of a structural member [3,4,7,10]. Hence it can form the basis for a general frame analysis program. Such a program would be capable of taking into consideration the various material and section phenomena that the fiber model can represent. In the case of reinforced concrete columns in particular, it would be possible to consider the moment-axial load interaction which is important for predicting the response of reinforced concrete frames in the working load range where the flexural stiffnesses are very sensitive to axial load and under inelastic cyclic loading where the section behaviour is significantly more complex than usually assumed in simplified analyses. Currently available micro-computers, however, may not be suitable for such a purpose because of the limited memory capacity and relatively low computational speed.

In spite of the versatility of the fiber model, it has some significant limitations. The assumption of plane sections remaining plane may be violated because of shearing deformations or, in the case of reinforced or prestressed concrete sections, shear cracks and bond slip. Uniaxial material properties are assumed, hence changes in the cross section at large deformations due to the Poisson effect are ignored. Moreover, effective uniaxial material properties may not be adequate in certain cases due to shear and transverse confinement in reinforced concrete sections. Investigations to assess and reduce the significance of these limitations are desirable.

REFERENCES

(1) Mahin, S.A., and Bertero, V.V., "RCCOLA, a Computer Program for Reinforced Concrete Column Analysis - User's Manual and Documentation," Department of Civil Engineering, University of California, Berkeley, August 1977.

(2) Ma, S.M., Bertero, V.V., and Popov, E.P., "Experimental and Analytical Studies of the Hysteretic Behavior of Reinforced Concrete Rectangular and T-Beams," EERC Report No. 76-2, Berkeley, May 1976.

(3) Bazant, Z.P., and Bhat, P.D., "Prediction of Hysteresis of Reinforced Concrete Members," Journal of the Structural Division, ASCE, Vol. 103, No. ST1, January 1977, pp. 153-167.

(4) Petersson, H., "GENFEM-S: A Computer Program for Nonlinear Dynamic Analysis of Concrete and Steel Structures by the Finite Element Method," Chalmers University of Technology, Department of Building Construction, Gothenburg, Sweden.

(5) Chen, W.F., and Atsutu, T., *Theory of Beam Columns,* McGraw-Hill, New York, 1976.

(6) Emori, K., and Schnobrich, W.C., "Analysis of Reinforced Concrete Frame-Wall Structures for Strong Motion Earthquakes," Civil Engineering Studies, Structural Research Series No. 457, University of Illinois, Urbana, December 1978.

(7) Iding, R., Bresler, B., and Nizamuddin, Z., "Fires-RC II, A Computer Program for the Fire Response of Structures-Reinforced Concrete Frames - Revised Edition," Fires Research Group, University of California, Berkeley, July 1977.

(8) Hays, C.O., and Santhanam, T.K., "Inelastic Section Response by Tangent Stiffness," Journal of the Structural Division, ASCE, Vol. 105, No. ST7, July 1979, pp. 1241-1259.

(9) Holzer, S.M., Somers, A.E., and Bradshaw, J.C., "Finite Response of Inelastic RC Structures," Journal of the Structural Division, ASCE, Vol. 105, No. ST1, January 1979, pp. 17-33.

(10) Mark, K.M.S., and Roesset, J.M., "Nonlinear Dynamic Response of Reinforced Concrete Frames," Publication R76-38, Department of Civil Engineering, M.I.T., August 1976.

(11) Massonet, C.E., and Save, M.A., *Plastic Analysis and Design,* Vol. 1, Blaisdell Publ. Co., 1965.

(12) Gilbert, R.I., and Warner, R.F., "Tension Stiffening in Reinforced Concrete Slabs," Journal of the Structural Division, ASCE, Vol. 104, No. ST12, Proc. Paper 14211, December 1978, pp. 1885-1899.

(13) Hognestad, E., "A Study of Combined Bending and Axial Load in Reinforced Concrete Members," The Reinforced Concrete Research Council of the Engineers Foundation, Bulletin No. 1, June 1951.

(14) Hognestad, E., "Inelastic Behavior in Tests of Eccentrically-loaded Short Reinforced Concrete Columns," The Reinforced Concrete Research Council of the Engineers Foundation, Bulletin No. 2, October 1952.

(15) Sheikh, S.A., and Uzumeri, S.M., "Strength and Ductility of Tied Concrete Columns,"

Proceedings, ASCE, Vol. 106, No. ST5, May 1980., pp. 1079-1102.

(16) Kent, D.C., and Park, R., "Flexural Members with Confined Concrete," Journal of the Structural Division, ASCE, Vol. 97, No. ST7, July 1971, pp. 1969-1990.

(17) Scott, B.D., Park, R., and Priestly, M.J.N., "Stress-Strain Behaviour of Concrete Confined by Overlapping Hoops at Low and High Strain Rates," Journal of the ACI, No. 1, Vol. 79, January-February 1982, pp.13-27.

(18) Vallenas, J., Bertero, V.V., and Popov, E.P., "Concrete Confined by Rectangular Hoops and Subjected to Axial Loads," Report No. UCB/EERC-77/13, Earthquake Engineering Research Center, University of California, Berkeley, August 1977.

(19) Sheikh, S.A., and Uzumeri, S.M., "Analytical Model for Concrete Confinement in Tied Columns," Journal of the Structural Division, ASCE, Vol. 108, No. ST12, December 1982, pp. 2703-2722.

(20) Blakeley, R.W.G., and Park, R., "Prestressed Concrete Sections with Cyclic Flexure," Journal of the Structural Division, ASCE, Vol. 99, No. ST8, August 1973, pp. 1717-1742.

(21) Kent, D.C., and Park, R., "Cyclic Load Behavior of Reinforcing Steel," *Strain* (Journal of the British Society for Strain Measurement), Vol. 9, No. 3, July 1973, pp. 98-103.

(22) Kent, D.C., "Inelastic Behaviour of Reinforced Concrete Members with Cyclic Loading," Ph.D. Thesis, University of Canterbury, Christchurch, New Zealand 1969.

(23) Park, R., and Paulay, T., *Reinforced Concrete Structures,* Wiley-Interscience, 1975, pp. 254-256.

(24) Conte and deBoor, *Elementary Numerical Analysis - An Algorithmic Approach,* McGraw-Hill, 1980.

(25) Bresler, B., and Gilbert, P.H., "Tie Requirements for Reinforced Concrete Columns," Journal of the ACI, No. 5, Vol. 58, November 1961, pp. 555-570.

(26) Dahlquist, G., and Björck, A., *Numerical Methods,* Prentice-Hall, 1974.

(27) Building Code Requirements for Reinforced Concrete, ACI 318-71, American Concerete Institute, 1971.

(28) Warwaruk, J., "Strength in Flexure of Bonded and Unbonded Prestressed Concrete Beams," Civil Engineering Studies, Structural Research Series No. 138, University of Illinois, August 1967.

(29) Bolong, Z., Mingshun, W., and Kunlian, Z., "A Study of the Hysteretic Curve of Reinforced Concrete Members Under Cyclic Loading," 7th. World Conference on Earthquake Engineering, Vol. 6, Istanbul, 1981.

(30) Lee, L.H.N., "Inelastic Behaviour of Reinforced Concrete Members Subjected to Short-time Static Loads," Proceedings ASCE Journal, Vol. 79, Separate No. 286, September 1953.

(31) Stanton, J.F., and McNiven, H.D., "The development of a Mathematical Model to Predict the Flexural Response of Reinforced Concrete Beams to Cyclic Loads, Using System Identification," EERC Report No. 79-2, Berkeley, January 1979.

(32) Burns, N.H., and Lin, T.Y., *Design of Prestressed Concrete Structures,* John Wiley and Sons, 3rd. Edition, 1981.

(33) Microsoft Corporation, 10700 Northup Way, Bellevue, Wash. 98004.

(34) Digital Research, CP/M 2.2 Operating System, "User Reference Manual," Morrow Designs, P.O.Box 579, Pacific Grove, Calif. 93950.

(35) Maxtek, Inc., 2908 Oregon Court, Torrance, Calif. 90503.

(36) Lifeboat Associates, 1651 Third Avenue, New York, N.Y. 10028.

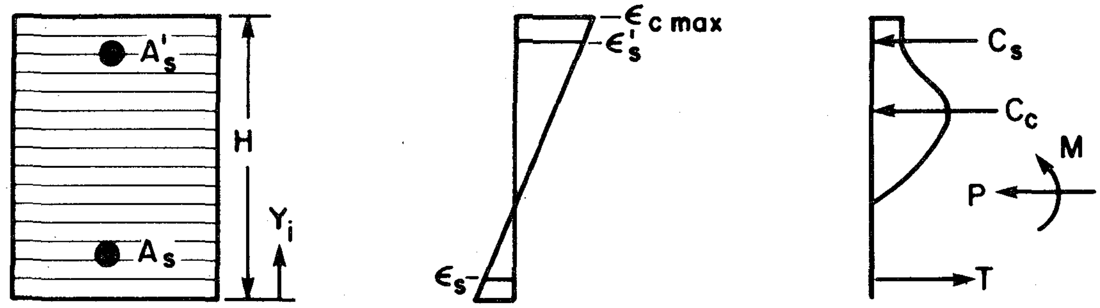

(a) Section idealization

(b) Strain distribution

(c) Stress distribution and force resultants

Fig. 2.1 The fiber model

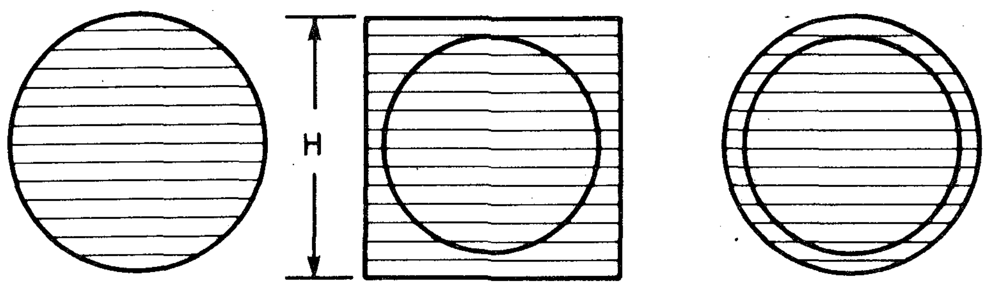

Fig. 2.2 Automatically generated sections

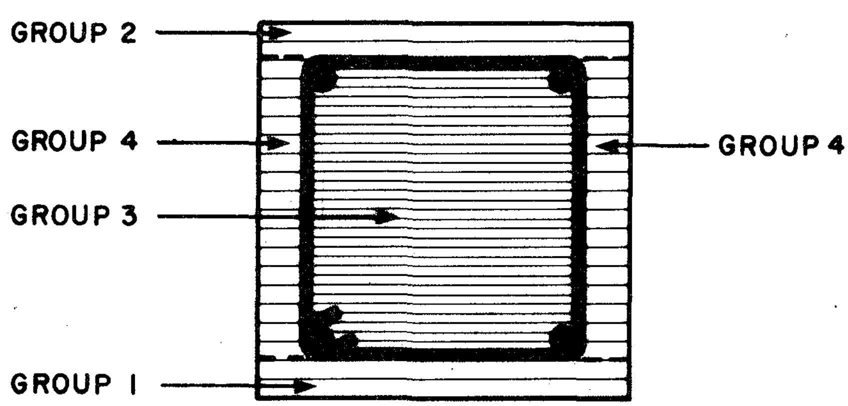

Fig. 2.3 Groups of layers in a typical section

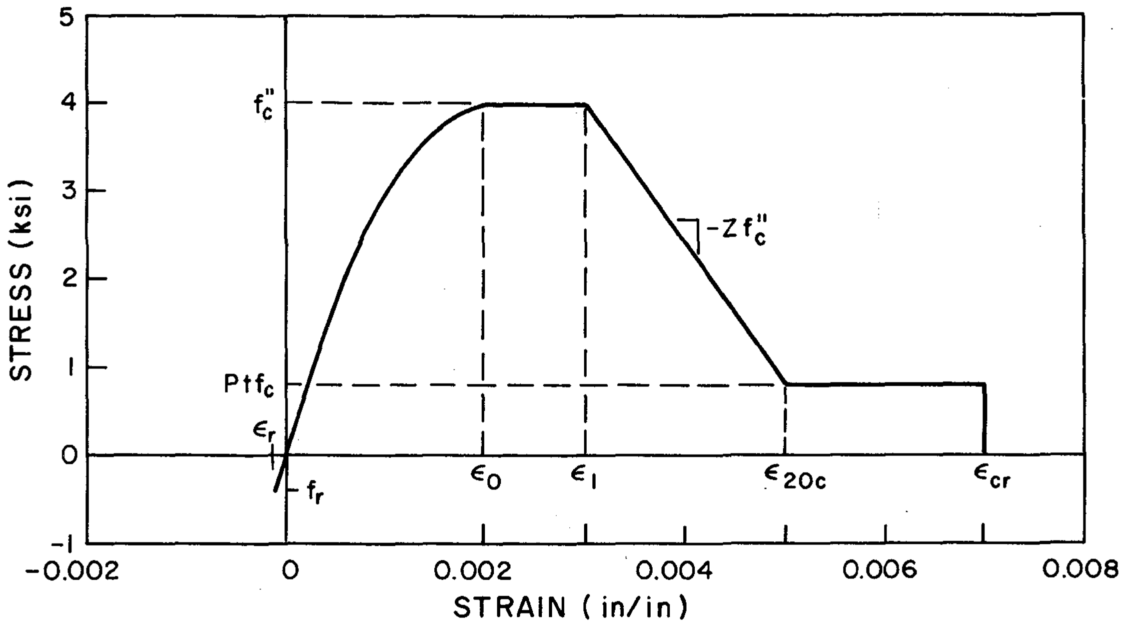

Fig. 2.4 Basic concrete model used (after Sheikh and Uzumeri)

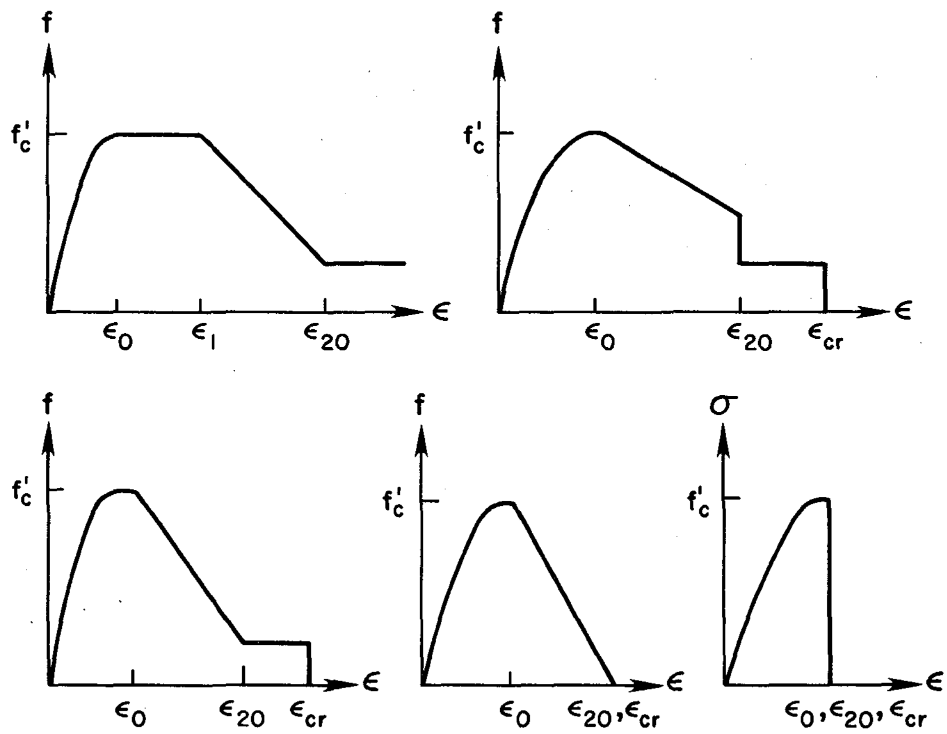

Fig. 2.5 Possible concrete models obtainable using basic model

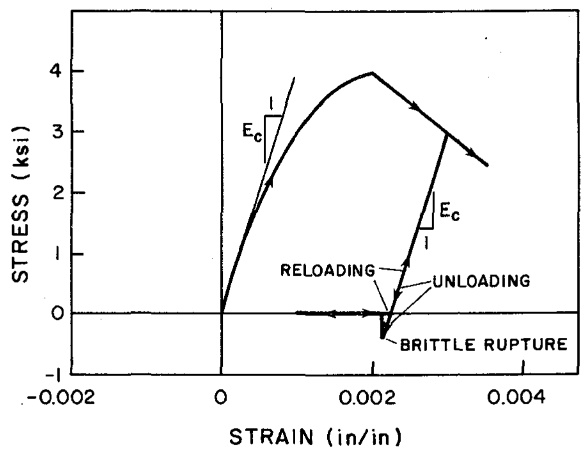

Fig. 2.6 Concrete model : unloading at E_c and reloading behaviour

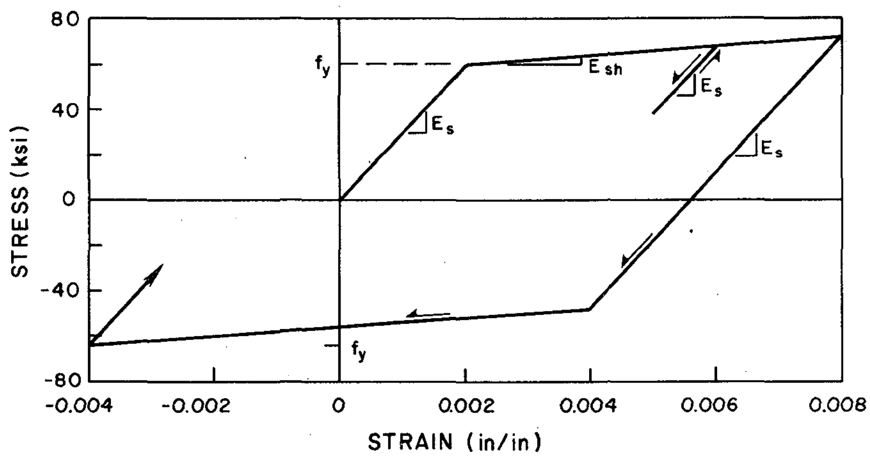

Fig. 2.7 Bilinear steel model

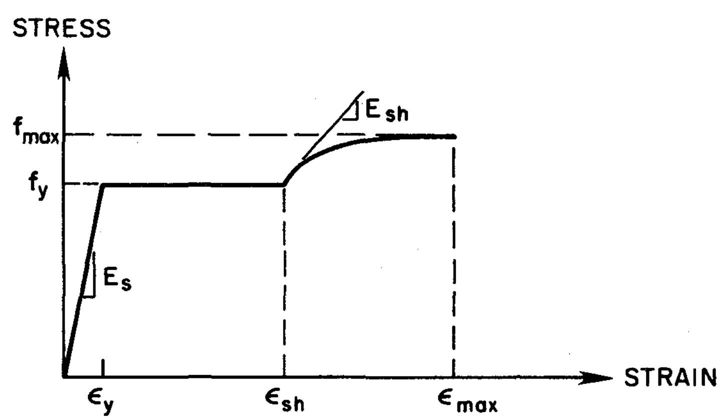

Fig. 2.8 Input parameters for the cubic and Ramberg-Osgood models

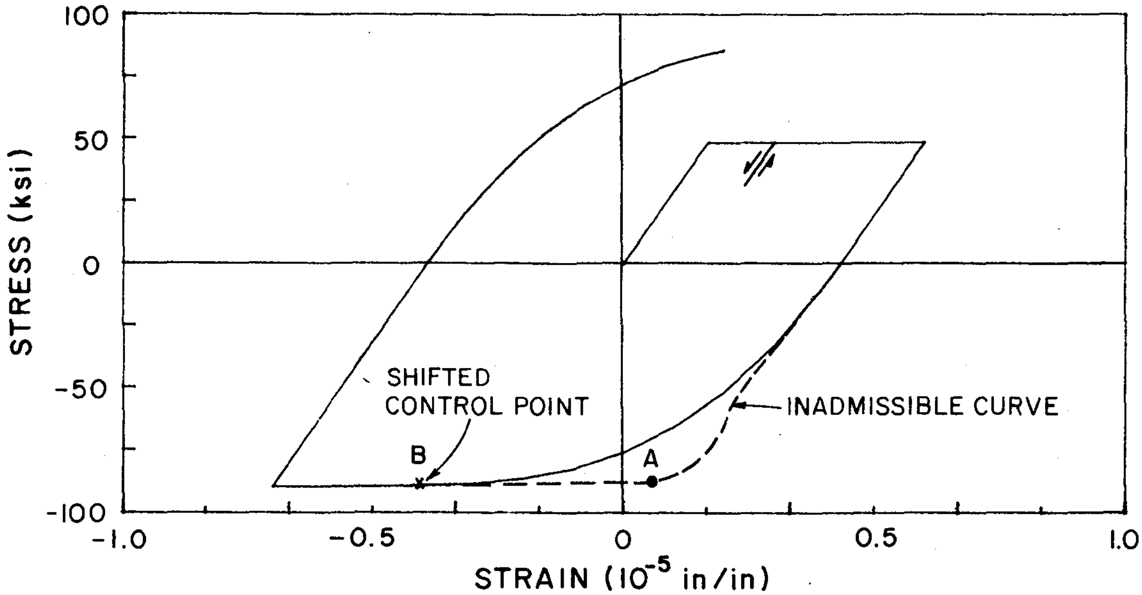

(a) Small strain cycles with shifting to ensure a smooth curve

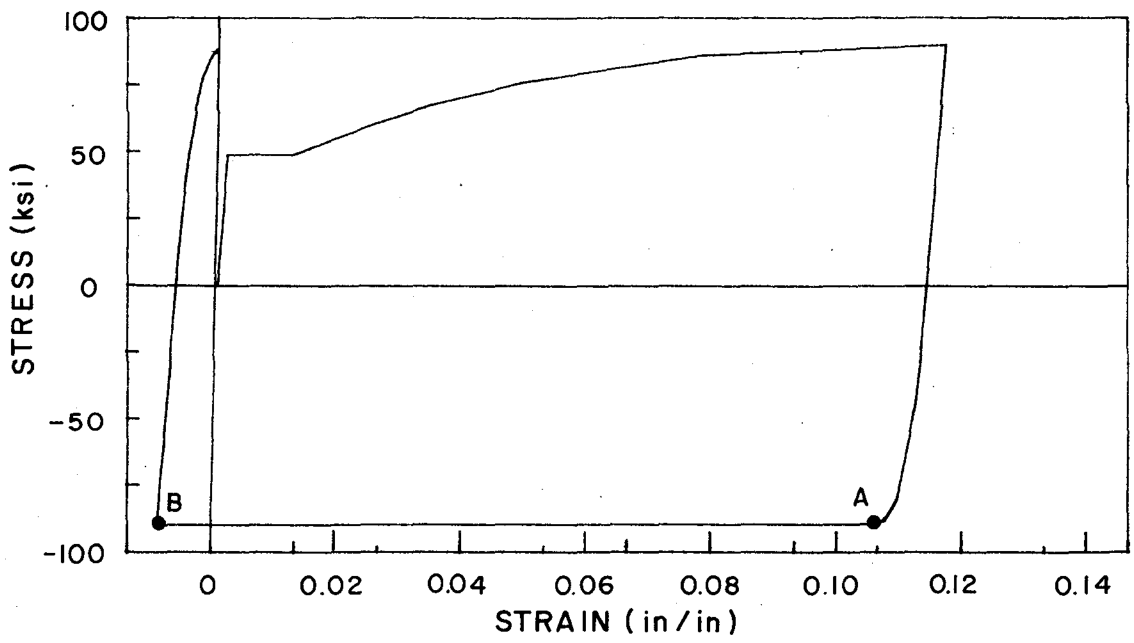

(b) Large strain cycles exhibiting flat portion

Fig. 2.9 Behaviour of the cubic steel model

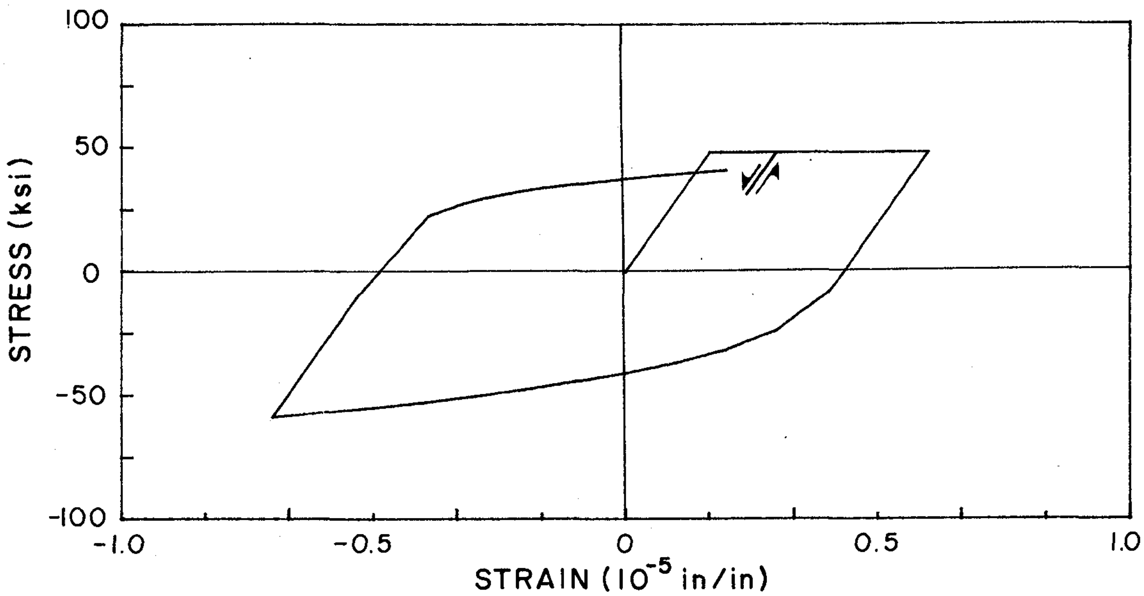

(a) Small strain cycles

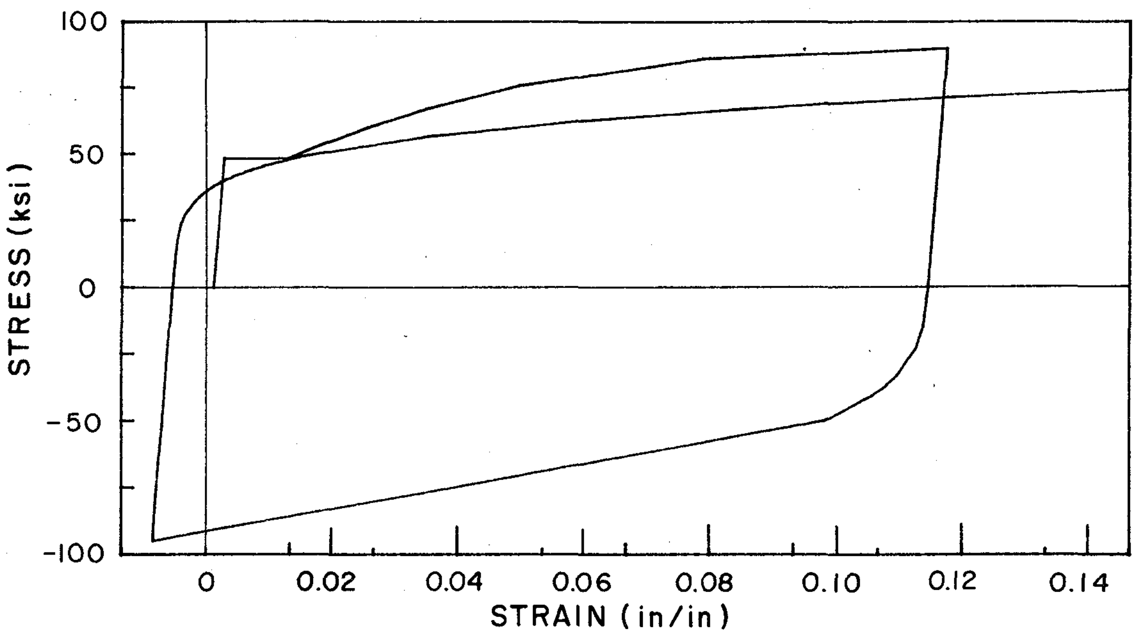

(b) Large strain cycles

Fig. 2.10 Behaviour of the Ramberg-Osgood steel model

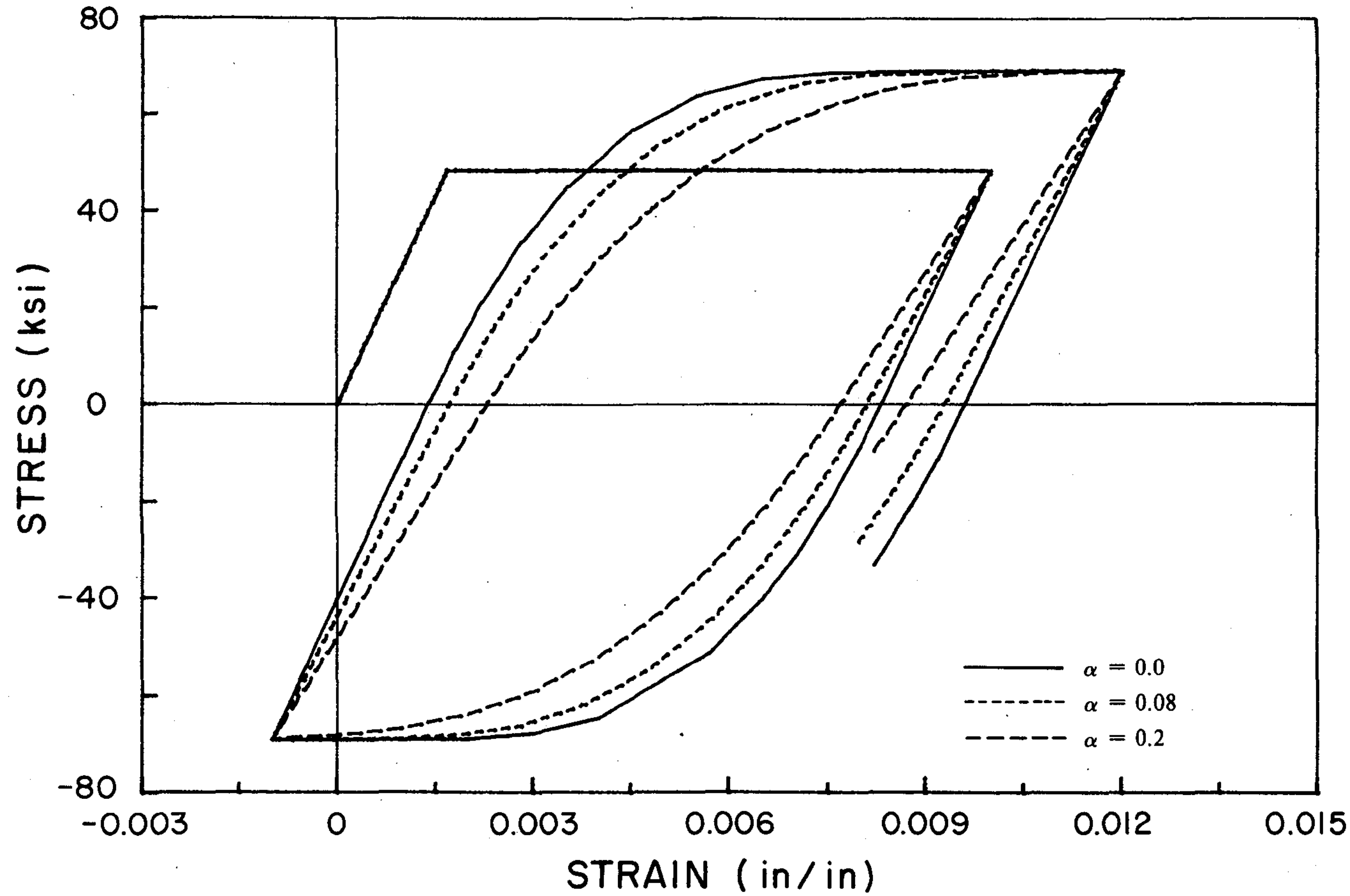

Fig. 2.11 Cubic steel model behaviour for various values of α

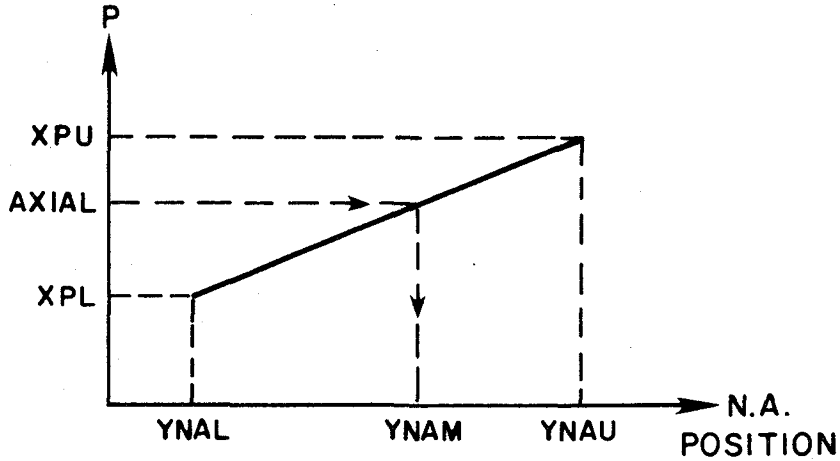

Fig. 2.12 Iteration for the position of neutral axis

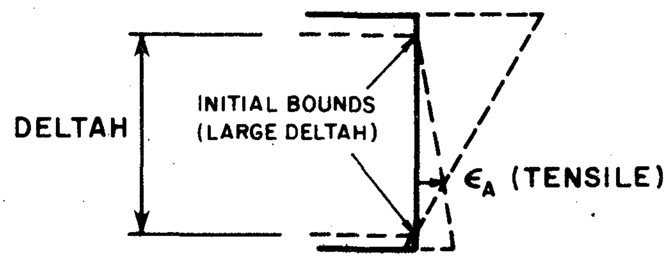

Fig. 2.13 No convergence for a large DELTAH in certain cases

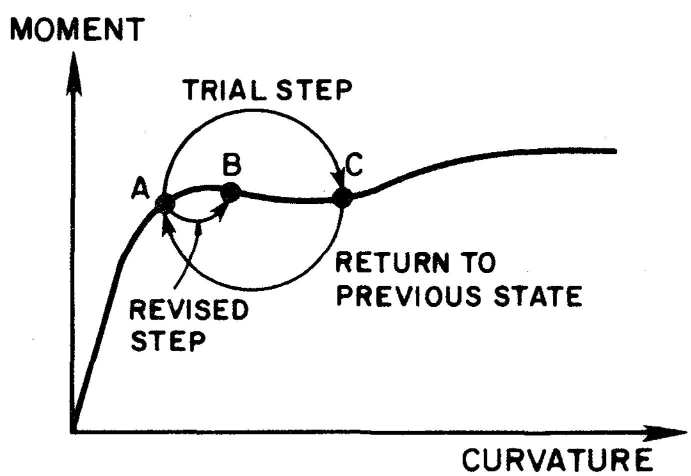

Fig. 2.14 The possibility of backing up during an analysis

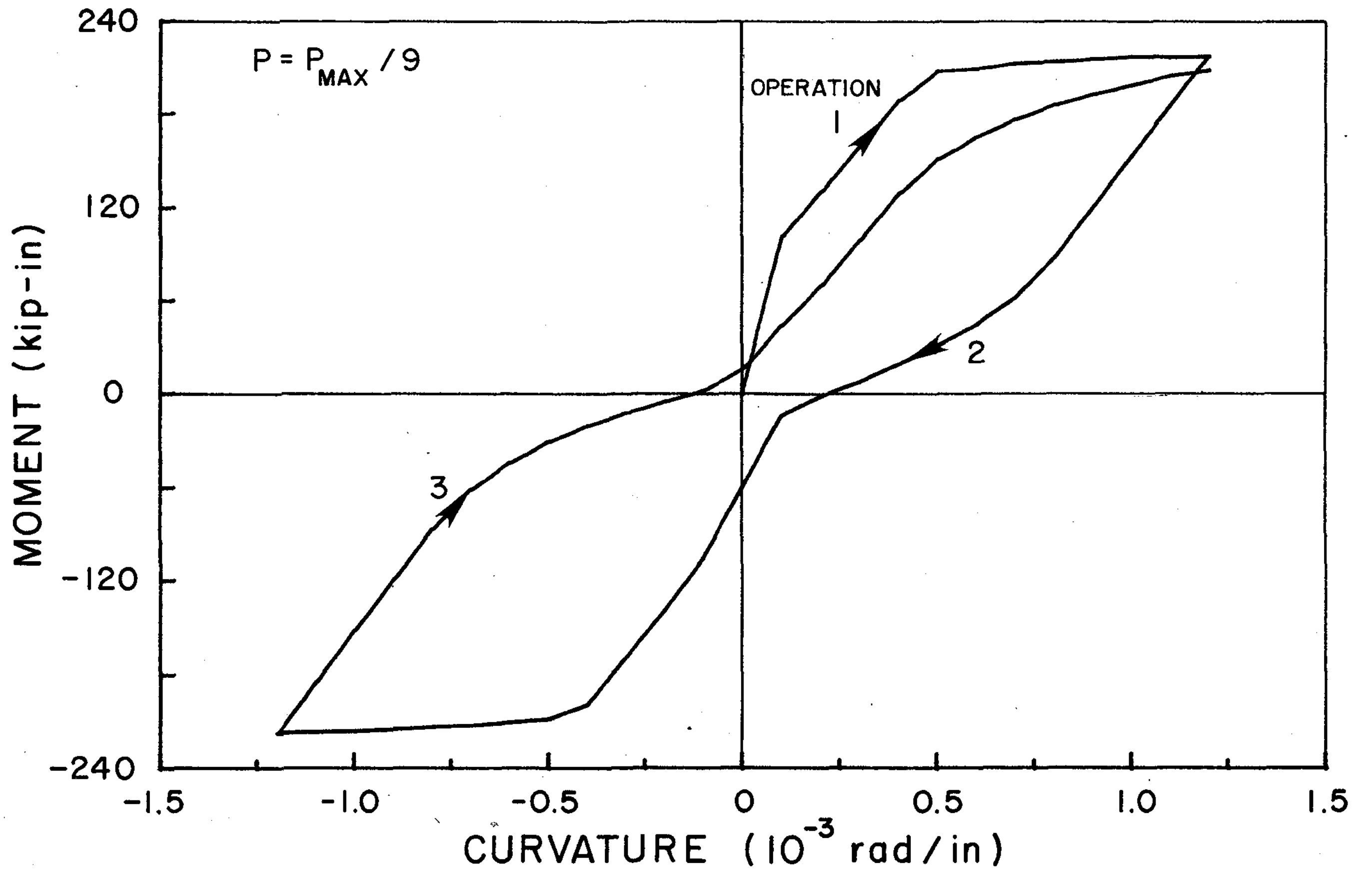

Fig. 2.15 Moment-curvature plot produced by chaining three operations

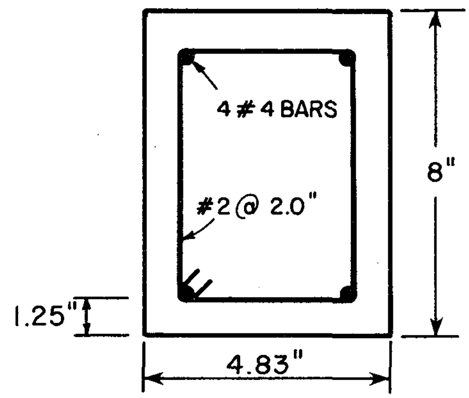

Fig. 3.1 Example reinforced concrete section

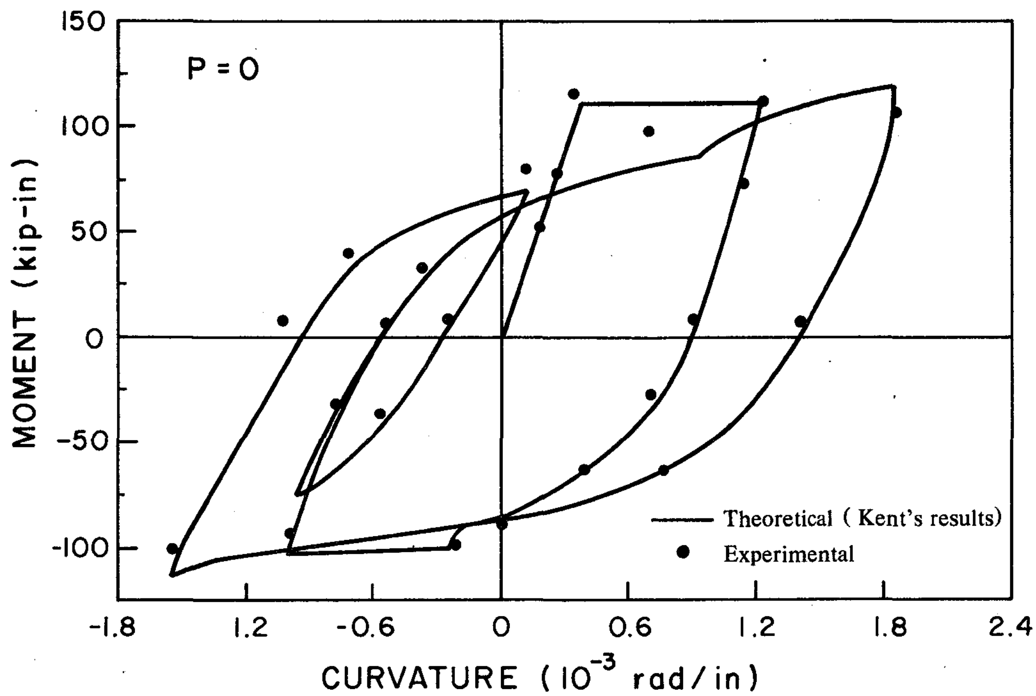

Fig. 3.2 Experimental moment-curvature plot for the example section

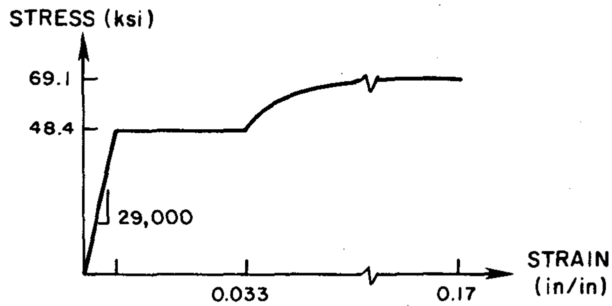

(a) Steel stress-strain relation

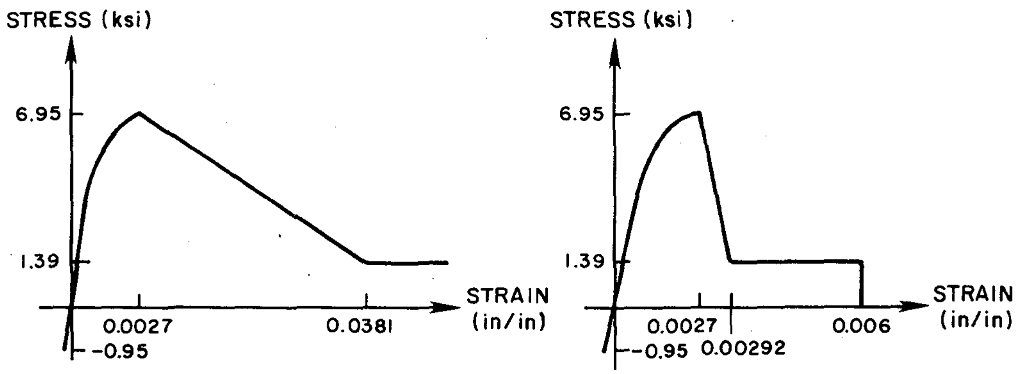

(b) Confined concrete model

(c) Unconfined concrete model

Fig. 3.3 Material models used to analyze Kent's beam # 24

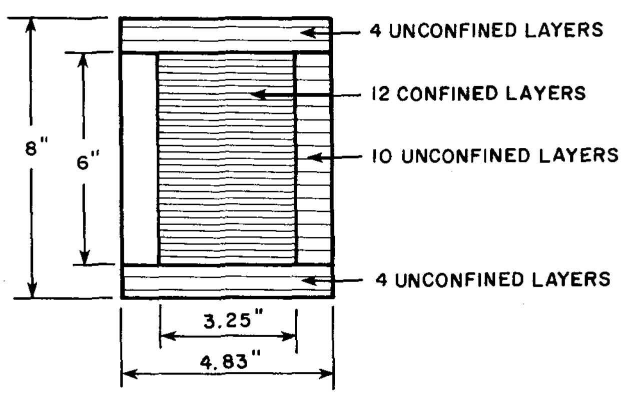

Fig. 3.4 Basic section idealization

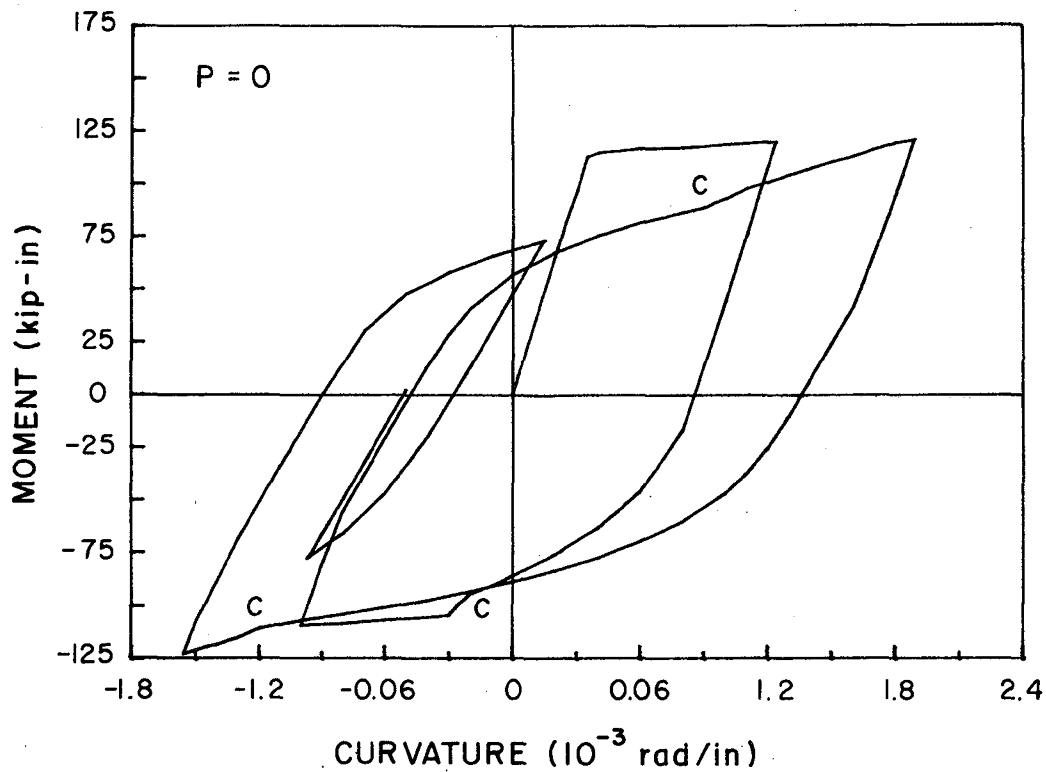

Fig. 3.5 Computed M-ϕ plot for the example section (compare with Fig. 3.2)

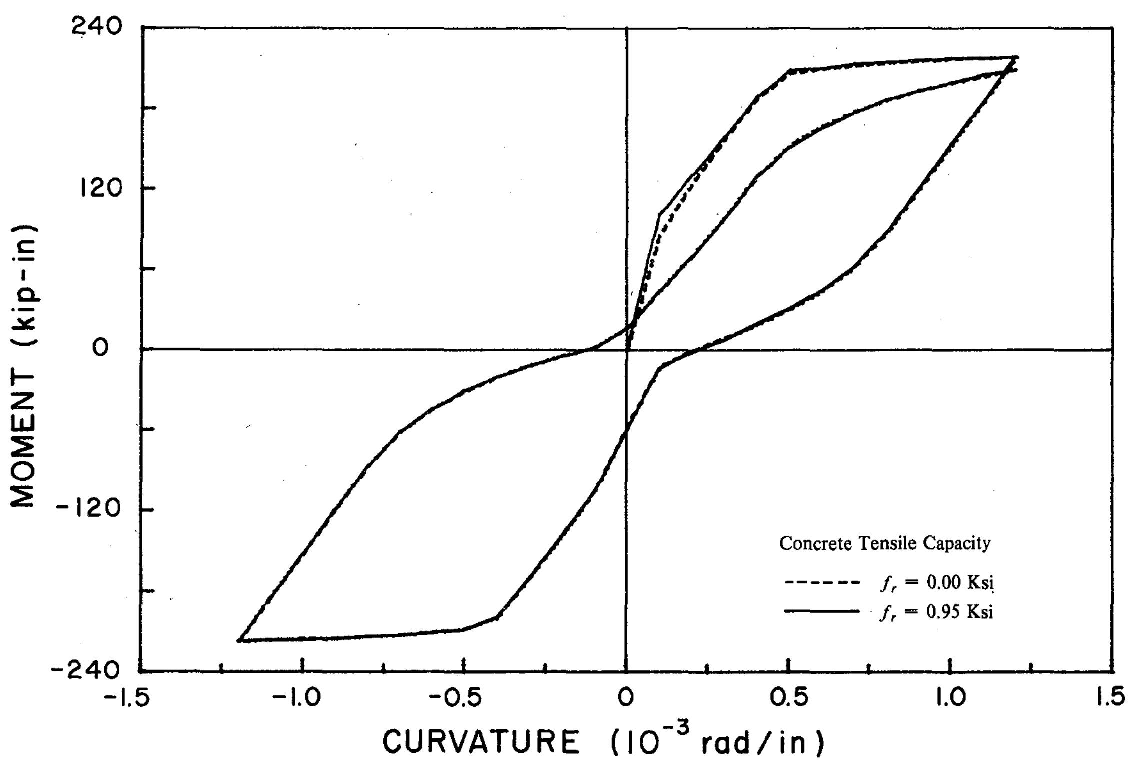

Fig. 3.6 Influence of concrete tensile capacity on cyclic section behaviour

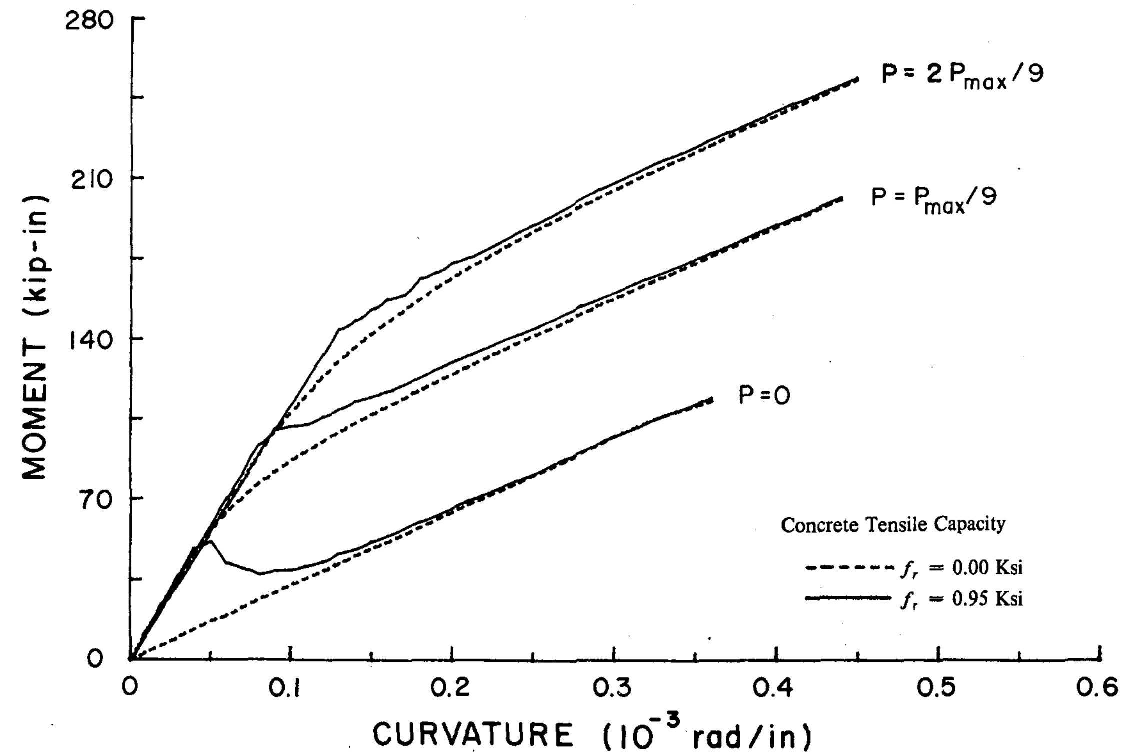

Fig. 3.7 Effect of concrete tensile capacity on section behaviour under service loads

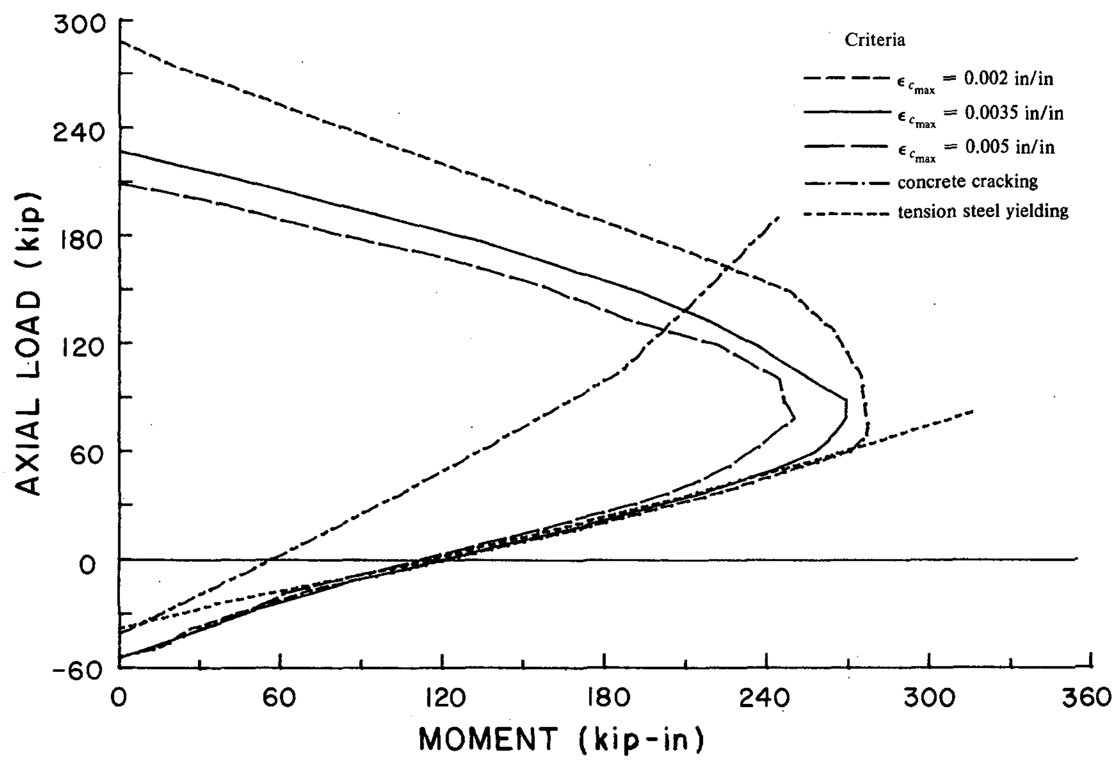

Fig. 3.8 Interaction diagrams for various criteria

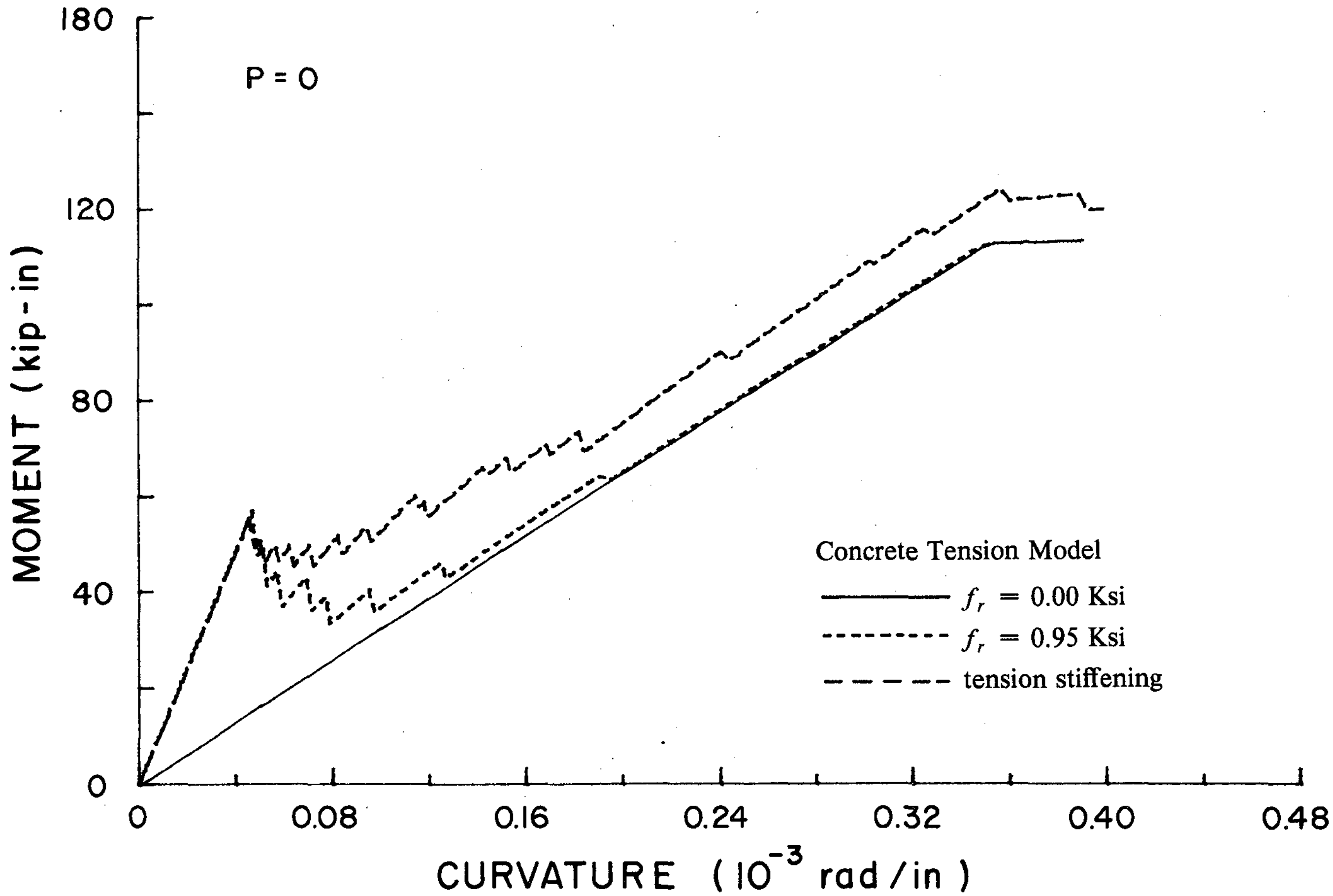

Fig. 3.9 Influence of tension stiffening on moment-average curvature

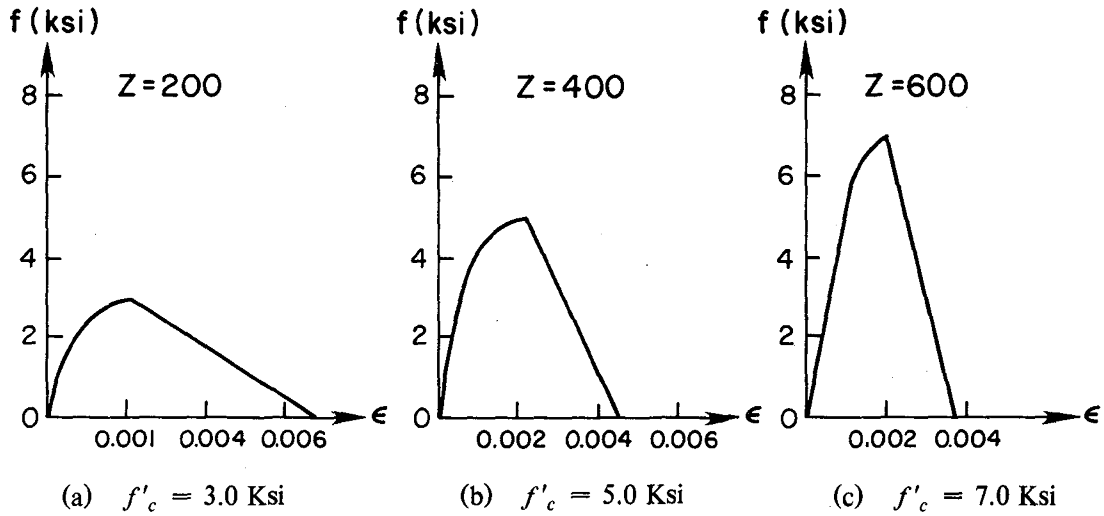

Fig. 3.10 Unconfined concrete models for different concrete strengths

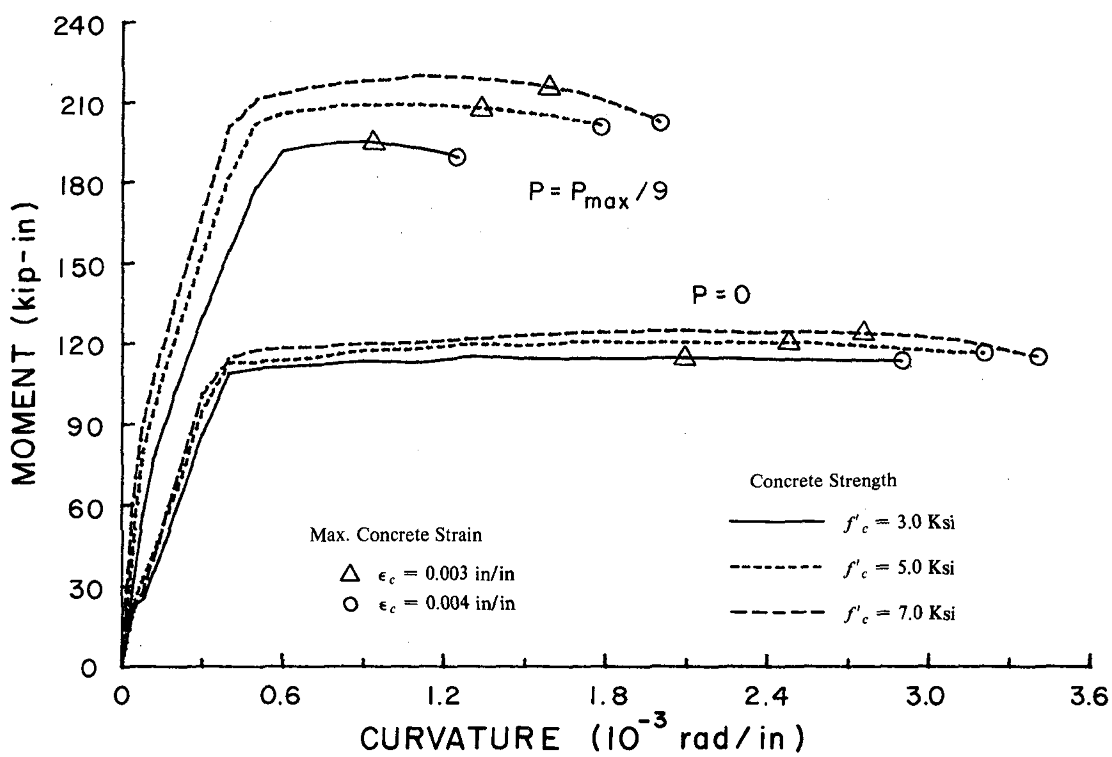

Fig. 3.11 Influence of concrete strength on section capacity and ductility

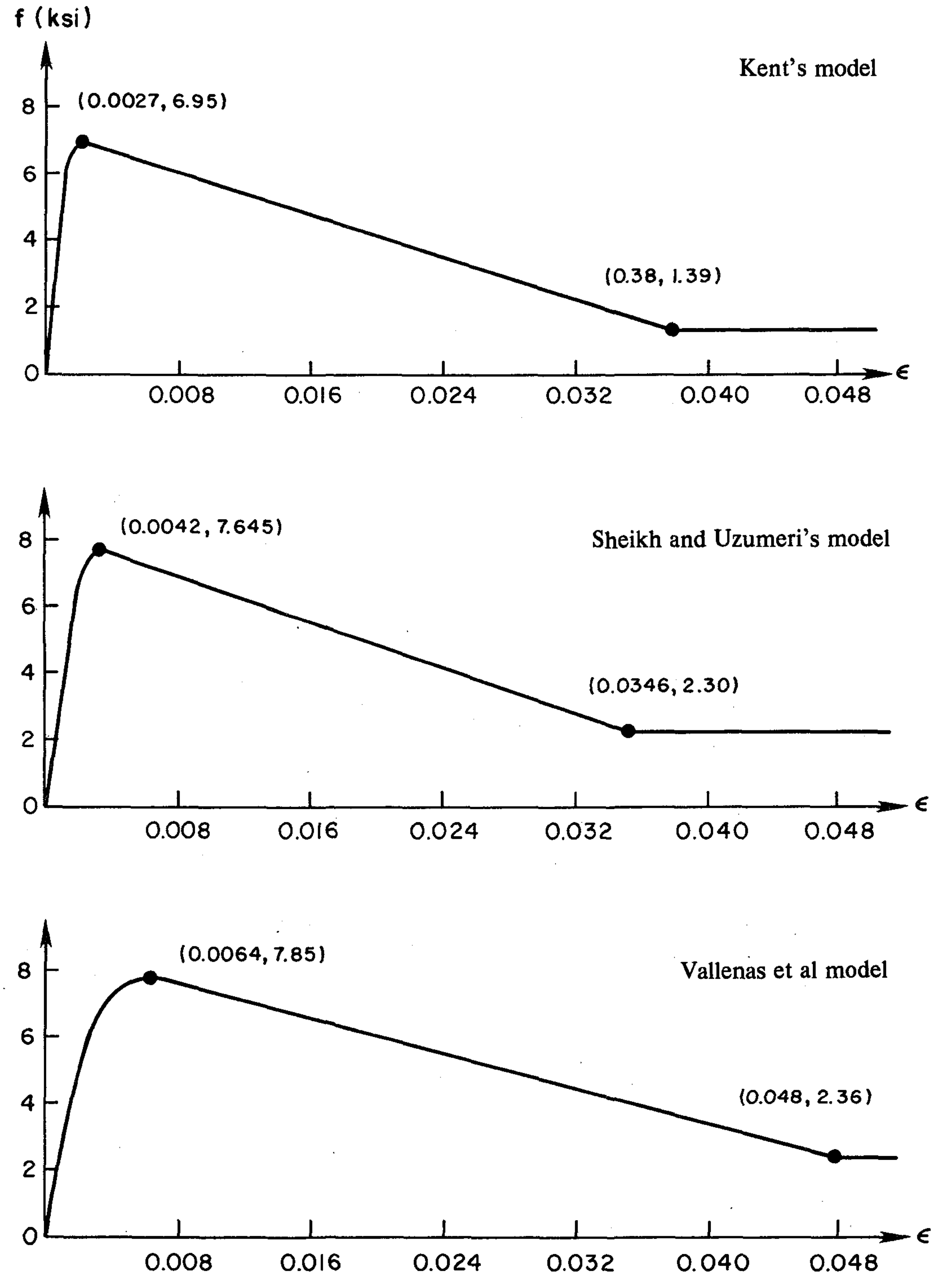

Fig. 3.12 Models for concrete behaviour for the example section

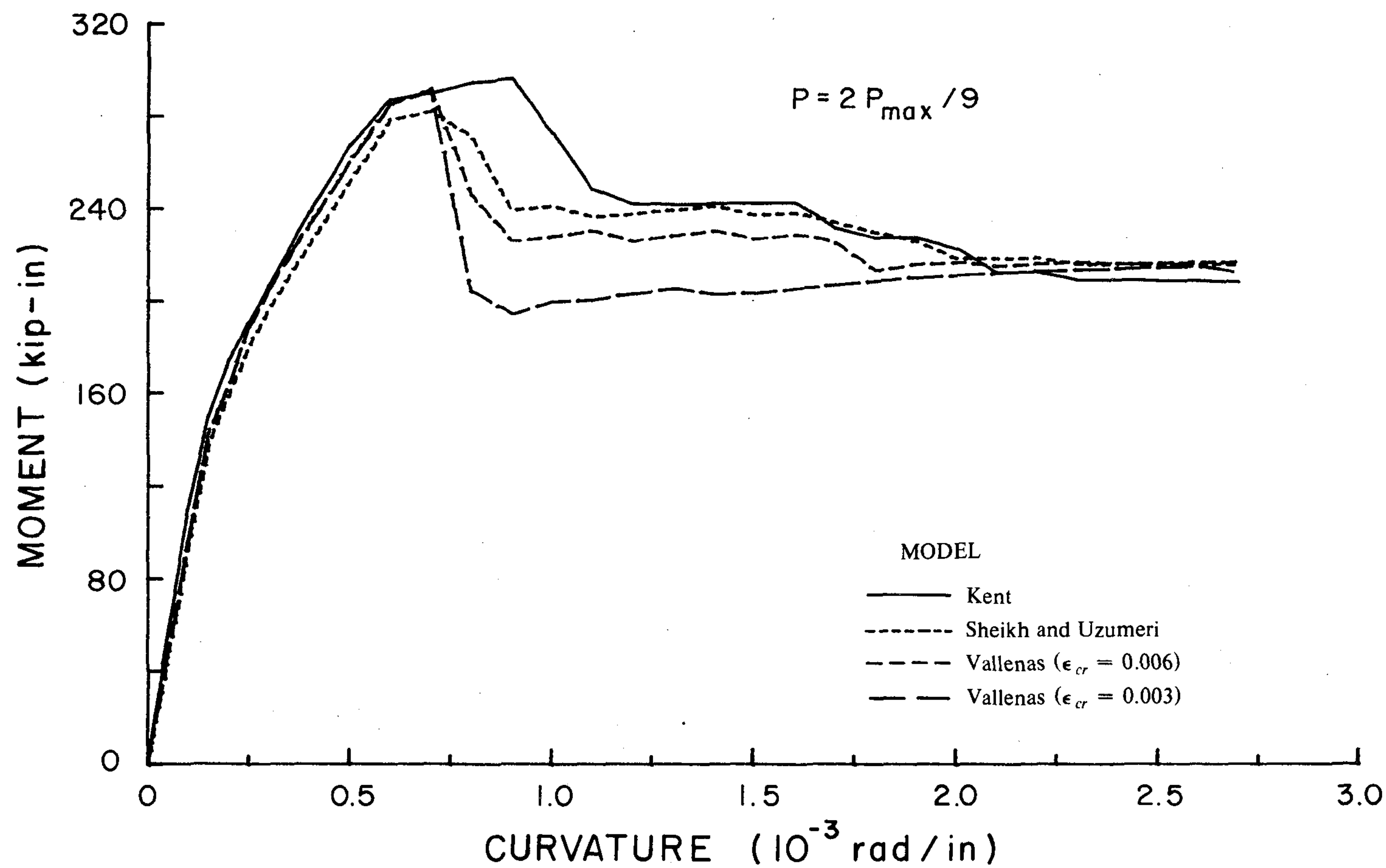

Fig. 3.13 Influence of concrete model on section behaviour

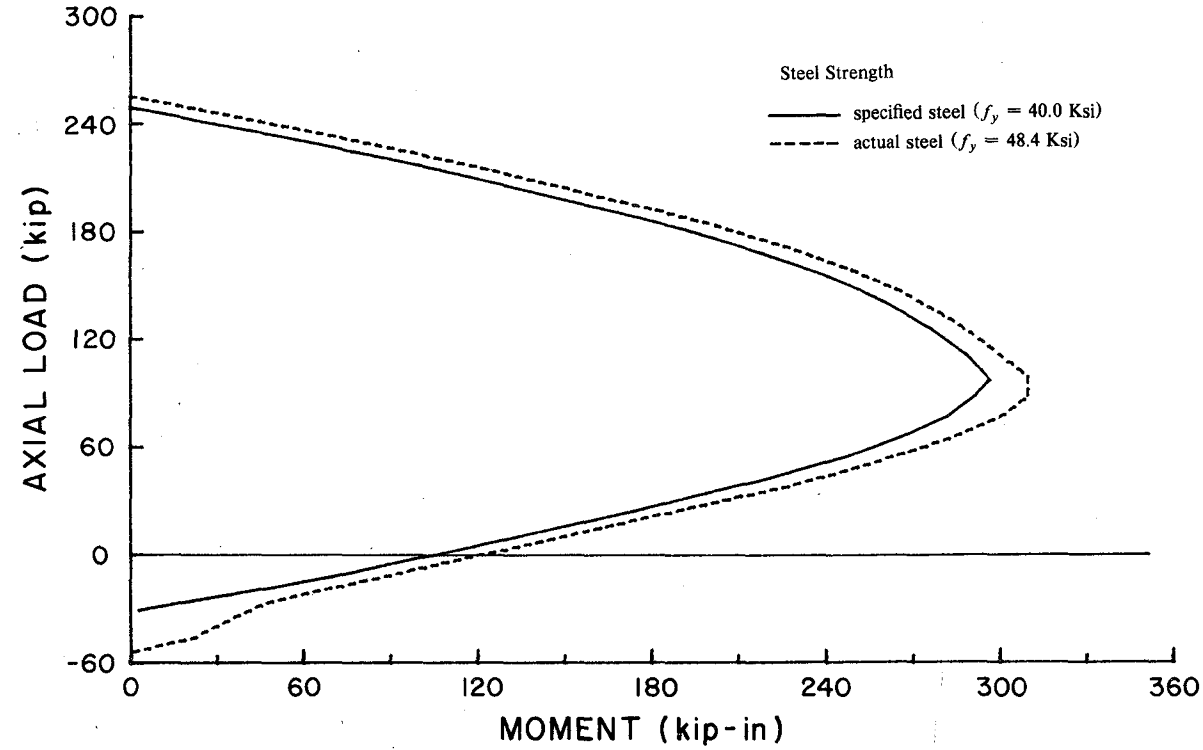

Fig. 3.14 Interaction diagrams for specified and actual steel yield stress

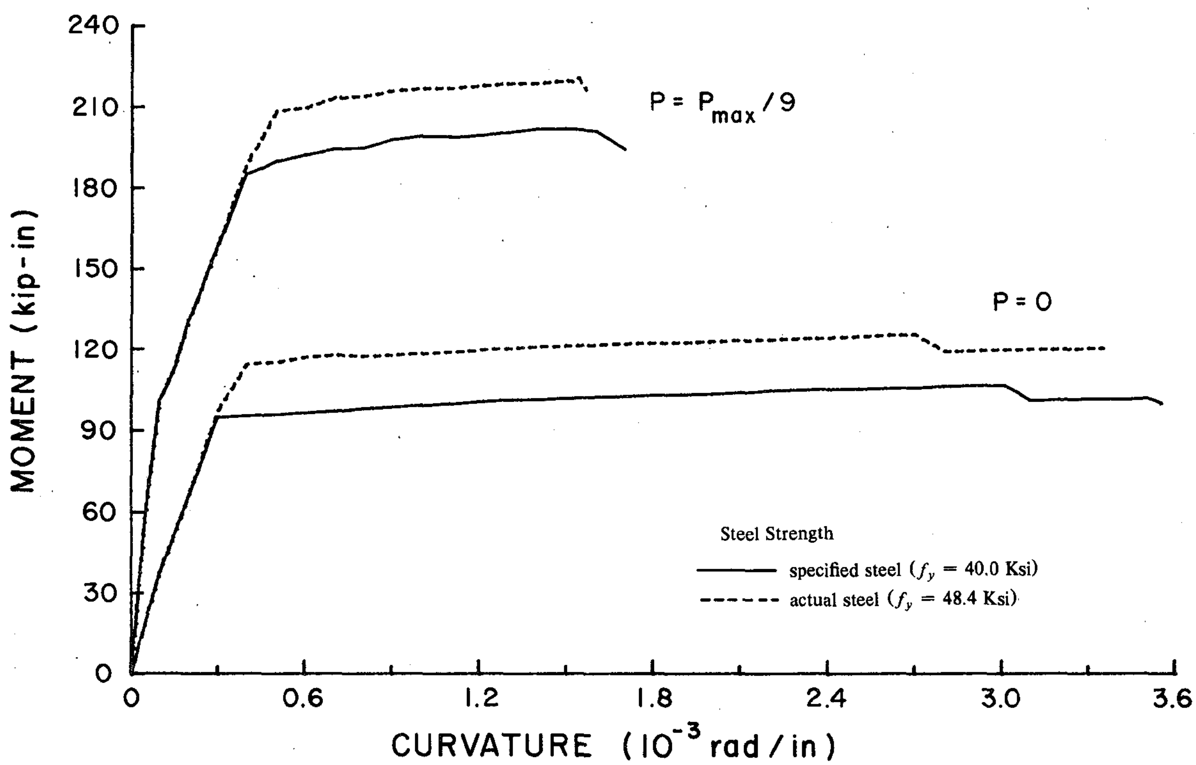

Fig. 3.15 Moment-curvature plots for specified and actual steel yield stress

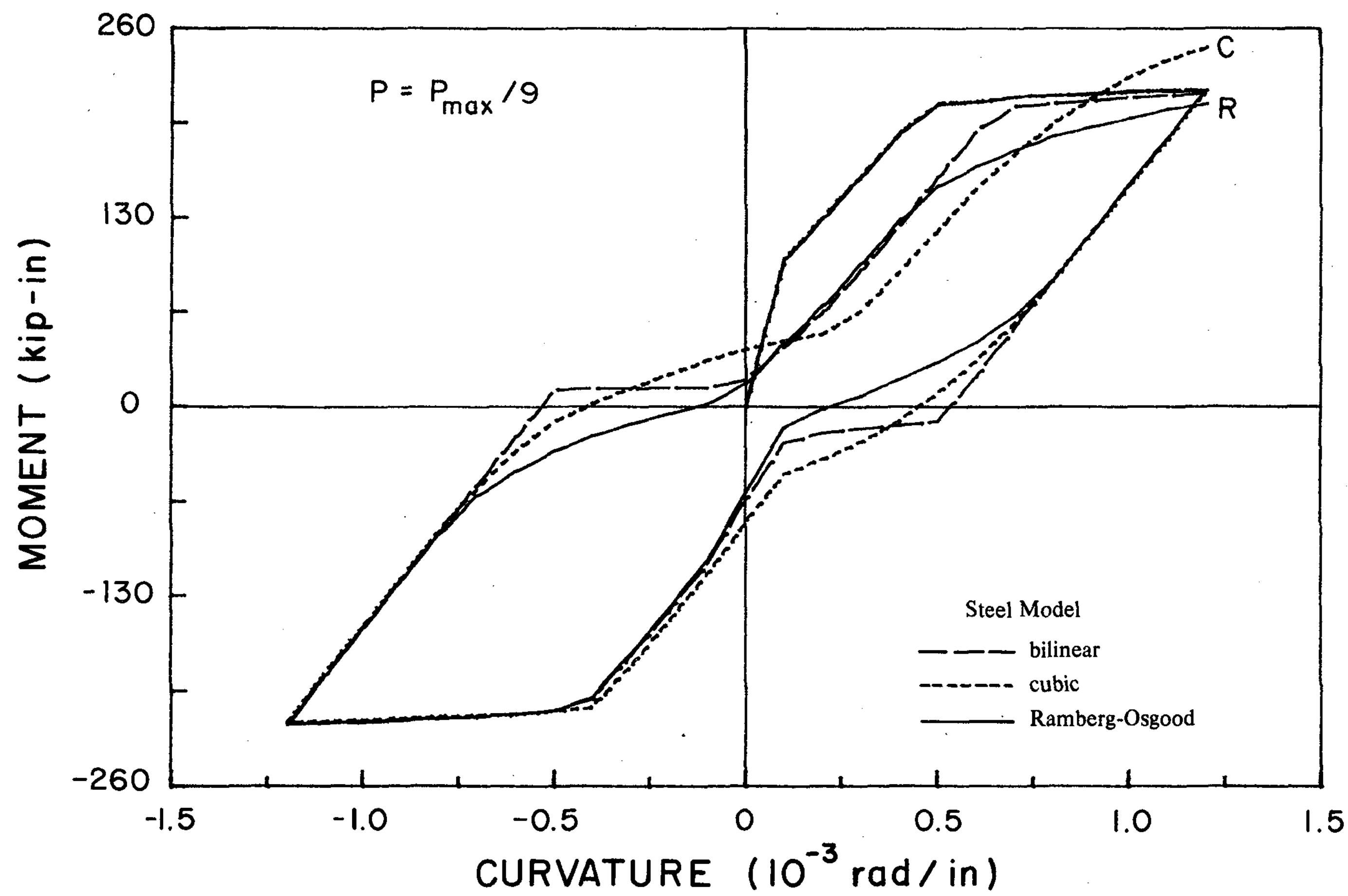

Fig. 3.16 Influence of steel model on section behaviour

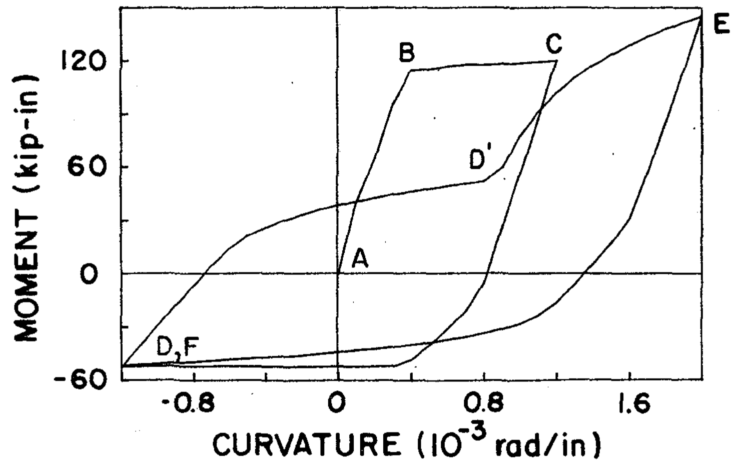

(a) Moment-curvature history showing "pinching"

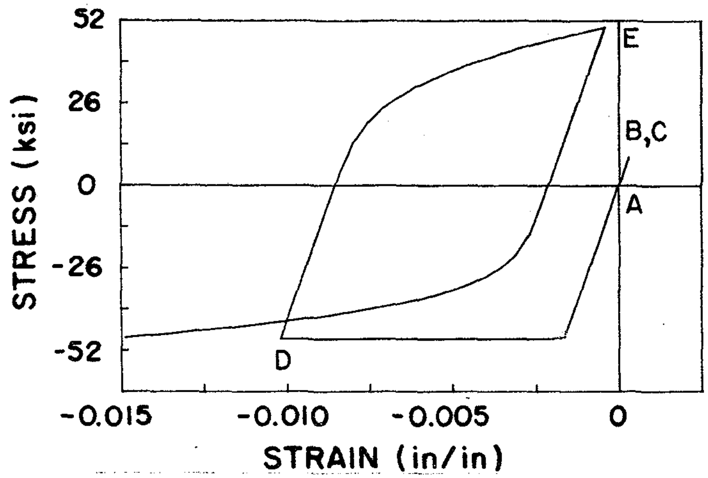

(b) Corresponding stress-strain history for top steel

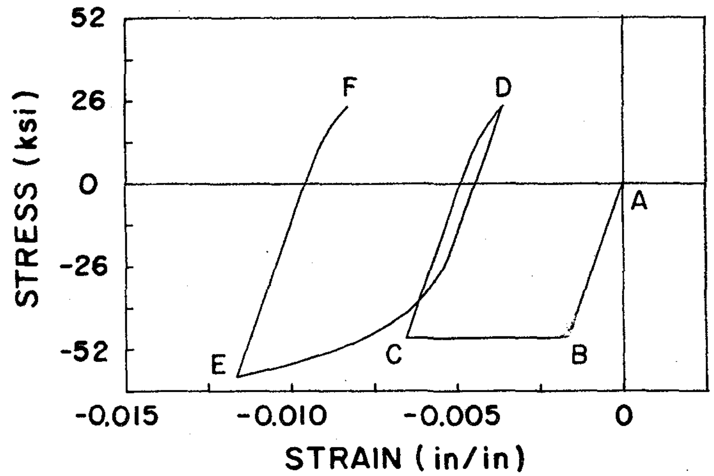

(c) Corresponding stress-strain history for bottom steel

Fig. 3.17 Influence of amount of compression steel under cyclic loading

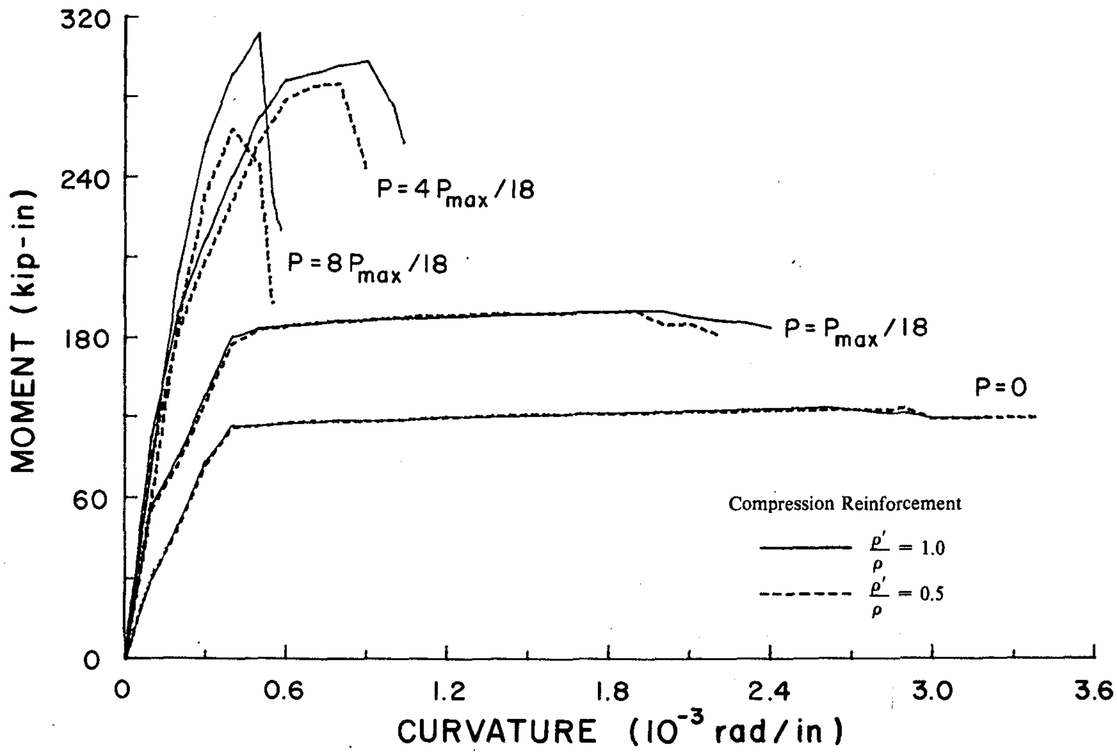

Fig 3.18 Influence of amount of compression steel for various axial loads

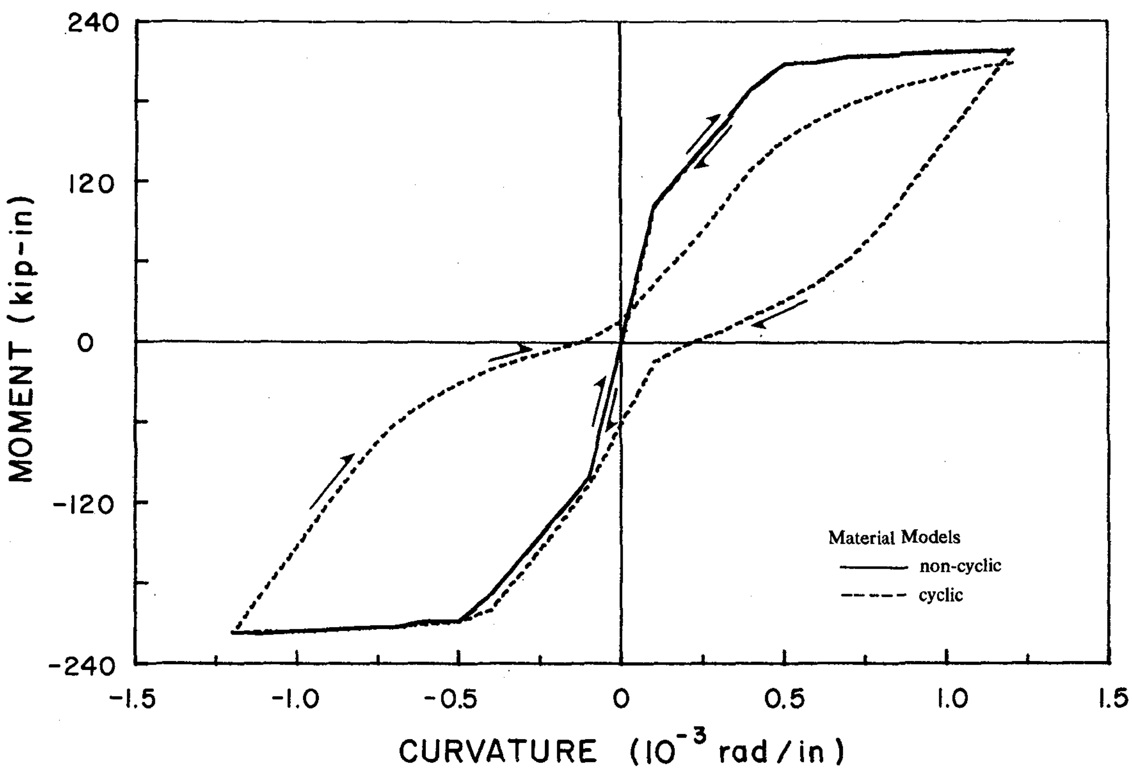

Fig 3.19 Cyclic and non-cyclic material behaviour under cyclic loading

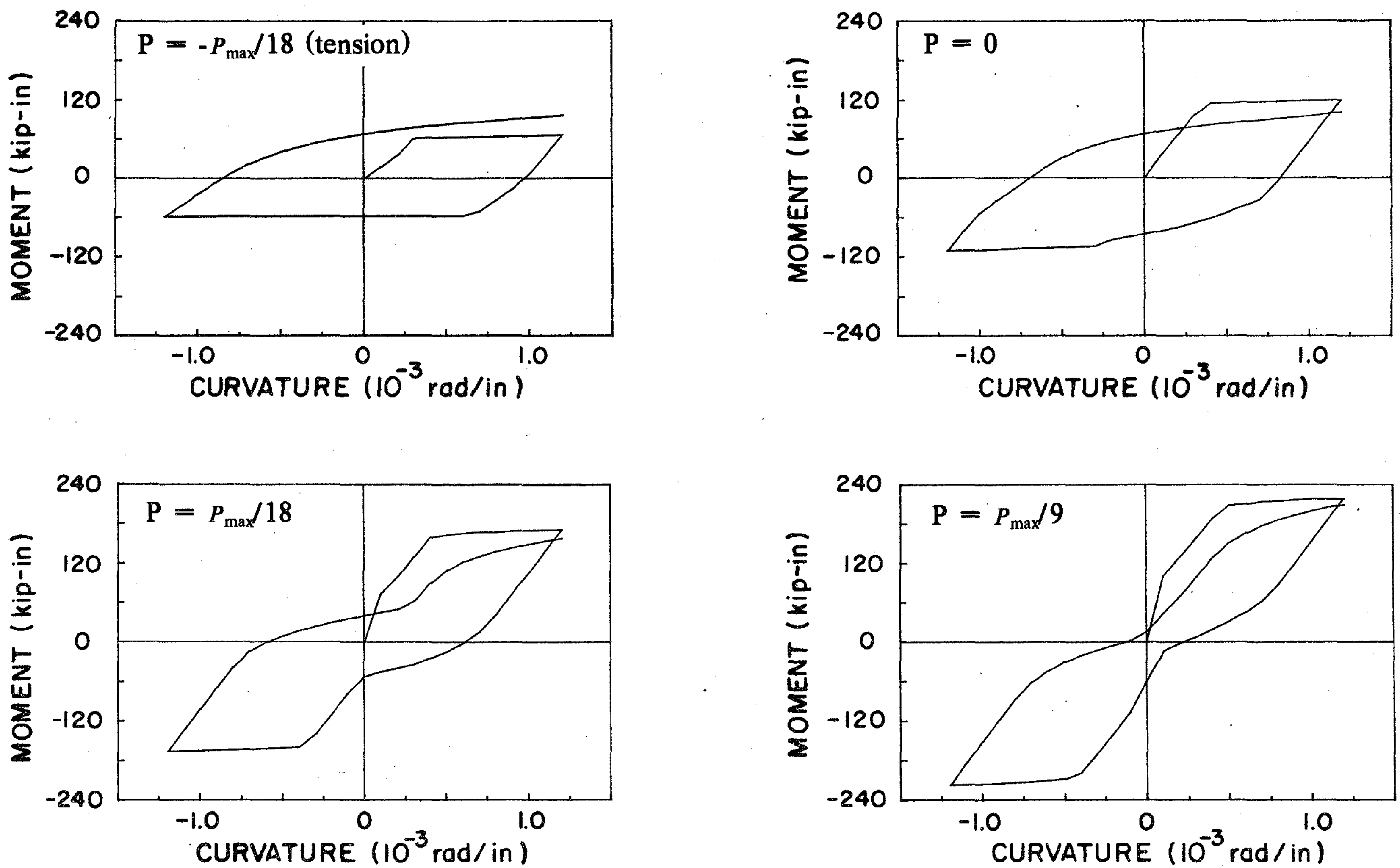

Fig 3.20 Effect of axial load on cyclic moment-curvature behaviour

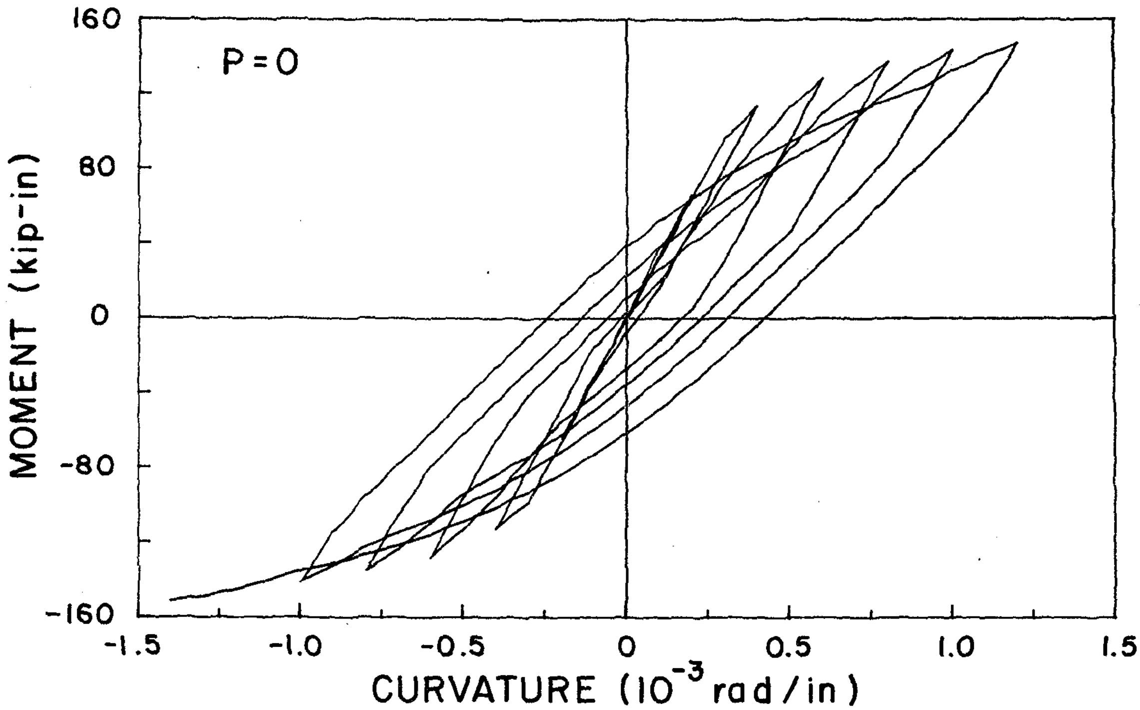

(a) Increasing amplitude curvature cycles

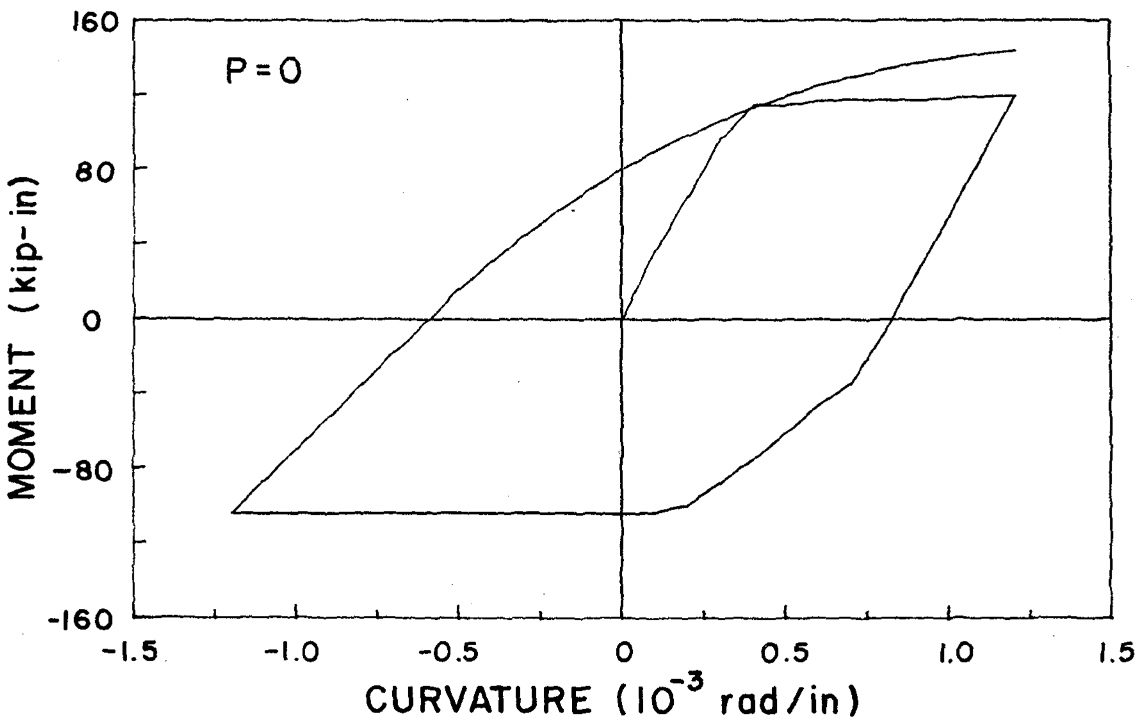

(b) Single large-amplitude cycle

Fig 3.21 Influence of curvature history on section behaviour

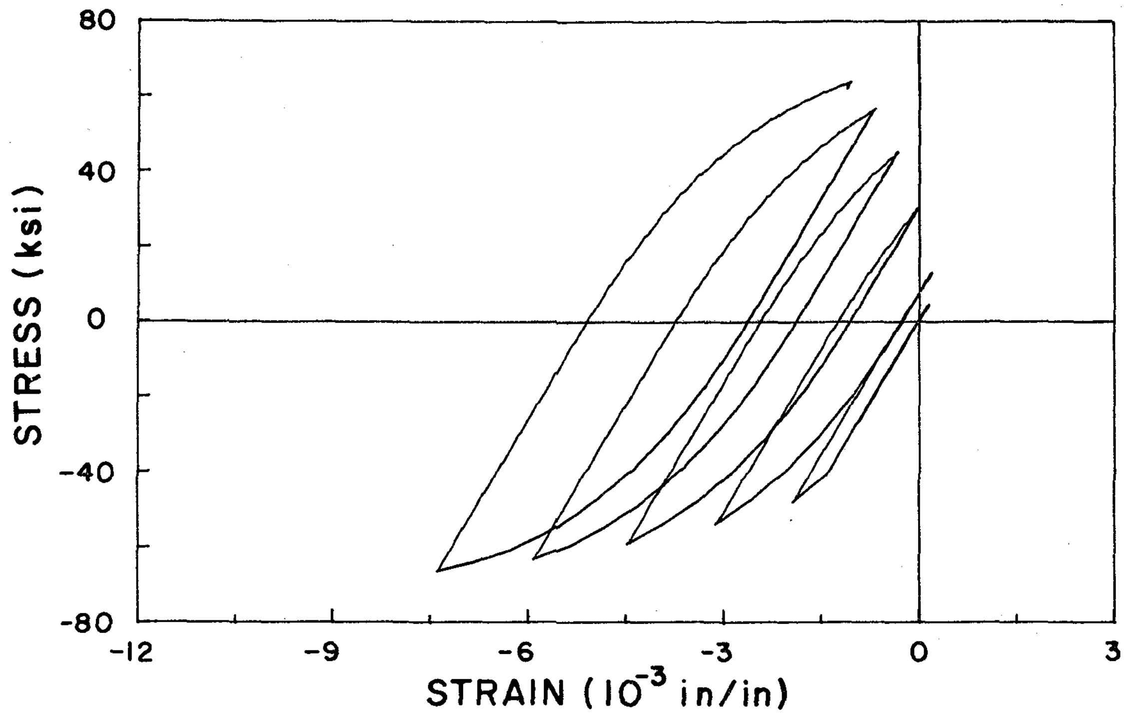

(a) σ-ϵ history corresponding to multi-cycle loading - Fig. 3.21(a)

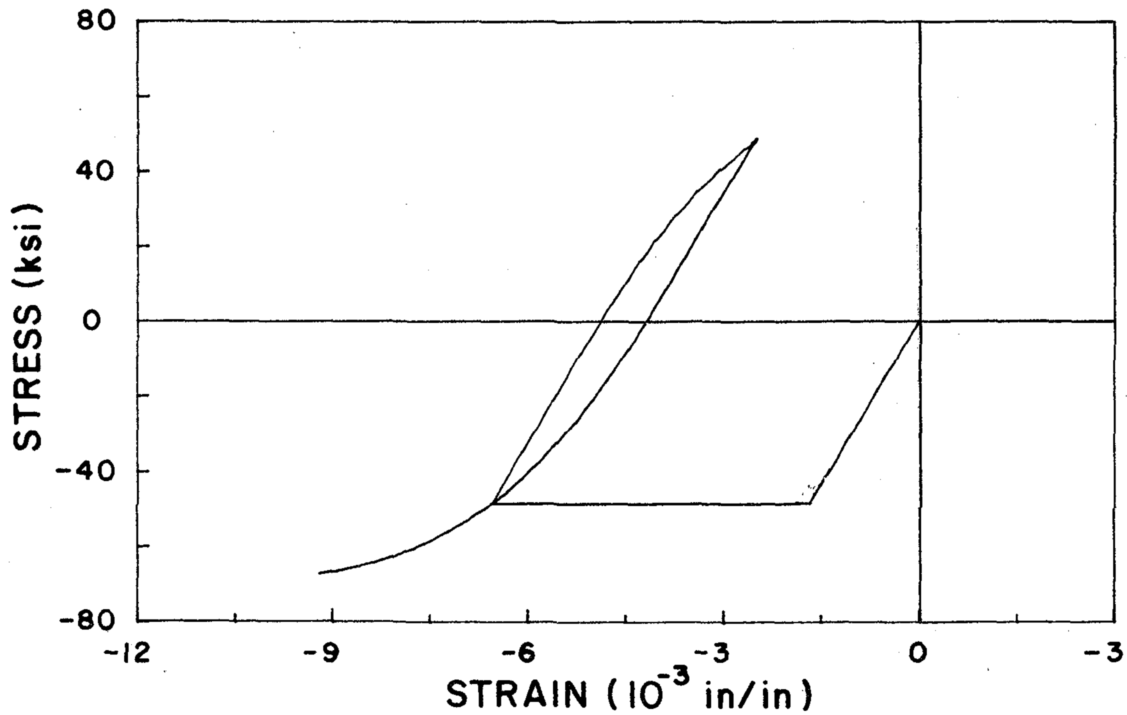

(b) σ-ϵ history corresponding to single-cycle loading - Fig. 3.21(b)

Fig 3.22 Bottom steel σ-ϵ histories for multi- and single- cycle loading

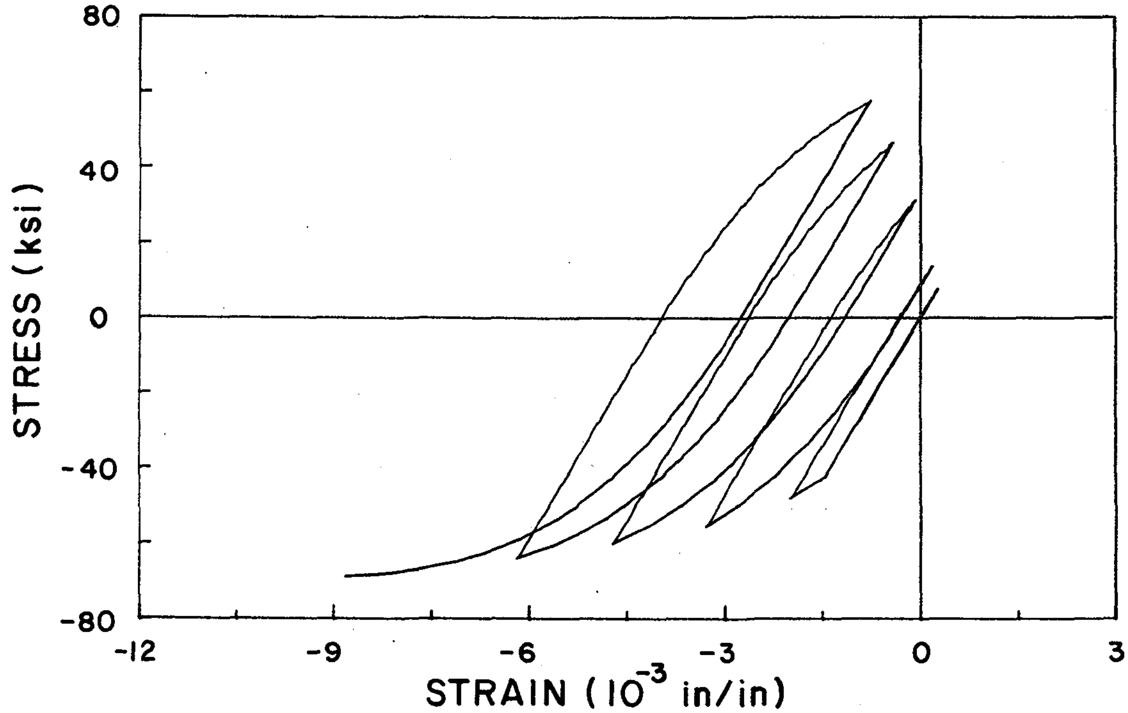

(a) σ-ϵ history corresponding to multi-cycle loading - Fig. 3.21(a)

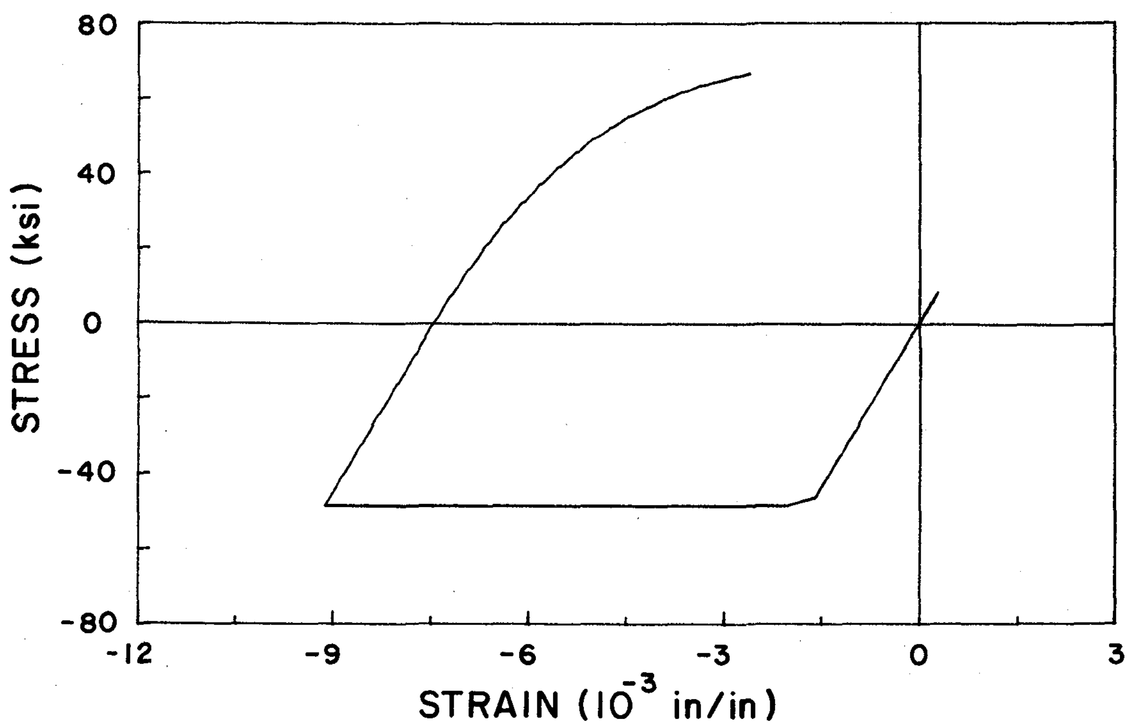

(b) σ-ϵ history corresponding to single-cycle loading - Fig. 3.21(b)

Fig. 3.23 Top steel σ-ϵ histories for multi- and single- cycle loading

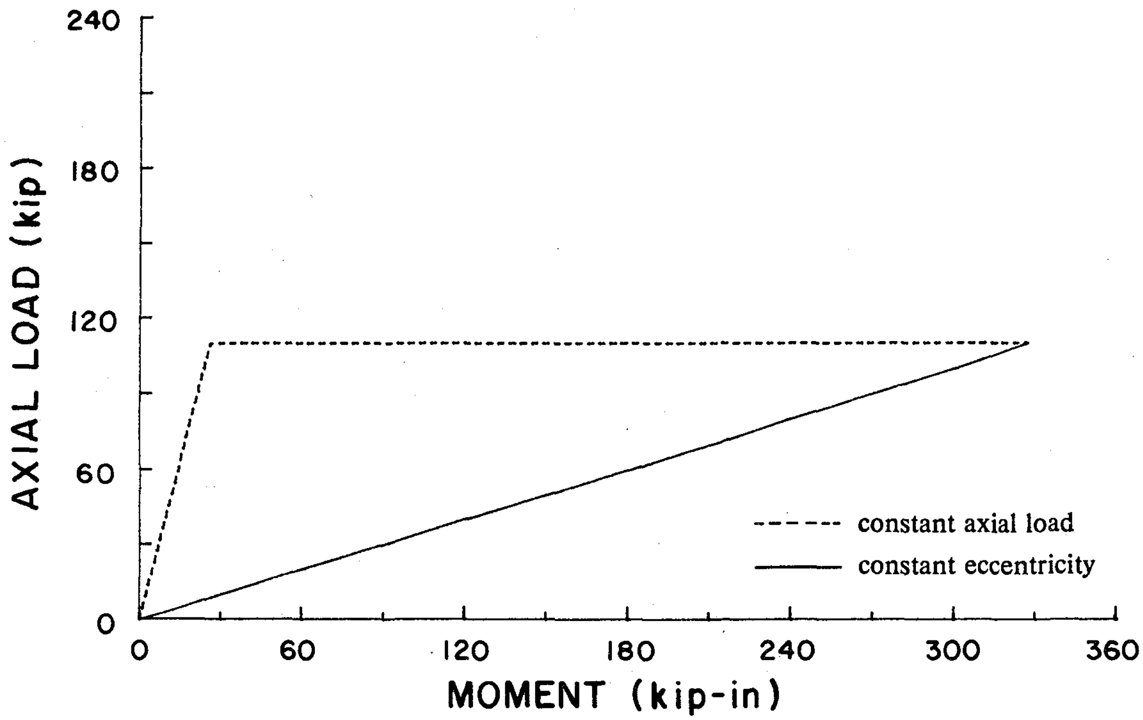

(a) Bending moment-axial load history

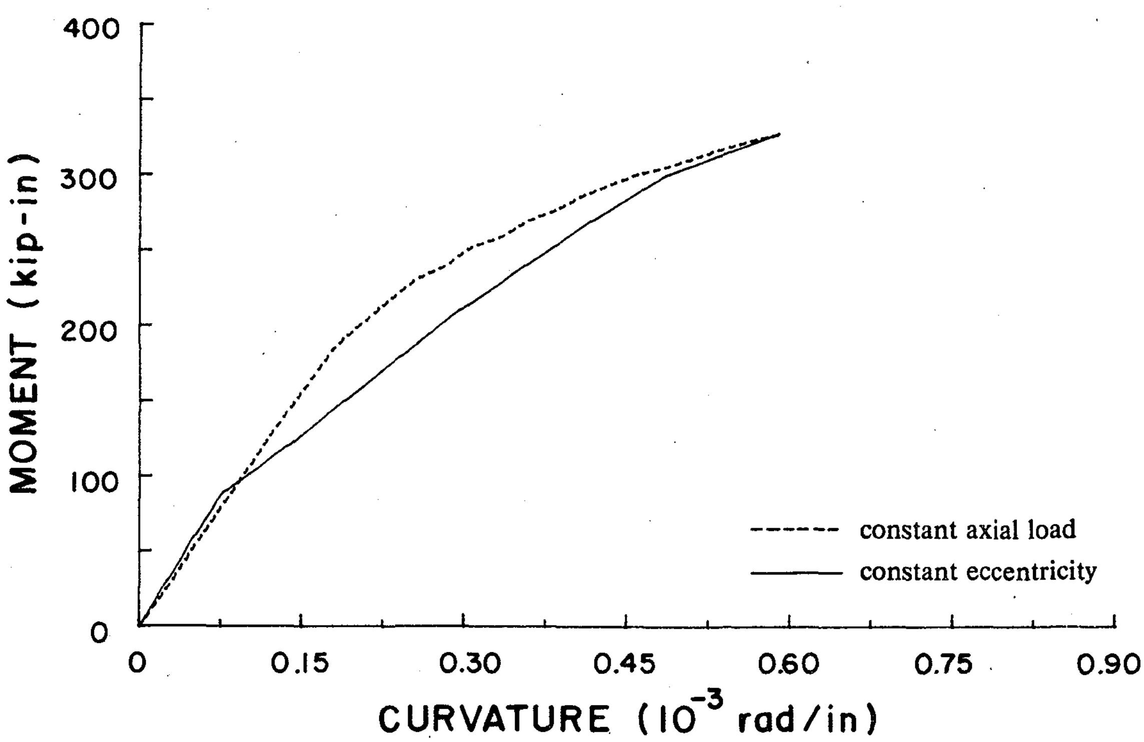

(b) Moment-curvature history

Fig. 3.24 Influence of axial load history on section behaviour

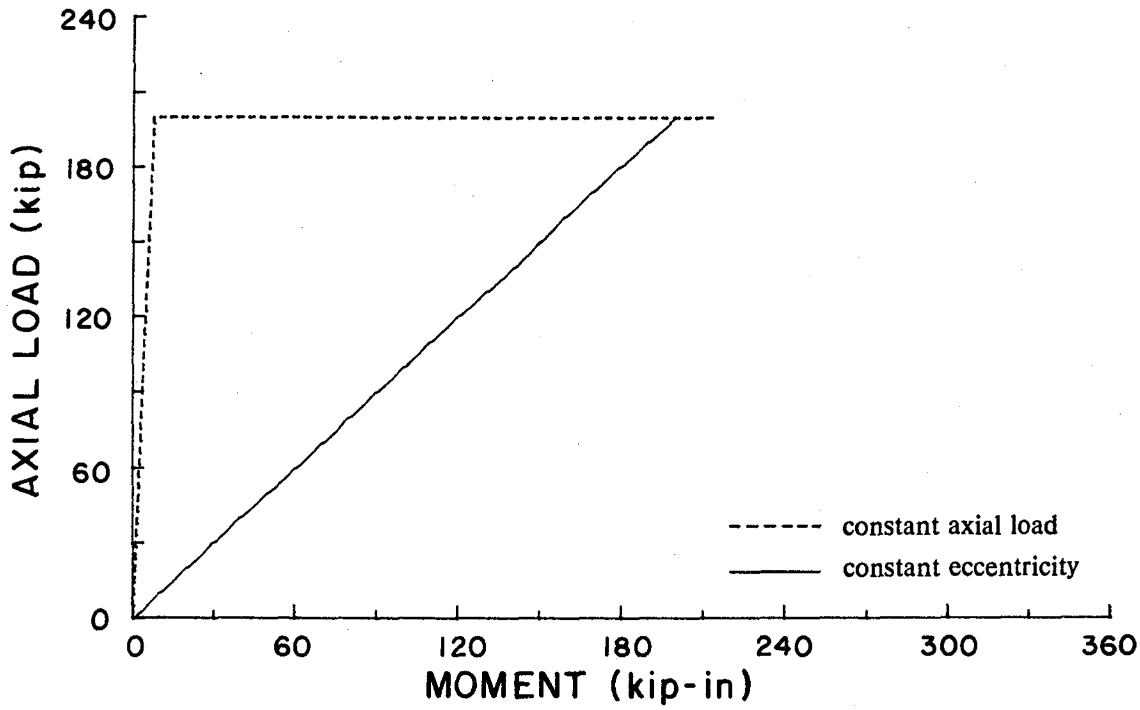

(a) Bending moment-axial load history

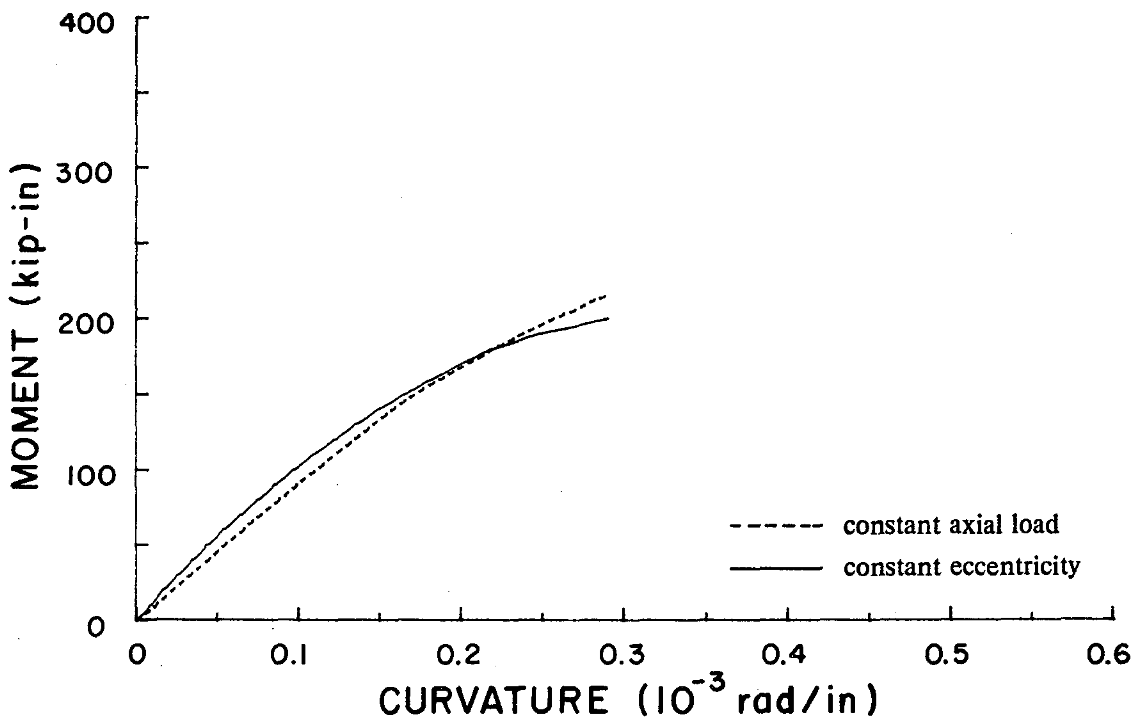

(b) Moment-curvature history

Fig. 3.25 Influence of axial load history on section behaviour

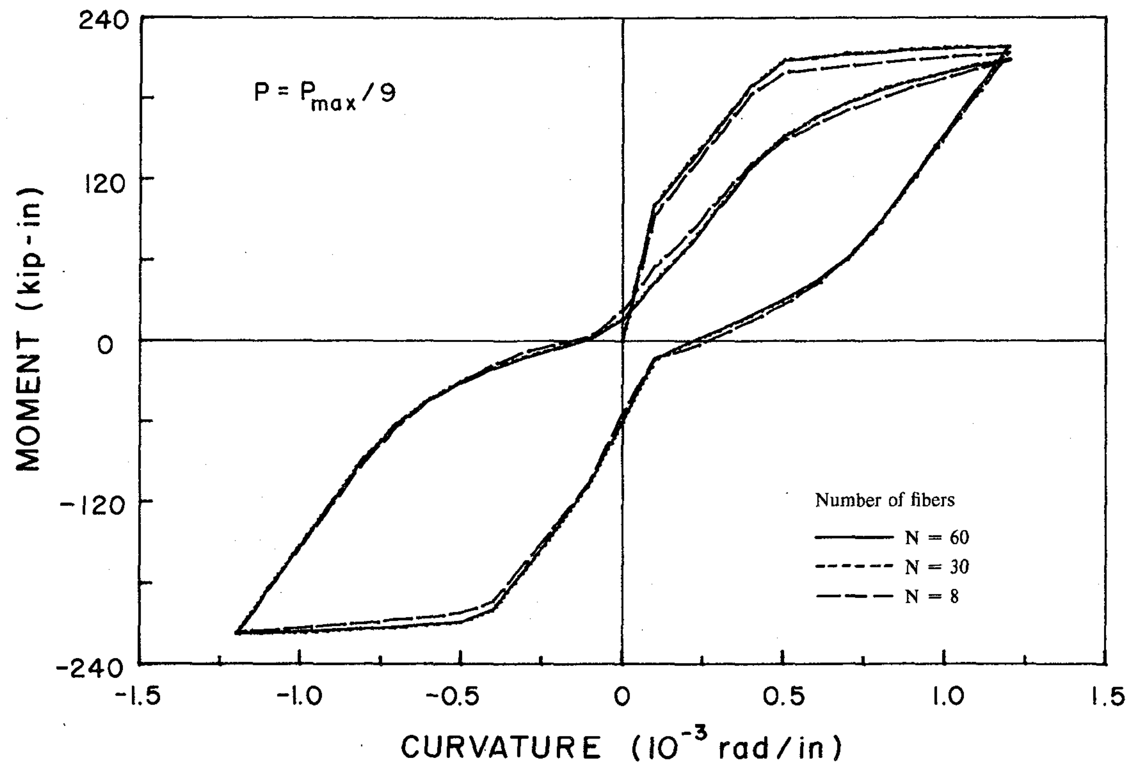

Fig. 3.26 Influence of number of fibers used to discretize the section

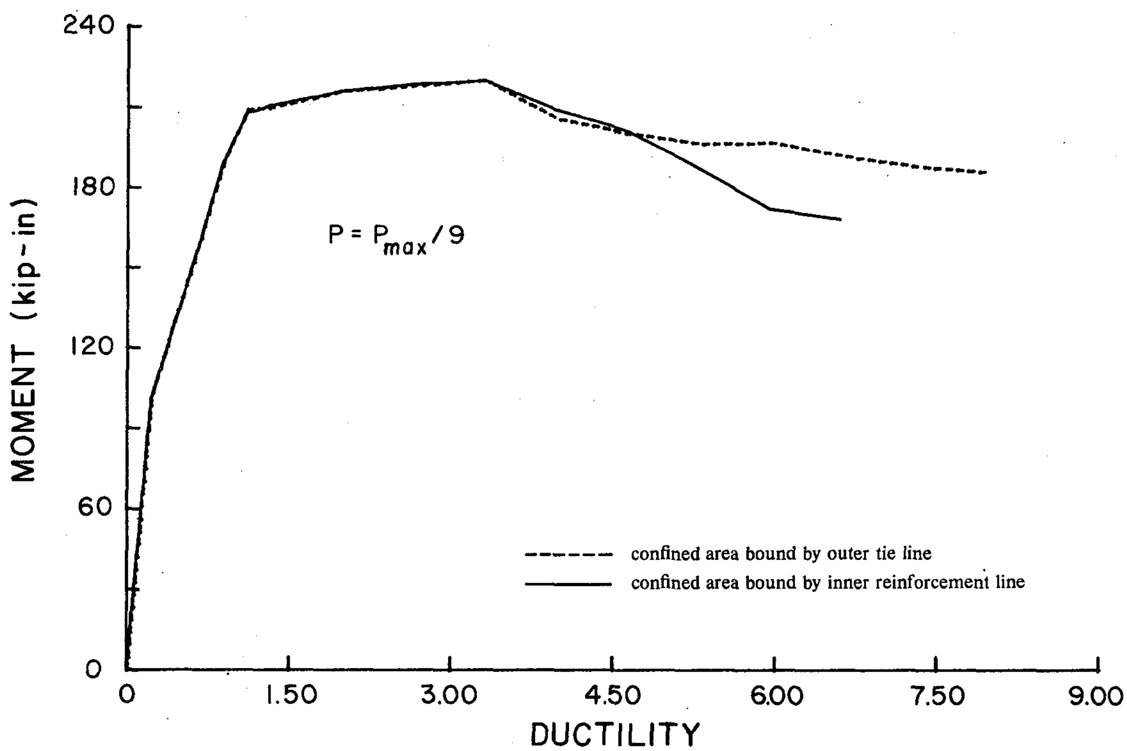

Fig. 3.27 Influence of assumed confined concrete area on computed section behaviour

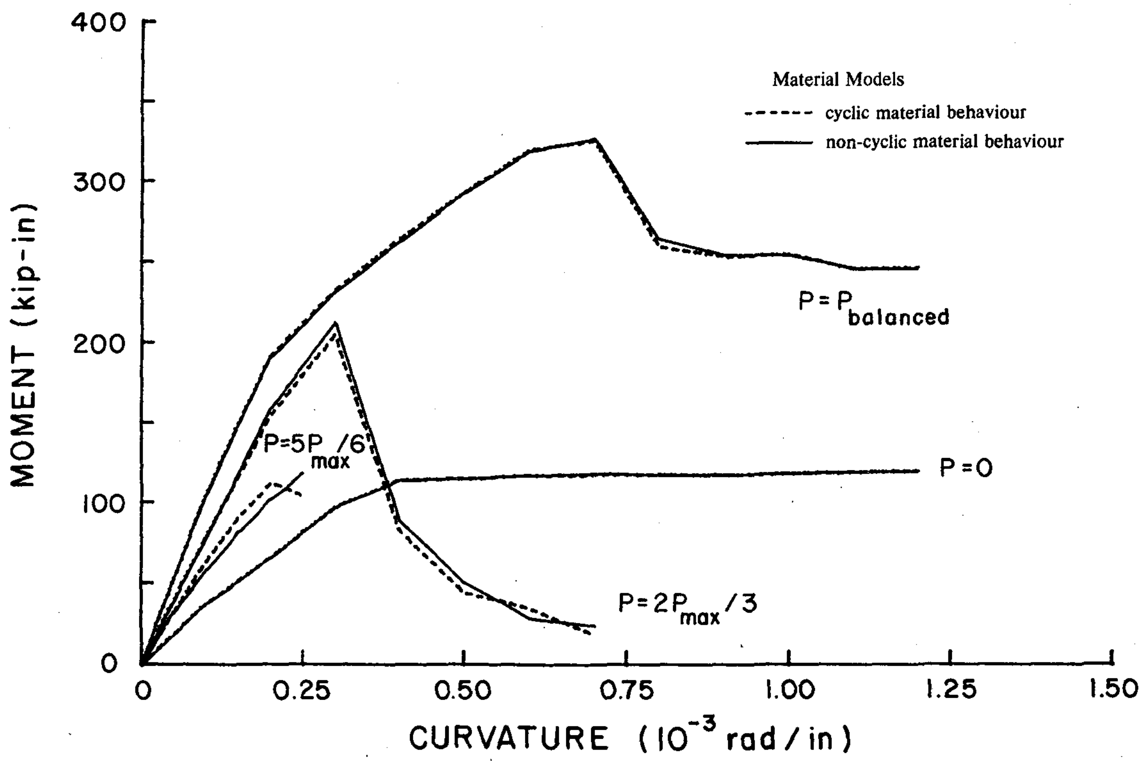

Fig. 3.28 Effect of cyclic and non-cyclic material models on section behaviour under monotonic loading

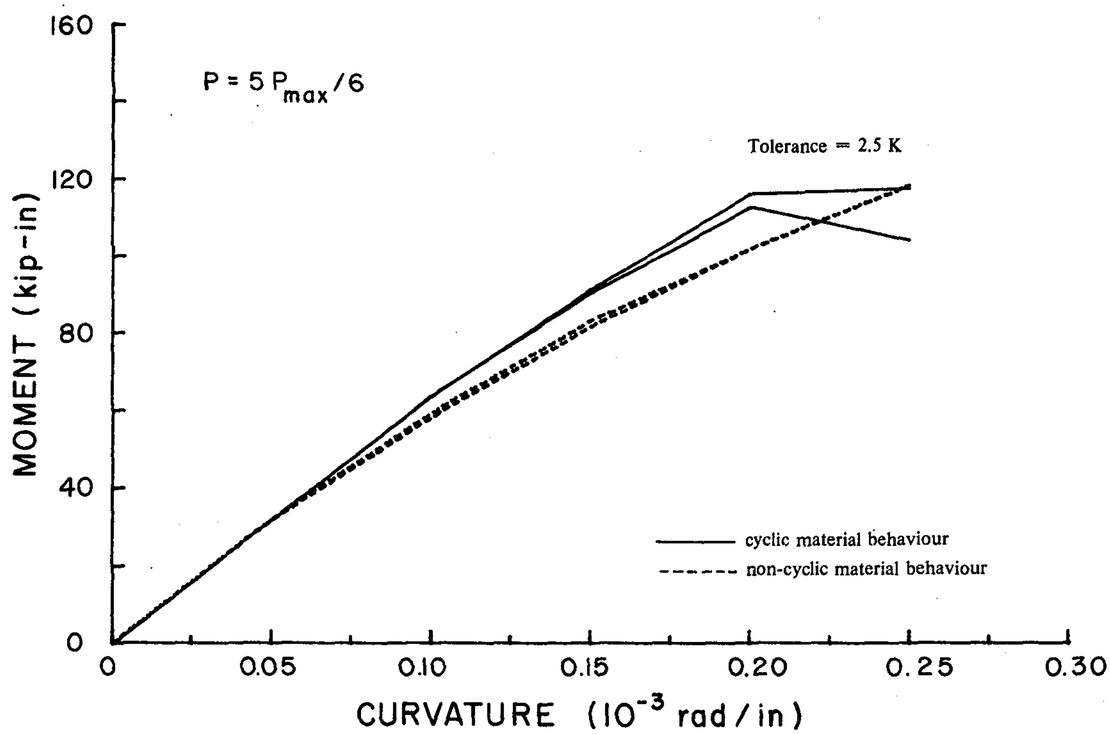

Fig. 3.29 Influence of convergence tolerance on computed behaviour at high axial load

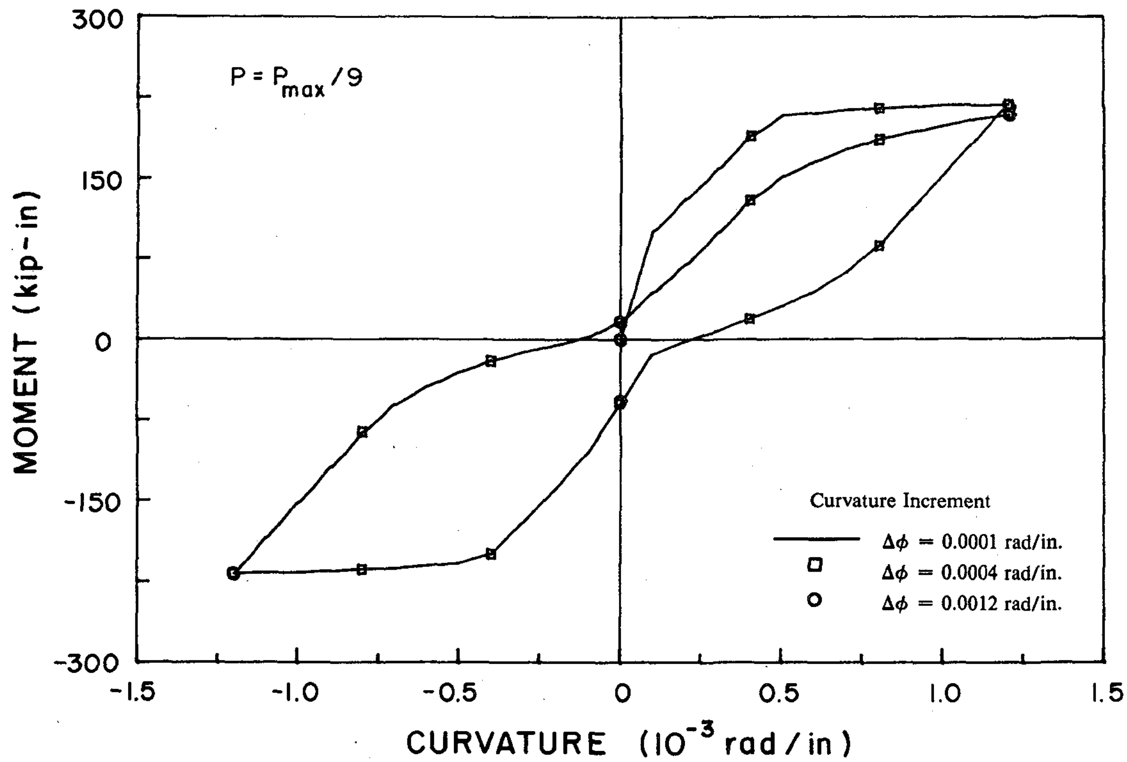

Fig 3.30 Influence of curvature increment size on computed behaviour at low axial load

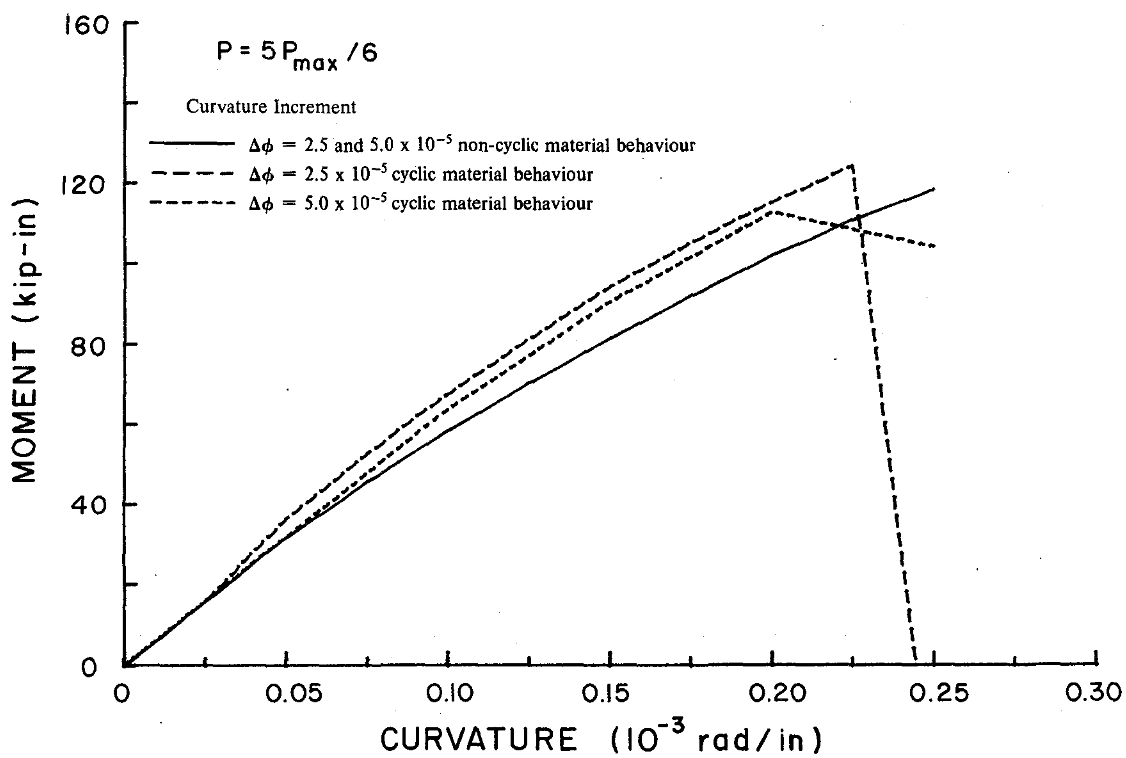

Fig 3.31 Influence of curvature increment size on computed behaviour at high axial load

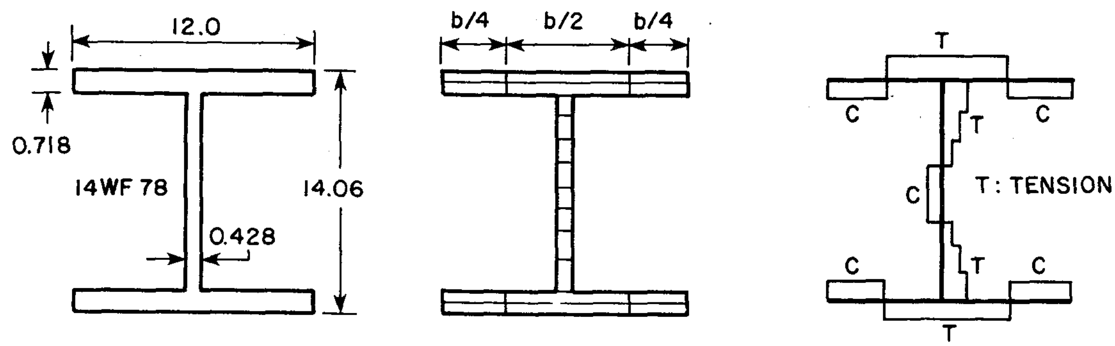

(a) Section Dimensions (b) Discretization (c) Residual Stresses

Fig. 4.1 Steel section used to study the effect of residual stresses

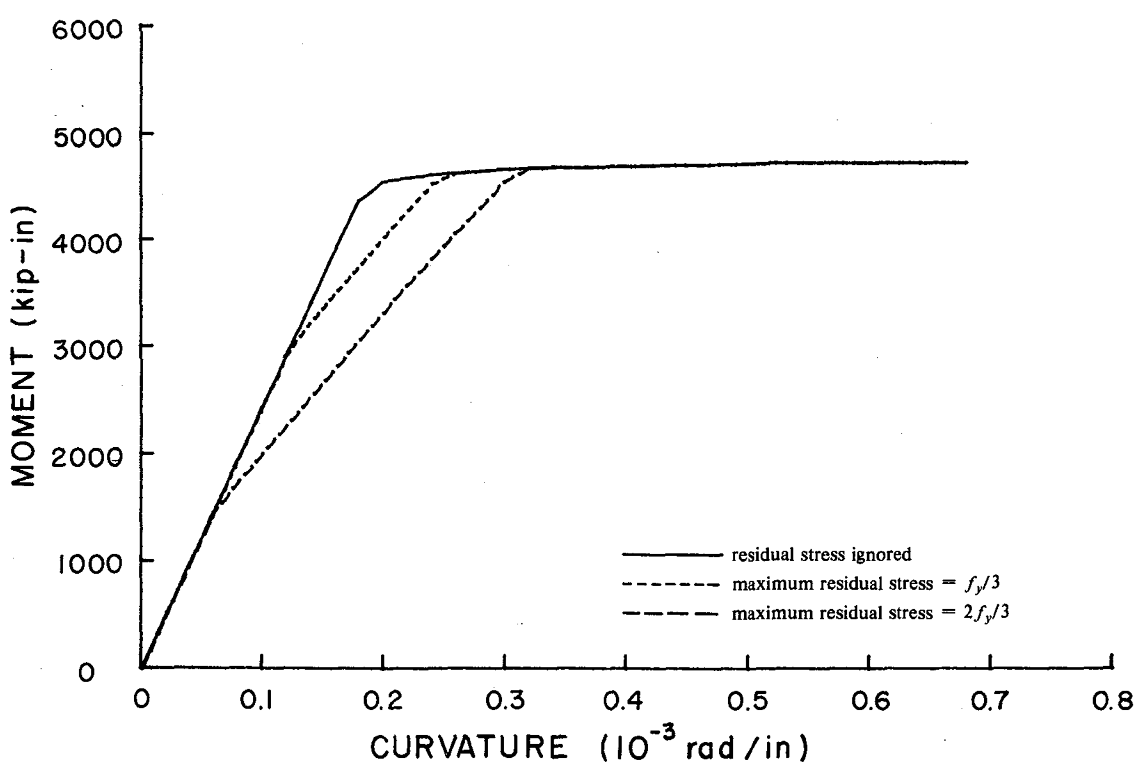

Fig. 4.2 Effect of residual stress on steel section behaviour

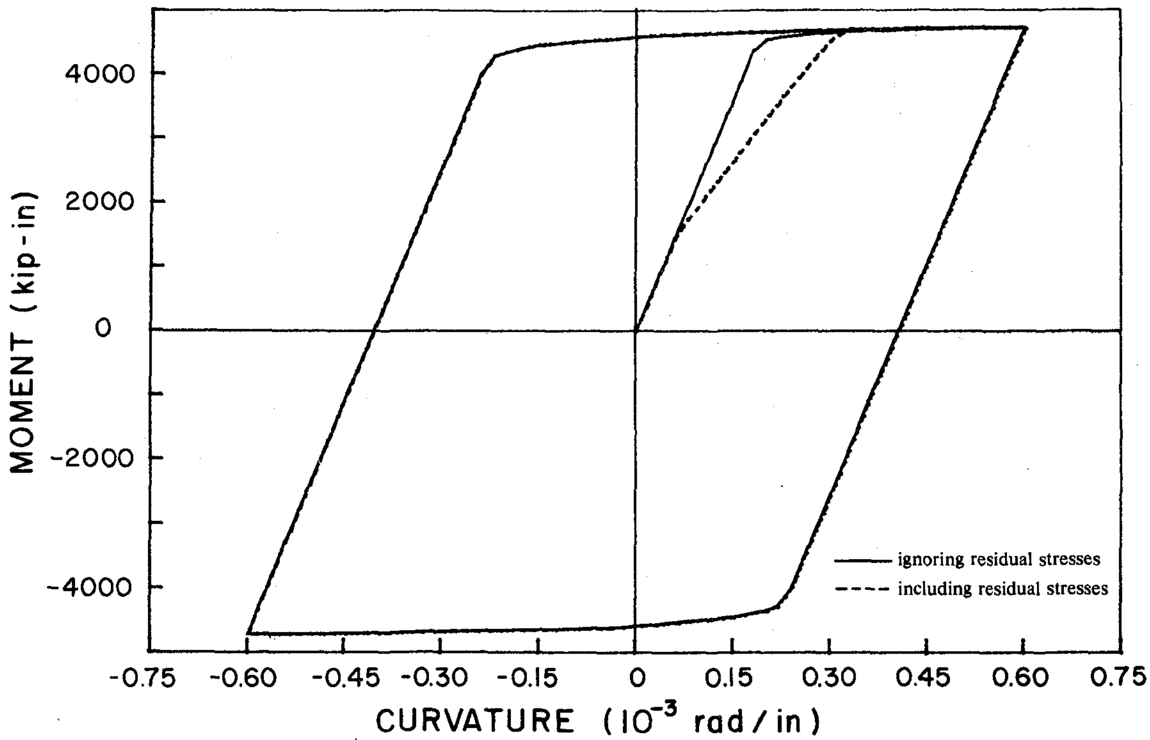

Fig. 4.3 Effect of residual stresses on steel section behaviour for cyclic loading

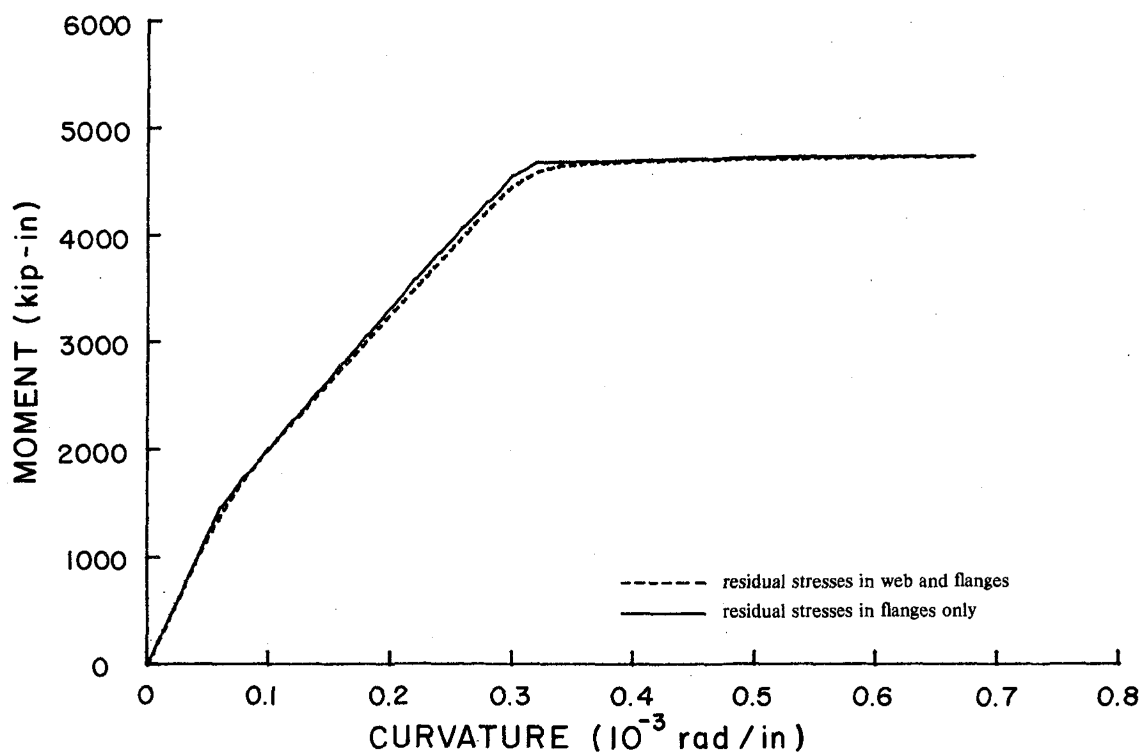

Fig. 4.4 Effect of residual stresses in the web

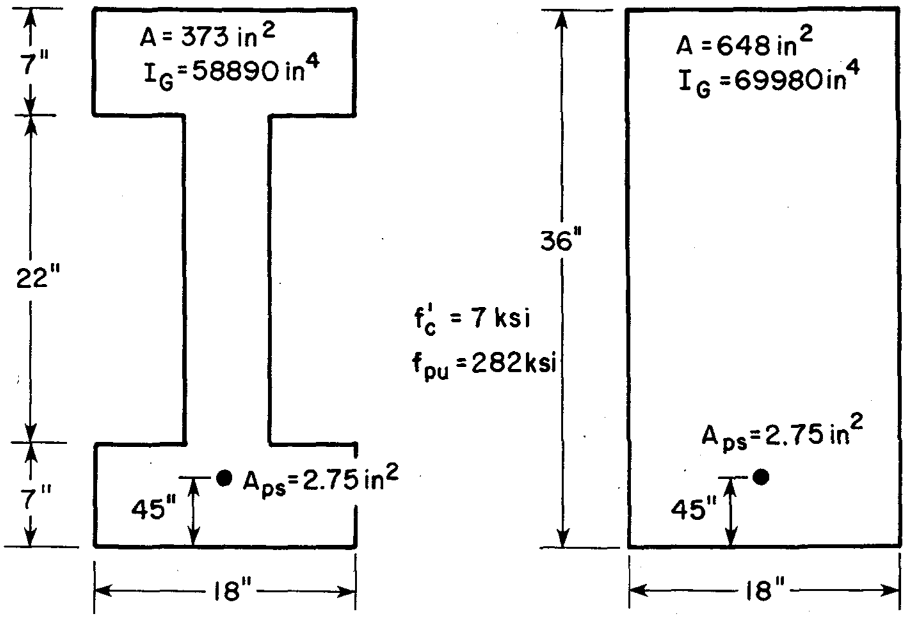

(a) I-Section

(b) Rectangular Section

Fig. 4.5 Sections used to study the effect of prestressing

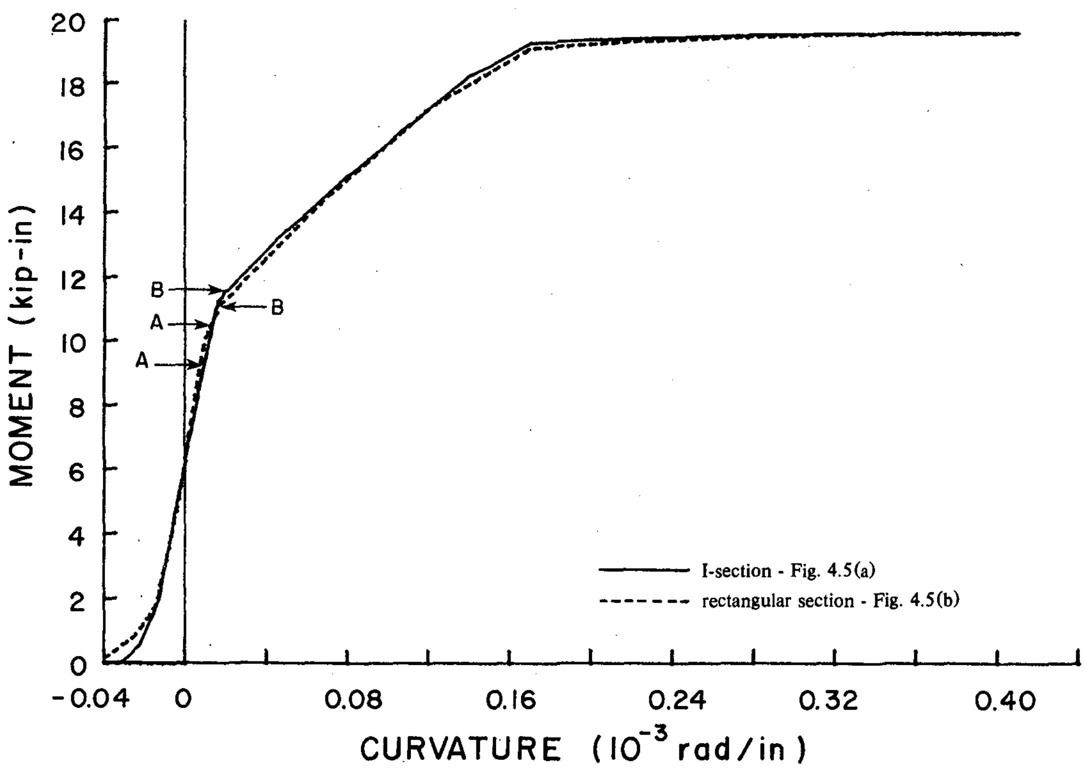

Fig. 4.6 Moment-curvature plots for prestressed concrete sections

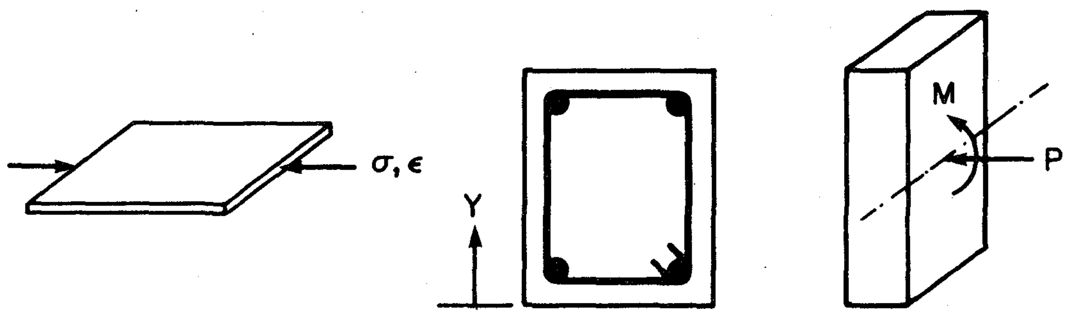

(a) Stress-strain (b) Locations (c) Force Resultants

Fig. A.1 Sign conventions (positive entities)

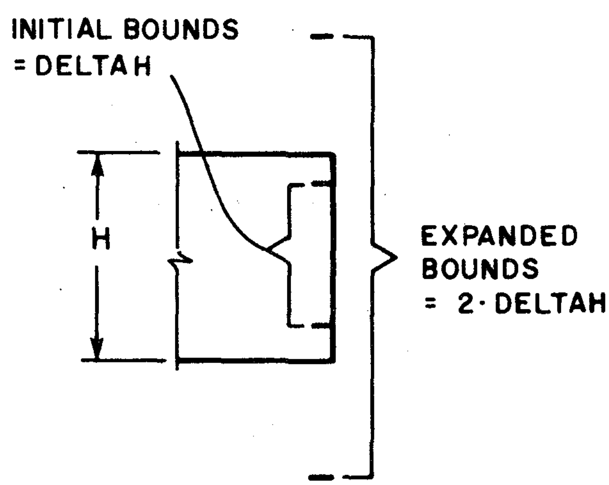

Fig. A.2 Expansion of bounds on neutral axis position

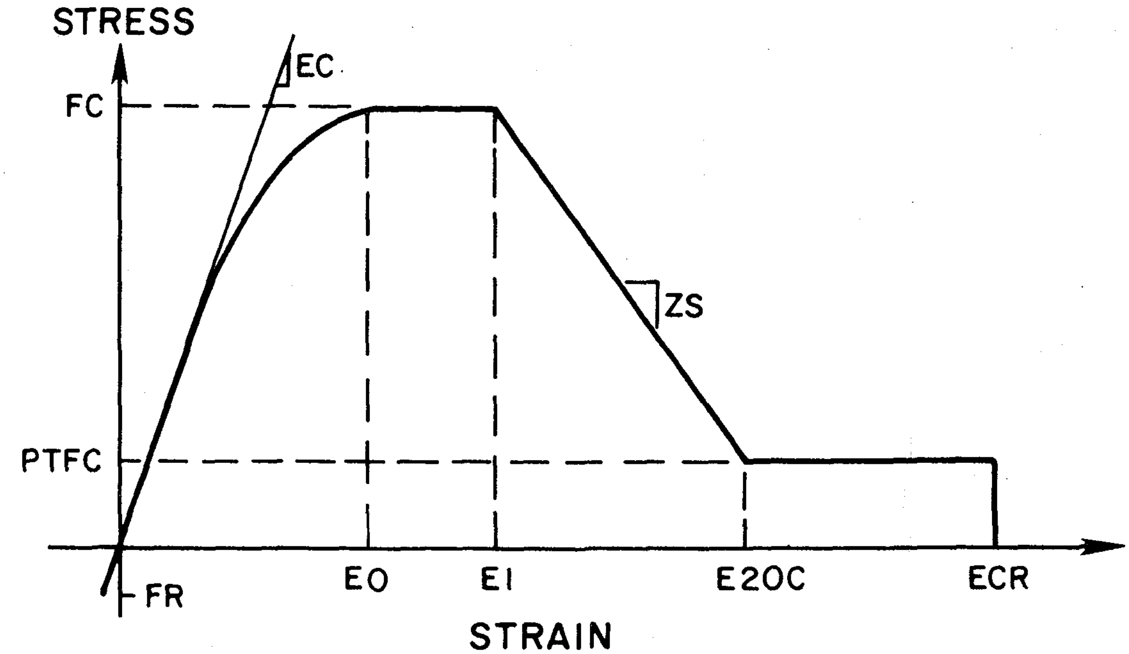

Fig. C.1 Variables used in the program to define concrete behaviour

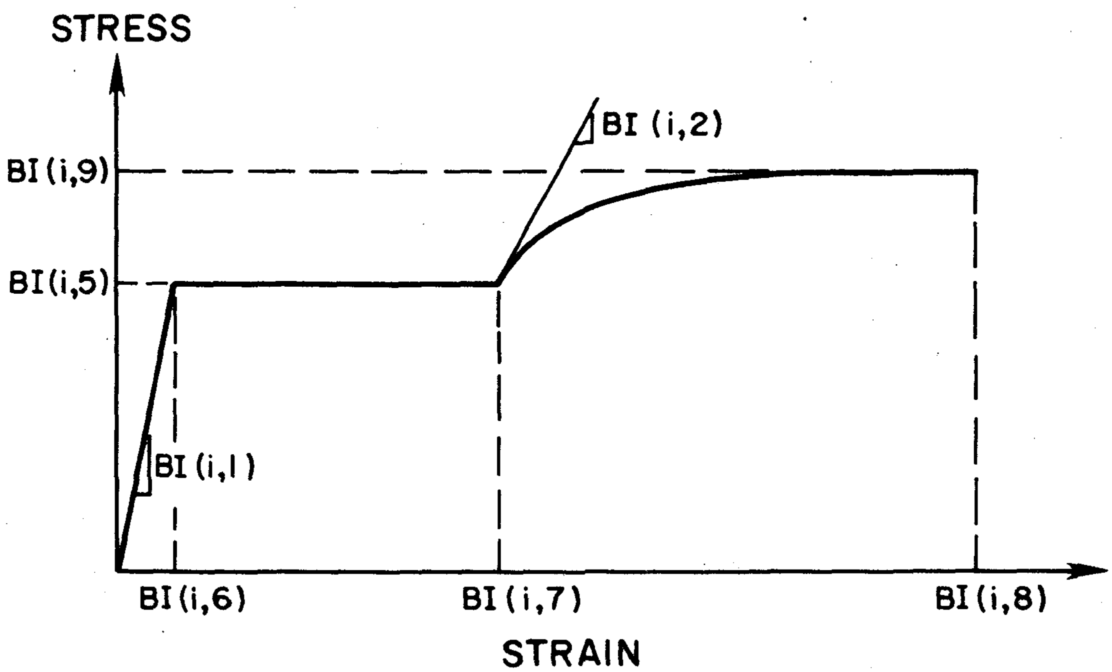

Fig. C.2 Variables used in the program to define steel behaviour

Appendix A

Notes on the Use of the Computer Program UNCOLA

The program, as written for a microcomputer, is interactive; hence the various input requirements are sequentially requested on the terminal by the program. Because of this a conventional batch processing user's guide is not possible. The purpose of the following notes is to further clarify some of the variables involved and to provide some hints which facilitate the use of the program.

1. The FORMAT associated with a READ statement is E15.0 in the case of real numbers and I5 in the case of integers. There is no need to right justify the data and control variables. Furthermore, decimal points are not necessary, and pressing the ENTER key is equivalent to feeding in a zero.

2. To prematurely terminate the program at any stage, simultaneously press the CNTRL and the C keys. Note however that this may result in the loss of output which would have otherwise been written to files.

3. Compressive strains, stresses, and axial load are defined as positive. A positive bending moment is one which would produce compression at the top of the section; positive curvature has the same sense as a positive moment. *All distances are referred to the bottom of the section.* The consistent sign convention allows the analysis of an inverted unsymmetrical section without the need for a new set of data, see Fig. A.1.

4. The program does not include any unit-dependent parameters or equations. Hence, any consistent system of units can be used to analyze a section. In some cases default values for material properties are implicitly unit dependent in which case the units are kips and inches.

5. The bending moments given by the program are computed about the plastic centroid of the section. To save on calculations, the location of the plastic centroid should be defined by the user whenever it is known *a priori* (i.e. as in the case of a double symmetric section). Otherwise, the program will locate it using the steel yield stresses and a concrete stress defined by

the user with a default value of $0.85 \cdot f_c'$. Note that it is possible to calculate the bending moments about any axis by simply feeding in the position of this axis as the plastic centroid location.

6. By setting MONCYC = 1, the program ignores cyclic behaviour and calculates concrete and steel stresses on the basis of the stress-strain envelopes. In this case, no memory of concrete cracking or crushing is retained. This is consistent with conventional hand calculations and is especially suited for producing conventional interaction diagrams.

7. The bounds on the location of the neutral axis are systematically expanded by DELTAH (with a default value of 0.25 x total depth of section, H) whenever a solution is unavailable within the current bounds, see Fig. A.2. Note that convergence is sometimes impossible with a given value of DELTAH. For example when a tensile strain is assigned to point A in Fig. 2.13 and a given compressive axial load is sought. In such a case a tensile axial force will be associated with the initial as well as any expanded bounds, for a sufficiently large DELTAH. This can be the case, for example, when calculating the yield curvature and moment. The user must therefore specify a small bound expansion increment DELTAH in such cases.

8. When the bounds are expanded, the maximum specified number of times (NBOUND) and the existence of a solution within the interval is still not ascertained, the program checks with the user on whether to expand the bounds further or to proceed to a new operation. The unavailability of a solution within very large bounds may be the result of specifying an axial load which is beyond the capacity of the section.

9. Similarly, if for some reason convergence is not achieved after the specified maximum number of iterations (NITER), the user is consulted for further instructions. Lack of convergence may result from specifying too large of increments in curvature or axial load, or too small a convergence tolerance.

10. Whenever the user moves from one operation to another INDEP should be set equal to 0 indicating that the two operations are independent and thus reinitializing the various arrays to virgin conditions. The output from the two operations is then automatically separated by a

row of zeros in the output files to make sure that the two groups of output are plotted separately - this also helps in separating the various groups of output. If, on the other hand, one operation is merely the continuation of the previous operation INDEP should be set equal to 1, hence preserving the conditions at the end of the last operation (no reinitialization).

11. The program generates a data file (DATA) which contains a description of the section geometry and material properties. Since this file contains titles and comments it is a self-contained description of the section. The program also generates two output files for every run (OUTPUT and STRNSTRS). It is possible, without exiting the program, to rename any of these files and thus save them for future reference. NOTE : these files must be renamed prior to executing a different problem since existing files with these names are overwritten during execution.

Appendix B

Modus Operandi

The program was written in Microsoft FORTRAN [33] using a RADIO SHACK TRS Model II micro-computer and the CP/M 2.2 [34] operating system which runs on an 8080, 8085, Z80 or any microprocessor which will execute 8080 machine language. With minor modifications the program should run on any computer that has a FORTRAN compiler. The plotting program and routines depend on the availability of XCEL graphics hardware and software [35].

The program is divided into three parts. The first part of the program (accessed by typing S) handles the section input and modification. It produces or modifies the input file called DATA, the PRESTR file which contains the initial steel stresses or strains and the BUCKLE file which has the data necessary for steel buckling considerations. Since this part of the program is independent of the rest, it is compiled and loaded separately. It does include, however, statements to chain it to the other parts of the program. This first part consists of two files (S and W) which are linked using PLINK [36] - because of their combined length, it is not possible to link them using L80 [33].

The second part of the program is used for analysis of the section. It is accessible from the first part of the program by menu selection or by typing A if the appropriate data files exist. The analysis section consists of two files (A and M); the first contains the analysis portion of the program, while the second contains the various subroutines relating to material behaviour. They are also linked using PLINK. This part of the program can produce two output files: OUTPUT contains a record of overall section results (moment, axial load, curvature, neutral axis position, etc.) and STRNSTRS contains the strain and stress histories of up to two user specified steel layers.

The third part (named P) is used for plotting, renaming and listing the output stored in files OUTPUT and STRNSTRS or a user specified file written in the same format. Plotting is possible when the XCEL graphics hardware and software are available. This section can also produce a summary of a given data file containing section geometry and material properties. Finally it can process a file containing the strain history of two layers (e.g. STRNSTRS) and produce the strain history of any point in the section.

Since the program consists of three independent but chained portions, the user can access the analysis portion (bypassing the input and modification portion) by typing A once the DATA file (and if necessary the buckling file: BUCKLE or initial strains or stresses file: PRESTR) has been created. Similarly, once the OUTPUT and STRNSTRS files are available, it is possible to bypass the input as well as the analysis sections and examine (or plot) those files by typing P.

Since the program is interactive, output is typically via console. However, the program produces output and data files which can be printed. In addition, pressing the CTRL and P keys simultaneously would result in transferring whatever appears on the screen to the printer. Hence it is possible to produce a hard copy of the entire session or parts thereof. Whenever the printer pauses, pressing CTRL and P again would suppress printing.

The following commands can be executed whenever the program execution is terminated (i.e., when control has been returned to the CPM operating system):

(1) To list the names of all files on the disk: DIR

(2) To erase a file: ERA *filename*

(3) To rename a file: REN *filename 2* = *filename 1* where *filename 2* is the new name and *filename 1* is the current one. This is essential if input and results are to be saved. The program input is always stored in files called DATA, BUCKLE, and PRESTR and the results are stored in OUTPUT and STRNSTRS. The output file will be destroyed when a new analysis is initiated unless they are renamed. Similarly to reanalyze a section, the input file should be called DATA.

(4) To type a file on the printer: press CTRL and P simultaneously followed by the command: TYPE *filename.*

Appendix C

Modifying Material Behaviour Models

It was mentioned earlier that the user could add subroutines to define material behaviour. The relevant material routines which have to be modified or replaced belong to the material description portion (M) of the program described in Appendix B. The following two sections explain the steps necessary to modify the material behaviour of concrete or steel.

(1) Modifying Concrete Behaviour:

The relevant subroutine is CONC(S,I) where S is the new strain and I is the layer number (total number of concrete layers = NC). Note that the type of concrete associated with this layer is given by II = MATCON (I) (total number of concrete types = NCON). The material properties corresponding to concrete types II are stored in the COMMON block labeled CONC2. It includes the following arrays: ZS, E20C, FR, ER, E0, E1, EC, ECR, and PTFC. For example, for II = 3, ECR (3) would contain the crushing concrete strain associated with concrete type 3. Fig. C.1 defines these parameters; note that the subroutine need not use all of them.

The subroutine should calculate the stress corresponding to the new strain S and place the value of the stress (compression being positive) in ACF (I,2). The arrays used for this purpose are stored in the COMMON block labeled CONC1. These arrays should be initialized in subroutine INIT and updated in subroutine UPDATE. In the following brief description of these arrays note that "I" refers to the number of the layer being considered:

ACF (I,1): the new strain - generated by the program.

ACF (I,2): the corresponding stress assigned by subroutine CONC.

ACF (I,3), ACF (I,4), ICRF (I), and INF (I) are storage locations available for describing the current state of this concrete layer (e.g. whether it has already cracked or is permanently crushed, etc.). These variables refer to the state of the concrete at the end of an operation, the corresponding variables ending with I instead of F refer to the state of concrete at the beginning of an operation.

The updating process is achieved by the following sequence of operations (I = 1, 2, 3,.....NC):

INI (I)	=	INF (I)
ICRI (I)	=	ICRF (I)
ACI (I,J)	=	ACF (I,J) J = 1, 2, 3, 4

IC (I) is an additional array, currently unused, that is also available for describing the state of a concrete layer. To avoid increasing the size of the program it is suggested that the user either modify the existing CONC subroutine or replace it by a new one. Note that the subroutine should also be capable of ignoring cyclic behaviour (when MONCYC is set equal to 1) and merely using the stress-strain envelope to calculate the stress corresponding to a new strain.

(2) Modifying Steel Behaviour:

In this case the user should eliminate the following subroutines: NONLIN, POLY, CUBIC, ROSGD, and BUCK. The new subroutine should be NONLIN (X,I), where X is the new strain set by the program and I is the layer number (total number of steel layers = NS). The type of steel associated with each layer is given by II = MATSTL (I) (number of types of steel = NBIL).

The material properties are stored in a common labeled STEEL2. BI (4,10) is the array with each row corresponding to a given type of steel and the ten columns are described in Fig. C.2 (note that the third and fourth columns are free and can be used to store other parameters, while the tenth column contains the α variable referred to in Equation (8)).

The condition of the steel layer is described by the arrays listed below (I being the number of the layer being considered).

ASI (I,1): strain at the end of the last operation

ASI (I,2): stress at the end of the last operation

ASI (I,J) J = 3, 4, 5, 6: left for the user

ASF (I,1): the new strain calculated by the program in subroutine STRAIN and passed to subroutine NONLIN (= X)

ASF (I,2): corresponding stress calculated by NONLIN

Some other arrays can be used as flags and parameters to describe the stress-strain state. These are: IS (I), NUNDL(I), INDEXI (I), INDEXF (I), EPMAX (I), NFLAG,INDI (I), INDF (I), SLOPE1 (I), SLOPE2 (I), and ISHIFT (I). These various arrays should be appropriately initialized in INIT and updated in UPDATE to reflect the new stress state and any changes that may have occurred. The subroutine should also be capable of ignoring the cyclic behaviour (when MONCYC = 1) and calculating the stress [ASF (I,2)] corresponding to a given strain [ASF (I,1)] from the stress-strain envelope.

Testing the newly added subroutine is a simple matter: create a section with one layer and set ICNTR = 1 and INTR = 1. Then feed as many strains as required and check that the resulting stresses do in fact correspond to the given strains.

Appendix D

Current Array Size Limitations

To facilitate modification of the section geometry during analysis by addition of layers or changing material properties all variables have fixed dimensions. The array sizes considered are indicated below. The bounds given can be relaxed by modifying the array sizes found in the various COMMON blocks.

NC	=	number of concrete layers (total)	65
NS	=	number of steel layers (total)	30
NGC	=	number of groups of concrete layers	30
NGS	=	number of groups of steel layers	20
NCON	=	number of types of concrete	9
NBIL	=	number of types of steel	4
NB	=	number of layers checked for buckling	10

Number of lines in files to be listed or plotted 600

Appendix E

Equations for Available Concrete Models

As discussed in Section 2.5(a), the concrete model available in the program has a sufficient number of parameters to fit a number of proposed concrete models. For convenient reference, the mathematical description of the models proposed by Kent [22], Vallenas et al [18], and Scott et al [17] is given below. Since [19] consists of a discussion of the model proposed by Sheikh and Uzumeri, it is felt that a description of the model here would be redundant and inappropriate.

Kent's model for confined concrete - see Fig. 2.5(c) - has an initial parabolic phase ($\epsilon \leqslant \epsilon_0$) defined by:

$$f_c = f_c' \frac{\epsilon}{\epsilon_0} \left(2 - \frac{\epsilon}{\epsilon_0} \right) \tag{1}$$

This equation implicitly means an initial slope of $E_c = 2 \cdot f_c' / \epsilon_0$. Furthermore, the maximum stress is equal to f_c' and is attained at a strain of ϵ_0.

The initial parabolic phase is followed by a linear descending portion ($\epsilon > \epsilon_0$) given by:

$$f_c = f_c' \left\{ 1 - z \left(\epsilon - \epsilon_0 \right) \right\} \tag{2}$$

but not less than $0.2 \cdot f_c'$

Where z, which sets the slope of this linear portion, is a function of the compressive strength and the confinement provided by the ties:

$$z = \frac{0.5}{\dfrac{3 + .002 f_c'(Psi)}{f_c'(Psi) - 1000} + \dfrac{3}{4} \rho_s \sqrt{\dfrac{h''}{s}} - \epsilon_0} \tag{3}$$

where: ρ_s = volumetric ratio of ties to concrete core (measured to the outside of the ties)

h'' = width of the concrete core to the outside of the ties

s = center to center spacing of the ties

Vallenas' model is similar to Kent's except that the maximum stress is assumed to increase with confinement to a value of $f_c''=k \cdot f_c'$ where k is given by:

$$k = 1+.0091\left(1-.245\frac{s}{h''}\right)\left(\rho + \frac{d''}{d}\rho\right)\frac{f_{yh}}{\sqrt{f_c'(Psi)}} \tag{4}$$

where ρ_s and s are as defined above and,

h'' = width of concrete core inside ties

d'' = tie diameter

d = longitudinal reinforcement diameter

ρ = longitudinal reinforcement ratio

f_{yh} = tie yield stress

Moreover, the peak concrete stress is attained at a strain ϵ_0 given by:

$$\epsilon_0=.0024+.0005\left(1-\frac{.734s}{h''}\right)\rho_s\frac{f_{yh}}{\sqrt{f_c'(Psi)}} \tag{5}$$

Finally the initial slope is no longer necessarily equal to $2\frac{f_c''}{\epsilon_0}$ but can be set at any value. To accomodate this additional restraint, the initial phase has to be slightly more elaborate than Kent's parabolic formulation and Vallenas suggests:

$$f_c = \frac{E_c\epsilon - f_c''\left(\frac{\epsilon}{\epsilon_0}\right)^2}{1 + \left[\frac{E_c\epsilon_0}{f_c''} - 2\right]\left(\frac{\epsilon}{\epsilon_0}\right)} \tag{6}$$

This is followed by a linear portion (for $\epsilon > \epsilon_0$) defined by:

$$f_c = f_c''\left[-z\left(\epsilon-\epsilon_0\right)\right] \tag{7}$$

but not less than $0.3 \cdot f_c''$

where z has the same value as that given by Equation (3).

For low strain rates, Scott proposes an initial parabolic phase that is similar to Kent's (Equation 1) except that f_c' is replaced by $k \cdot f_c'$ and ϵ_0 by $0.002k$ where k is given by:

$$k = 1+\rho_s \frac{f_{yh}}{f_c'} \tag{8}$$

The linear descending portion is the one proposed by Kent (Equation 2) but again f_c' is replaced by $k \cdot f_c'$ and ϵ_0 by $0.002k$.

EARTHQUAKE ENGINEERING RESEARCH CENTER REPORTS

NOTE: Numbers in parentheses are Accession Numbers assigned by the National Technical Information Service; these are followed by a price code. Copies of the reports may be ordered from the National Technical Information Service, 5285 Port Royal Road, Springfield, Virginia, 22161. Accession Numbers should be quoted on orders for reports (PB --- ---) and remittance must accompany each order. Reports without this information were not available at time of printing. The complete list of EERC reports (from EERC 67-1) is available upon request from the Earthquake Engineering Research Center, University of California, Berkeley, 47th Street and Hoffman Boulevard, Richmond, California 94804.

UCB/EERC-77/01 "PLUSH - A Computer Program for Probabilistic Finite Element Analysis of Seismic Soil-Structure Interaction," by M.P. Romo Organista, J. Lysmer and H.B. Seed - 1977 (PB81 177 651)A05

UCB/EERC-77/02 "Soil-Structure Interaction Effects at the Humboldt Bay Power Plant in the Ferndale Earthquake of June 7, 1975," by J.E. Valera, H.B. Seed, C.F. Tsai and J. Lysmer - 1977 (PB 265 795)A04

UCB/EERC-77/03 "Influence of Sample Disturbance on Sand Response to Cyclic Loading," by K. Mori, H.B. Seed and C.K. Chan - 1977 (PB 267 352)A04

UCB/EERC-77/04 "Seismological Studies of Strong Motion Records," by J. Shoja-Taheri - 1977 (PB 269 655)A10

UCB/EERC-77/05 Unassigned

UCB/EERC-77/06 "Developing Methodologies for Evaluating the Earthquake Safety of Existing Buildings," by No. 1 - B. Bresler; No. 2 - B. Bresler, T. Okada and D. Zisling; No. 3 - T. Okada and B. Bresler; No. 4 - V.V. Bertero and B. Bresler - 1977 (PB 267 354)A08

UCB/EERC-77/07 "A Literature Survey - Transverse Strength of Masonry Walls," by Y. Omote, R.L. Mayes, S.W. Chen and R.W. Clough - 1977 (PB 277 933)A07

UCB/EERC-77/08 "DRAIN-TABS: A Computer Program for Inelastic Earthquake Response of Three Dimensional Buildings," by R. Guendelman-Israel and G.H. Powell - 1977 (PB 270 693)A07

UCB/EERC-77/09 "SUBWALL: A Special Purpose Finite Element Computer Program for Practical Elastic Analysis and Design of Structural Walls with Substructure Option," by D.Q. Le, H. Peterson and E.P. Popov - 1977 (PB 270 567)A05

UCB/EERC-77/10 "Experimental Evaluation of Seismic Design Methods for Broad Cylindrical Tanks," by D.P. Clough (PB 272 280)A13

UCB/EERC-77/11 "Earthquake Engineering Research at Berkeley - 1976," - 1977 (PB 273 507)A09

UCB/EERC-77/12 "Automated Design of Earthquake Resistant Multistory Steel Building Frames," by N.D. Walker, Jr. - 1977 (PB 276 526)A09

UCB/EERC-77/13 "Concrete Confined by Rectangular Hoops Subjected to Axial Loads," by J. Vallenas, V.V. Bertero and E.P. Popov - 1977 (PB 275 165)A06

UCB/EERC-77/14 "Seismic Strain Induced in the Ground During Earthquakes," by Y. Sugimura - 1977 (PB 284 201)A04

UCB/EERC-77/15 Unassigned

UCB/EERC-77/16 "Computer Aided Optimum Design of Ductile Reinforced Concrete Moment Resisting Frames," by S.W. Zagajeski and V.V. Bertero - 1977 (PB 280 137)A07

UCB/EERC-77/17 "Earthquake Simulation Testing of a Stepping Frame with Energy-Absorbing Devices," by J.M. Kelly and D.F. Tsztoo - 1977 (PB 273 506)A04

UCB/EERC-77/18 "Inelastic Behavior of Eccentrically Braced Steel Frames under Cyclic Loadings," by C.W. Roeder and E.P. Popov - 1977 (PB 275 526)A15

UCB/EERC-77/19 "A Simplified Procedure for Estimating Earthquake-Induced Deformations in Dams and Embankments," by F.I. Makdisi and H.B. Seed - 1977 (PB 276 820)A04

UCB/EERC-77/20 "The Performance of Earth Dams during Earthquakes," by H.B. Seed, F.I. Makdisi and P. de Alba - 1977 (PB 276 821)A04

UCB/EERC-77/21 "Dynamic Plastic Analysis Using Stress Resultant Finite Element Formulation," by P. Lukkunapvasit and J.M. Kelly - 1977 (PB 275 453)A04

UCB/EERC-77/22 "Preliminary Experimental Study of Seismic Uplift of a Steel Frame," by R.W. Clough and A.A. Huckelbridge 1977 (PB 278 769)A08

UCB/EERC-77/23 "Earthquake Simulator Tests of a Nine-Story Steel Frame with Columns Allowed to Uplift," by A.A. Huckelbridge - 1977 (PB 277 944)A09

UCB/EERC-77/24 "Nonlinear Soil-Structure Interaction of Skew Highway Bridges," by M.-C. Chen and J. Penzien - 1977 (PB 276 176)A07

UCB/EERC-77/25 "Seismic Analysis of an Offshore Structure Supported on Pile Foundations," by D.D.-N. Liou and J. Penzien 1977 (PB 283 180)A06

UCB/EERC-77/26 "Dynamic Stiffness Matrices for Homogeneous Viscoelastic Half-Planes," by G. Dasgupta and A.K. Chopra - 1977 (PB 279 654)A06

Preceding page blank

UCB/EERC-77/27 "A Practical Soft Story Earthquake Isolation System," by J.M. Kelly, J.M. Eidinger and C.J. Derham - 1977 (PB 276 814)A07

UCB/EERC-77/28 "Seismic Safety of Existing Buildings and Incentives for Hazard Mitigation in San Francisco: An Exploratory Study," by A.J. Meltsner - 1977 (PB 281 970)A05

UCB/EERC-77/29 "Dynamic Analysis of Electrohydraulic Shaking Tables," by D. Rea, S. Abedi-Hayati and Y. Takahashi 1977 (PB 282 569)A04

UCB/EERC-77/30 "An Approach for Improving Seismic - Resistant Behavior of Reinforced Concrete Interior Joints," by B. Galunic, V.V. Bertero and E.P. Popov - 1977 (PB 290 870)A06

UCB/EERC-78/01 "The Development of Energy-Absorbing Devices for Aseismic Base Isolation Systems," by J.M. Kelly and D.F. Tsztoo - 1978 (PB 284 978)A04

UCB/EERC-78/02 "Effect of Tensile Prestrain on the Cyclic Response of Structural Steel Connections, by J.G. Bouwkamp and A. Mukhopadhyay - 1978

UCB/EERC-78/03 "Experimental Results of an Earthquake Isolation System using Natural Rubber Bearings," by J.M. Eidinger and J.M. Kelly - 1978 (PB 281 686)A04

UCB/EERC-78/04 "Seismic Behavior of Tall Liquid Storage Tanks," by A. Niwa - 1978 (PB 284 017)A14

UCB/EERC-78/05 "Hysteretic Behavior of Reinforced Concrete Columns Subjected to High Axial and Cyclic Shear Forces," by S.W. Zagajeski, V.V. Bertero and J.G. Bouwkamp - 1978 (PB 283 858)A13

UCB/EERC-78/06 "Three Dimensional Inelastic Frame Elements for the ANSR-I Program," by A. Riahi, D.G. Row and G.H. Powell - 1978 (PB 295 755)A04

UCB/EERC-78/07 "Studies of Structural Response to Earthquake Ground Motion," by O.A. Lopez and A.K. Chopra - 1978 (PB 282 790)A05

UCB/EERC-78/08 "A Laboratory Study of the Fluid-Structure Interaction of Submerged Tanks and Caissons in Earthquakes," by R.C. Byrd - 1978 (PB 284 957)A08

UCB/EERC-78/09 Unassigned

UCB/EERC-78/10 "Seismic Performance of Nonstructural and Secondary Structural Elements," by I. Sakamoto - 1978 (PB81 154 593)A05

UCB/EERC-78/11 "Mathematical Modelling of Hysteresis Loops for Reinforced Concrete Columns," by S. Nakata, T. Sproul and J. Penzien - 1978 (PB 298 274)A05

UCB/EERC-78/12 "Damageability in Existing Buildings," by T. Blejwas and B. Bresler - 1978 (PB 80 166 978)A05

UCB/EERC-78/13 "Dynamic Behavior of a Pedestal Base Multistory Building," by R.M. Stephen, E.L. Wilson, J.G. Bouwkamp and M. Button - 1978 (PB 286 650)A08

UCB/EERC-78/14 "Seismic Response of Bridges - Case Studies," by R.A. Imbsen, V. Nutt and J. Penzien - 1978 (PB 286 503)A10

UCB/EERC-78/15 "A Substructure Technique for Nonlinear Static and Dynamic Analysis," by D.G. Row and G.H. Powell - 1978 (PB 288 077)A10

UCB/EERC-78/16 "Seismic Risk Studies for San Francisco and for the Greater San Francisco Bay Area," by C.S. Oliveira - 1978 (PB 81 120 115)A07

UCB/EERC-78/17 "Strength of Timber Roof Connections Subjected to Cyclic Loads," by P. Gülkan, R.L. Mayes and R.W. Clough - 1978 (HUD-000 1491)A07

UCB/EERC-78/18 "Response of K-Braced Steel Frame Models to Lateral Loads," by J.G. Bouwkamp, R.M. Stephen and E.P. Popov - 1978

UCB/EERC-78/19 "Rational Design Methods for Light Equipment in Structures Subjected to Ground Motion," by J.L. Sackman and J.M. Kelly - 1978 (PB 292 357)A04

UCB/EERC-78/20 "Testing of a Wind Restraint for Aseismic Base Isolation," by J.M. Kelly and D.E. Chitty - 1978 (PB 292 833)A03

UCB/EERC-78/21 "APOLLO - A Computer Program for the Analysis of Pore Pressure Generation and Dissipation in Horizontal Sand Layers During Cyclic or Earthquake Loading," by P.P. Martin and H.B. Seed - 1978 (PB 292 835)A04

UCB/EERC-78/22 "Optimal Design of an Earthquake Isolation System," by M.A. Bhatti, K.S. Pister and E. Polak - 1978 (PB 294 735)A06

UCB/EERC-78/23 "MASH - A Computer Program for the Non-Linear Analysis of Vertically Propagating Shear Waves in Horizontally Layered Deposits," by P.P. Martin and H.B. Seed - 1978 (PB 293 101)A05

UCB/EERC-78/24 "Investigation of the Elastic Characteristics of a Three Story Steel Frame Using System Identification," by I. Kaya and H.D. McNiven - 1978 (PB 296 225)A06

UCB/EERC-78/25 "Investigation of the Nonlinear Characteristics of a Three-Story Steel Frame Using System Identification," by I. Kaya and H.D. McNiven - 1978 (PB 301 363)A05

UCB/EERC-80/24 "U-Bar Restraint Element (Type 11) for the ANSR-II Program," by C. Oughourlian and G.H. Powell July 1980(PB81 122 293)A03

UCB/EERC-80/25 "Testing of a Natural Rubber Base Isolation System by an Explosively Simulated Earthquake," by J.M. Kelly - August 1980(PB81 201 360)A04

UCB/EERC-80/26 "Input Identification from Structural Vibrational Response," by Y. Hu - August 1980(PB81 152 308)A05

UCB/EERC-80/27 "Cyclic Inelastic Behavior of Steel Offshore Structures," by V.A. Zayas, S.A. Mahin and E.P. Popov August 1980(PB81 196 180)A15

UCB/EERC-80/28 "Shaking Table Testing of a Reinforced Concrete Frame with Biaxial Response," by M.G. Oliva October 1980(PB81 154 304)A10

UCB/EERC-80/29 "Dynamic Properties of a Twelve-Story Prefabricated Panel Building," by J.G. Bouwkamp, J.P. Kollegger and R.M. Stephen - October 1980(PB82 117 128)A06

UCB/EERC-80/30 "Dynamic Properties of an Eight-Story Prefabricated Panel Building," by J.G. Bouwkamp, J.P. Kollegger and R.M. Stephen - October 1980(PB81 200 313)A05

UCB/EERC-80/31 "Predictive Dynamic Response of Panel Type Structures Under Earthquakes," by J.P. Kollegger and J.G. Bouwkamp - October 1980(PB81 152 316)A04

UCB/EERC-80/32 "The Design of Steel Energy-Absorbing Restrainers and their Incorporation into Nuclear Power Plants for Enhanced Safety (Vol 3): Testing of Commercial Steels in Low-Cycle Torsional Fatigue," by P. Spencer, E.R. Parker, E. Jongewaard and M. Drory

UCB/EERC-80/33 "The Design of Steel Energy-Absorbing Restrainers and their Incorporation into Nuclear Power Plants for Enhanced Safety (Vol 4): Shaking Table Tests of Piping Systems with Energy-Absorbing Restrainers," by S.F. Stiemer and W.G. Godden - Sept. 1980

UCB/EERC-80/34 "The Design of Steel Energy-Absorbing Restrainers and their Incorporation into Nuclear Power Plants for Enhanced Safety (Vol 5): Summary Report," by P. Spencer

UCB/EERC-80/35 "Experimental Testing of an Energy-Absorbing Base Isolation System," by J.M. Kelly, M.S. Skinner and K.E. Beucke - October 1980(PB81 154 072)A04

UCB/EERC-80/36 "Simulating and Analyzing Artificial Non-Stationary Earthquake Ground Motions," by R.F. Nau, R.M. Oliver and K.S. Pister - October 1980(PB81 153 397)A04

UCB/EERC-80/37 "Earthquake Engineering at Berkeley - 1980," - Sept. 1980(PB81 205 874)A09

UCB/EERC-80/38 "Inelastic Seismic Analysis of Large Panel Buildings," by V. Schricker and G.H. Powell - Sept. 1980 (PB81 154 338)A13

UCB/EERC-80/39 "Dynamic Response of Embankment, Concrete-Gravity and Arch Dams Including Hydrodynamic Interaction," by J.F. Hall and A.K. Chopra - October 1980(PB81 152 324)A11

UCB/EERC-80/40 "Inelastic Buckling of Steel Struts Under Cyclic Load Reversal," by R.G. Black, W.A. Wenger and E.P. Popov - October 1980(PB81 154 312)A08

UCB/EERC-80/41 "Influence of Site Characteristics on Building Damage During the October 3, 1974 Lima Earthquake," by P. Repetto, I. Arango and H.B. Seed - Sept. 1980(PB81 161 739)A05

UCB/EERC-80/42 "Evaluation of a Shaking Table Test Program on Response Behavior of a Two Story Reinforced Concrete Frame," by J.M. Blondet, R.W. Clough and S.A. Mahin

UCB/EERC-80/43 "Modelling of Soil-Structure Interaction by Finite and Infinite Elements," by F. Medina - December 1980(PB81 229 270)A04

UCB/EERC-81/01 "Control of Seismic Response of Piping Systems and Other Structures by Base Isolation," edited by J.M. Kelly - January 1981 (PB81 200 735)A05

UCB/EERC-81/02 "OPTNSR - An Interactive Software System for Optimal Design of Statically and Dynamically Loaded Structures with Nonlinear Response," by M.A. Bhatti, V. Ciampi and K.S. Pister - January 1981 (PB81 218 851)A09

UCB/EERC-81/03 "Analysis of Local Variations in Free Field Seismic Ground Motions," by J.-C. Chen, J. Lysmer and H.B. Seed - January 1981 (AD-A099508)A13

UCB/EERC-81/04 "Inelastic Structural Modeling of Braced Offshore Platforms for Seismic Loading," by V.A. Zayas, P.-S.B. Shing, S.A. Mahin and E.P. Popov - January 1981(PB82 138 777)A07

UCB/EERC-81/05 "Dynamic Response of Light Equipment in Structures," by A. Der Kiureghian, J.L. Sackman and B. Nour-Omid - April 1981 (PB81 218 497)A04

UCB/EERC-81/06 "Preliminary Experimental Investigation of a Broad Base Liquid Storage Tank," by J.G. Bouwkamp, J.P. Kollegger and R.M. Stephen - May 1981(PB82 140 385)A03

UCB/EERC-81/07 "The Seismic Resistant Design of Reinforced Concrete Coupled Structural Walls," by A.E. Aktan and V.V. Bertero - June 1981(PB82 113 358)A11

UCB/EERC-81/08 "The Undrained Shearing Resistance of Cohesive Soils at Large Deformations," by M.R. Pyles and H.B. Seed - August 1981

UCB/EERC-81/09 "Experimental Behavior of a Spatial Piping System with Steel Energy Absorbers Subjected to a Simulated Differential Seismic Input," by S.F. Stiemer, W.G. Godden and J.M. Kelly - July 1981

UCB/EERC-81/10 "Evaluation of Seismic Design Provisions for Masonry in the United States," by B.I. Sveinsson, R.L. Mayes and H.D. McNiven - August 1981 (PB82 166 075)A08

UCB/EERC-81/11 "Two-Dimensional Hybrid Modelling of Soil-Structure Interaction," by T.-J. Tzong, S. Gupta and J. Penzien - August 1981(PB82 142 118)A04

UCB/EERC-81/12 "Studies on Effects of Infills in Seismic Resistant R/C Construction," by S. Brokken and V.V. Bertero - September 1981 (PB82 166 190)A09

UCB/EERC-81/13 "Linear Models to Predict the Nonlinear Seismic Behavior of a One-Story Steel Frame," by H. Valdimarsson, A.H. Shah and H.D. McNiven - September 1981(PB82 138 793)A07

UCB/EERC-81/14 "TLUSH: A Computer Program for the Three-Dimensional Dynamic Analysis of Earth Dams," by T. Kagawa, L.H. Mejia, H.B. Seed and J. Lysmer - September 1981(PB82 139 940)A06

UCB/EERC-81/15 "Three Dimensional Dynamic Response Analysis of Earth Dams," by L.H. Mejia and H.B. Seed - September 1981 (PB82 137 274)A12

UCB/EERC-81/16 "Experimental Study of Lead and Elastomeric Dampers for Base Isolation Systems," by J.M. Kelly and S.B. Hodder - October 1981 (PB82 166 182)A05

UCB/EERC-81/17 "The Influence of Base Isolation on the Seismic Response of Light Secondary Equipment," by J.M. Kelly - April 1981 (PB82 255 266)A04

UCB/EERC-81/18 "Studies on Evaluation of Shaking Table Response Analysis Procedures," by J. Marcial Blondet - November 1981 (PB82 197 278)A10

UCB/EERC-81/19 "DELIGHT.STRUCT: A Computer-Aided Design Environment for Structural Engineering," by R.J. Balling, K.S. Pister and E. Polak - December 1981 (PB82 218 496)A07

UCB/EERC-81/20 "Optimal Design of Seismic-Resistant Planar Steel Frames," by R.J. Balling, V. Ciampi, K.S. Pister and E. Polak - December 1981 (PB82 220 179)A07

UCB/EERC-82/01 "Dynamic Behavior of Ground for Seismic Analysis of Lifeline Systems," by T. Sato and A. Der Kiureghian - January 1982 (PB82 218 926)A05

UCB/EERC-82/02 "Shaking Table Tests of a Tubular Steel Frame Model," by Y. Ghanaat and R. W. Clough - January 1982 (PB82 220 161)A07

UCB/EERC-82/03 "Behavior of a Piping System under Seismic Excitation: Experimental Investigations of a Spatial Piping System supported by Mechanical Shock Arrestors and Steel Energy Absorbing Devices under Seismic Excitation," by S. Schneider, H.-M. Lee and W. G. Godden - May 1982 (PB83 172 544)A09

UCB/EERC-82/04 "New Approaches for the Dynamic Analysis of Large Structural Systems," by E. L. Wilson - June 1982 (PB83 148 080)A05

UCB/EERC-82/05 "Model Study of Effects of Damage on the Vibration Properties of Steel Offshore Platforms," by F. Shahrivar and J. G. Bouwkamp - June 1982 (PB83 148 742)A10

UCB/EERC-82/06 "States of the Art and Practice in the Optimum Seismic Design and Analytical Response Prediction of R/C Frame-Wall Structures," by A. E. Aktan and V. V. Bertero - July 1982 (PB83 147 736)A05

UCB/EERC-82/07 "Further Study of the Earthquake Response of a Broad Cylindrical Liquid-Storage Tank Model," by G. C. Manos and R. W. Clough - July 1982 (PB83 147 744)A11

UCB/EERC-82/08 "An Evaluation of the Design and Analytical Seismic Response of a Seven Story Reinforced Concrete Frame - Wall Structure," by F. A. Charney and V. V. Bertero - July 1982(PB83 157 628)A09

UCB/EERC-82/09 "Fluid-Structure Interactions: Added Mass Computations for Incompressible Fluid," by J. S.-H. Kuo - August 1982 (PB83 156 281)A07

UCB/EERC-82/10 "Joint-Opening Nonlinear Mechanism: Interface Smeared Crack Model," by J. S.-H. Kuo - August 1982 (PB83 149 195)A05

UCB/EERC-82/11 "Dynamic Response Analysis of Techi Dam," by R. W. Clough, R. M. Stephen and J. S.-H. Kuo - August 1982 (PB83 147 496)A06

UCB/EERC-82/12 "Prediction of the Seismic Responses of R/C Frame-Coupled Wall Structures," by A. E. Aktan, V. V. Bertero and M. Piazza - August 1982 (PB83 149 203)A09

UCB/EERC-82/13 "Preliminary Report on the SMART 1 Strong Motion Array in Taiwan," by B. A. Bolt, C. H. Loh, J. Penzien, Y. B. Tsai and Y. T. Yeh - August 1982 (PB83 159 400)A10

UCB/EERC-82/14 "Shaking-Table Studies of an Eccentrically X-Braced Steel Structure," by M. S. Yang - September 1982

UCB/EERC-82/15 "The Performance of Stairways in Earthquakes," by C. Roha, J. W. Axley and V. V. Bertero - September 1982 (PB83 157 693)A07

UCB/EERC-82/16 "The Behavior of Submerged Multiple Bodies in Earthquakes," by W.-G. Liao - Sept. 1982 (PB83 158 709)A07

UCB/EERC-82/17 "Effects of Concrete Types and Loading Conditions on Local Bond-Slip Relationships," by A. D. Cowell, E. P. Popov and V. V. Bertero - September 1982 (PB83 153 577)A04

UCB/EERC-78/26 "Studies of Strong Ground Motion in Taiwan," by Y.M. Hsiung, B.A. Bolt and J. Penzien - 1978 (PB 298 436)A06

UCB/EERC-78/27 "Cyclic Loading Tests of Masonry Single Piers: Volume 1 - Height to Width Ratio of 2," by P.A. Hidalgo, R.L. Mayes, H.D. McNiven and R.W. Clough - 1978 (PB 296 211)A07

UCB/EERC-78/28 "Cyclic Loading Tests of Masonry Single Piers: Volume 2 - Height to Width Ratio of 1," by S.-W.J. Chen, P.A. Hidalgo, R.L. Mayes, R.W. Clough and H.D. McNiven - 1978 (PB 296 212)A09

UCB/EERC-78/29 "Analytical Procedures in Soil Dynamics," by J. Lysmer - 1978 (PB 298 445)A06

UCB/EERC-79/01 "Hysteretic Behavior of Lightweight Reinforced Concrete Beam-Column Subassemblages," by B. Forzani, E.P. Popov and V.V. Bertero - April 1979(PB 298 267)A06

UCB/EERC-79/02 "The Development of a Mathematical Model to Predict the Flexural Response of Reinforced Concrete Beams to Cyclic Loads, Using System Identification," by J. Stanton & H. McNiven - Jan. 1979(PB 295 875)A10

UCB/EERC-79/03 "Linear and Nonlinear Earthquake Response of Simple Torsionally Coupled Systems," by C.L. Kan and A.K. Chopra - Feb. 1979(PB 298 262)A06

UCB/EERC-79/04 "A Mathematical Model of Masonry for Predicting its Linear Seismic Response Characteristics," by Y. Mengi and H.D. McNiven - Feb. 1979(PB 298 266)A06

UCB/EERC-79/05 "Mechanical Behavior of Lightweight Concrete Confined by Different Types of Lateral Reinforcement," by M.A. Manrique, V.V. Bertero and E.P. Popov - May 1979(PB 301 114)A06

UCB/EERC-79/06 "Static Tilt Tests of a Tall Cylindrical Liquid Storage Tank," by R.W. Clough and A. Niwa - Feb. 1979 (PB 301 167)A06

UCB/EERC-79/07 "The Design of Steel Energy Absorbing Restrainers and Their Incorporation into Nuclear Power Plants for Enhanced Safety: Volume 1 - Summary Report," by P.N. Spencer, V.F. Zackay, and E.R. Parker - Feb. 1979(UCB/EERC-79/07)A09

UCB/EERC-79/08 "The Design of Steel Energy Absorbing Restrainers and Their Incorporation into Nuclear Power Plants for Enhanced Safety: Volume 2 - The Development of Analyses for Reactor System Piping,""Simple Systems" by M.C. Lee, J. Penzien, A.K. Chopra and K, Suzuki "Complex Systems" by G.H. Powell, E.L. Wilson, R.W. Clough and D.G. Row - Feb. 1979(UCB/EERC-79/08)A10

UCB/EERC-79/09 "The Design of Steel Energy Absorbing Restrainers and Their Incorporation into Nuclear Power Plants for Enhanced Safety: Volume 3 - Evaluation of Commercial Steels," by W.S. Owen, R.M.N. Pelloux, R.O. Ritchie, M. Faral, T. Ohhashi, J. Toplosky, S.J. Hartman, V.F. Zackay and E.R. Parker - Feb. 1979(UCB/EERC-79/09)A04

UCB/EERC-79/10 "The Design of Steel Energy Absorbing Restrainers and Their Incorporation into Nuclear Power Plants for Enhanced Safety: Volume 4 - A Review of Energy-Absorbing Devices," by J.M. Kelly and M.S. Skinner - Feb. 1979(UCB/EERC-79/10)A04

UCB/EERC-79/11 "Conservatism In Summation Rules for Closely Spaced Modes," by J.M. Kelly and J.L. Sackman - May 1979(PB 301 328)A03

UCB/EERC-79/12 "Cyclic Loading Tests of Masonry Single Piers; Volume 3 - Height to Width Ratio of 0.5," by P.A. Hidalgo, R.L. Mayes, H.D. McNiven and R.W. Clough - May 1979(PB 301 321)A08

UCB/EERC-79/13 "Cyclic Behavior of Dense Course-Grained Materials in Relation to the Seismic Stability of Dams," by N.G. Banerjee, H.B. Seed and C.K. Chan - June 1979(PB 301 373)A13

UCB/EERC-79/14 "Seismic Behavior of Reinforced Concrete Interior Beam-Column Subassemblages," by S. Viwathanatepa, E.P. Popov and V.V. Bertero - June 1979(PB 301 326)A10

UCB/EERC-79/15 "Optimal Design of Localized Nonlinear Systems with Dual Performance Criteria Under Earthquake Excitations," by M.A. Bhatti - July 1979(PB 80 167 109)A06

UCB/EERC-79/16 "OPTDYN - A General Purpose Optimization Program for Problems with or without Dynamic Constraints," by M.A. Bhatti, E. Polak and K.S. Pister - July 1979(PB 80 167 091)A05

UCB/EERC-79/17 "ANSR-II, Analysis of Nonlinear Structural Response, Users Manual," by D.P. Mondkar and G.H. Powell July 1979(PB 80 113 301)A05

UCB/EERC-79/18 "Soil Structure Interaction in Different Seismic Environments," A. Gomez-Masso, J. Lysmer, J.-C. Chen and H.B. Seed - August 1979(PB 80 101 520)A04

UCB/EERC-79/19 "ARMA Models for Earthquake Ground Motions," by M.K. Chang, J.W. Kwiatkowski, R.F. Nau, R.M. Oliver and K.S. Pister - July 1979(PB 301 166)A05

UCB/EERC-79/20 "Hysteretic Behavior of Reinforced Concrete Structural Walls," by J.M. Vallenas, V.V. Bertero and E.P. Popov - August 1979(PB 80 165 905)A12

UCB/EERC-79/21 "Studies on High-Frequency Vibrations of Buildings - 1: The Column Effect," by J. Lubliner - August 1979 (PB 80 158 553)A03

UCB/EERC-79/22 "Effects of Generalized Loadings on Bond Reinforcing Bars Embedded in Confined Concrete Blocks," by S. Viwathanatepa, E.P. Popov and V.V. Bertero - August 1979(PB 81 124 018)A14

UCB/EERC-79/23 "Shaking Table Study of Single-Story Masonry Houses, Volume 1: Test Structures 1 and 2," by P. Gülkan, R.L. Mayes and R.W. Clough - Sept. 1979 (HUD-000 1763)A12

UCB/EERC-79/24 "Shaking Table Study of Single-Story Masonry Houses, Volume 2: Test Structures 3 and 4," by P. Gülkan, R.L. Mayes and R.W. Clough - Sept. 1979 (HUD-000 1836)A12

UCB/EERC-79/25 "Shaking Table Study of Single-Story Masonry Houses, Volume 3: Summary, Conclusions and Recommendations," by R.W. Clough, R.L. Mayes and P. Gülkan - Sept. 1979 (HUD-000 1837)A06

UCB/EERC-79/26 "Recommendations for a U.S.-Japan Cooperative Research Program Utilizing Large-Scale Testing Facilities," by U.S.-Japan Planning Group - Sept. 1979(PB 301 407)A06

UCB/EERC-79/27 "Earthquake-Induced Liquefaction Near Lake Amatitlan, Guatemala," by H.B. Seed, I. Arango, C.K. Chan, A. Gomez-Masso and R. Grant de Ascoli - Sept. 1979(NUREG-CR1341)A03

UCB/EERC-79/28 "Infill Panels: Their Influence on Seismic Response of Buildings," by J.W. Axley and V.V. Bertero Sept. 1979(PB 80 163 371)A10

UCB/EERC-79/29 "3D Truss Bar Element (Type 1) for the ANSR-II Program," by D.P. Mondkar and G.H. Powell - Nov. 1979 (PB 80 169 709)A02

UCB/EERC-79/30 "2D Beam-Column Element (Type 5 - Parallel Element Theory) for the ANSR-II Program," by D.G. Row, G.H. Powell and D.P. Mondkar - Dec. 1979(PB 80 167 224)A03

UCB/EERC-79/31 "3D Beam-Column Element (Type 2 - Parallel Element Theory) for the ANSR-II Program," by A. Riahi, G.H. Powell and D.P. Mondkar - Dec. 1979(PB 80 167 216)A03

UCB/EERC-79/32 "On Response of Structures to Stationary Excitation," by A. Der Kiureghian - Dec. 1979(PB 80166 929)A03

UCB/EERC-79/33 "Undisturbed Sampling and Cyclic Load Testing of Sands," by S. Singh, H.B. Seed and C.K. Chan Dec. 1979(ADA 087 298)A07

UCB/EERC-79/34 "Interaction Effects of Simultaneous Torsional and Compressional Cyclic Loading of Sand," by P.M. Griffin and W.N. Houston - Dec. 1979(ADA 092 352)A15

UCB/EERC-80/01 "Earthquake Response of Concrete Gravity Dams Including Hydrodynamic and Foundation Interaction Effects," by A.K. Chopra, P. Chakrabarti and S. Gupta - Jan. 1980(AD-A087297)A10

UCB/EERC-80/02 "Rocking Response of Rigid Blocks to Earthquakes," by C.S. Yim, A.K. Chopra and J. Penzien - Jan. 1980 (PB80 166 002)A04

UCB/EERC-80/03 "Optimum Inelastic Design of Seismic-Resistant Reinforced Concrete Frame Structures," by S.W. Zagajeski and V.V. Bertero - Jan. 1980(PB80 164 635)A06

UCB/EERC-80/04 "Effects of Amount and Arrangement of Wall-Panel Reinforcement on Hysteretic Behavior of Reinforced Concrete Walls," by R. Iliya and V.V. Bertero - Feb. 1980(PB81 122 525)A09

UCB/EERC-80/05 "Shaking Table Research on Concrete Dam Models," by A. Niwa and R.W. Clough - Sept. 1980(PB81 122 368)A06

UCB/EERC-80/06 "The Design of Steel Energy-Absorbing Restrainers and their Incorporation into Nuclear Power Plants for Enhanced Safety (Vol 1A): Piping with Energy Absorbing Restrainers: Parameter Study on Small Systems," by G.H. Powell, C. Oughourlian and J. Simons - June 1980

UCB/EERC-80/07 "Inelastic Torsional Response of Structures Subjected to Earthquake Ground Motions," by Y. Yamazaki April 1980(PB81 122 327)A08

UCB/EERC-80/08 "Study of X-Braced Steel Frame Structures Under Earthquake Simulation," by Y. Ghanaat - April 1980 (PB81 122 335)A11

UCB/EERC-80/09 "Hybrid Modelling of Soil-Structure Interaction," by S. Gupta, T.W. Lin, J. Penzien and C.S. Yeh May 1980(PB81 122 319)A07

UCB/EERC-80/10 "General Applicability of a Nonlinear Model of a One Story Steel Frame," by B.I. Sveinsson and H.D. McNiven - May 1980(PB81 124 877)A06

UCB/EERC-80/11 "A Green-Function Method for Wave Interaction with a Submerged Body," by W. Kioka - April 1980 (PB81 122 269)A07

UCB/EERC-80/12 "Hydrodynamic Pressure and Added Mass for Axisymmetric Bodies," by F. Nilrat - May 1980(PB81 122 343)A08

UCB/EERC-80/13 "Treatment of Non-Linear Drag Forces Acting on Offshore Platforms," by B.V. Dao and J. Penzien May 1980(PB81 153 413)A07

UCB/EERC-80/14 "2D Plane/Axisymmetric Solid Element (Type 3 - Elastic or Elastic-Perfectly Plastic) for the ANSR-II Program," by D.P. Mondkar and G.H. Powell - July 1980(PB81 122 350)A03

UCB/EERC-80/15 "A Response Spectrum Method for Random Vibrations," by A. Der Kiureghian - June 1980(PB81 122 301)A03

UCB/EERC-80/16 "Cyclic Inelastic Buckling of Tubular Steel Braces," by V.A. Zayas, E.P. Popov and S.A. Mahin June 1980(PB81 124 885)A10

UCB/EERC-80/17 "Dynamic Response of Simple Arch Dams Including Hydrodynamic Interaction," by C.S. Porter and A.K. Chopra - July 1980(PB81 124 000)A13

UCB/EERC-80/18 "Experimental Testing of a Friction Damped Aseismic Base Isolation System with Fail-Safe Characteristics," by J.M. Kelly, K.E. Beucke and M.S. Skinner - July 1980(PB81 148 595)A04

UCB/EERC-80/19 "The Design of Steel Energy-Absorbing Restrainers and their Incorporation into Nuclear Power Plants for Enhanced Safety (Vol 1B): Stochastic Seismic Analyses of Nuclear Power Plant Structures and Piping Systems Subjected to Multiple Support Excitations," by M.C. Lee and J. Penzien - June 1980

UCB/EERC-80/20 "The Design of Steel Energy-Absorbing Restrainers and their Incorporation into Nuclear Power Plants for Enhanced Safety (Vol 1C): Numerical Method for Dynamic Substructure Analysis," by J.M. Dickens and E.L. Wilson - June 1980

UCB/EERC-80/21 "The Design of Steel Energy-Absorbing Restrainers and their Incorporation into Nuclear Power Plants for Enhanced Safety (Vol 2): Development and Testing of Restraints for Nuclear Piping Systems," by J.M. Kelly and M.S. Skinner - June 1980

UCB/EERC-80/22 "3D Solid Element (Type 4-Elastic or Elastic-Perfectly-Plastic) for the ANSR-II Program," by D.P. Mondkar and G.H. Powell - July 1980(PB81 123 242)A03

UCB/EERC-80/23 "Gap-Friction Element (Type 5) for the ANSR-II Program," by D.P. Mondkar and G.H. Powell - July 1980 (PB81 122 285)A03

UCB/EERC-82/18 "Mechanical Behavior of Shear Wall Vertical Boundary Members: An Experimental Investigation," by M. T. Wagner and V. V. Bertero - October 1982 (PB83 159 764)A05

UCB/EERC-82/19 "Experimental Studies of Multi-support Seismic Loading on Piping Systems," by J. M. Kelly and A. D. Cowell - November 1982

UCB/EERC-82/20 "Generalized Plastic Hinge Concepts for 3D Beam-Column Elements," by P. F.-S. Chen and G. H. Powell - November 1982

UCB/EERC-82/21 "ANSR-III: General Purpose Computer Program for Nonlinear Structural Analysis," by C. V. Oughourlian and G. H. Powell - November 1982

UCB/EERC-82/22 "Solution Strategies for Statically Loaded Nonlinear Structures," by J. W. Simons and G. H. Powell - November 1982

UCB/EERC-82/23 "Analytical Model of Deformed Bar Anchorages under Generalized Excitations," by V. Ciampi, R. Eligehausen, V. V. Bertero and E. P. Popov - November 1982 (PB83 169 532)A06

UCB/EERC-82/24 "A Mathematical Model for the Response of Masonry Walls to Dynamic Excitations," by H. Sucuoğlu, Y. Mengi and H. D. McNiven - November 1982 (PB83 169 011)A07

UCB/EERC-82/25 "Earthquake Response Considerations of Broad Liquid Storage Tanks," by F. J. Cambra - November 1982

UCB/EERC-82/26 "Computational Models for Cyclic Plasticity, Rate Dependence and Creep," by B. Mosaddad and G. H. Powell - November 1982

UCB/EERC-82/27 "Inelastic Analysis of Piping and Tubular Structures," by M. Mahasuverachai and G. H. Powell - November 1982

UCB/EERC-83/01 "The Economic Feasibility of Seismic Rehabilitation of Buildings by Base Isolation," by J. M. Kelly - January 1983

UCB/EERC-83/02 "Seismic Moment Connections for Moment-Resisting Steel Frames," by E. P. Popov - January 1983

UCB/EERC-83/03 "Design of Links and Beam-to-Column Connections for Eccentrically Braced Steel Frames," by E. P. Popov and J. O. Malley - January 1983

UCB/EERC-83/04 "Numerical Techniques for the Evaluation of Soil-Structure Interaction Effects in the Time Domain," by E. Bayo and E. L. Wilson - February 1983

UCB/EERC-83/05 "A Transducer for Measuring the Internal Forces in the Columns of a Frame-Wall Reinforced Concrete Structure," by R. Sause and V. V. Bertero - May 1983

UCB/EERC-83/06 "Dynamic Interactions between Floating Ice and Offshore Structures," by P. Croteau - May 1983

UCB/EERC-83/07 "Dynamic Analysis of Multiply Tuned and Arbitrarily Supported Secondary Systems," by T. Igusa and A. Der Kiureghian - June 1983

UCB/EERC-83/08 "A Laboratory Study of Submerged Multi-body Systems in Earthquakes," by G. R. Ansari - June 1983

UCB/EERC-83/09 "Effects of Transient Foundation Uplift on Earthquake Response of Structures," by C.-S. Yim and A. K. Chopra - June 1983

UCB/EERC-83/10 "Optimal Design of Friction-Braced Frames under Seismic Loading," by M. A. Austin and K. S. Pister - June 1983

UCB/EERC-83/11 "Shaking Table Study of Single-Story Masonry Houses: Dynamic Performance under Three Component Seismic Input and Recommendations," by G. C. Manos, R. W. Clough and R. L. Mayes - June 1983

UCB/EERC-83/12 "Experimental Error Propagation in Pseudodynamic Testing," by P. B. Shing and S. A. Mahin - June 1983

UCB/EERC-83/13 "Experimental and Analytical Predictions of the Mechanical Characteristics of a 1/5-scale Model of a 7-story R/C Frame-Wall Building Structure," by A. E. Aktan, V. V. Bertero, A. A. Chowdhury and T. Nagashima - August 1983

UCB/EERC-83/14 "Shaking Table Tests of Large-Panel Precast Concrete Building System Assemblages," by M. G. Oliva and R. W. Clough - August 1983

UCB/EERC-83/15 "Seismic Behavior of Active Beam Links in Eccentrically Braced Frames," by K. D. Hjelmstad and E. P. Popov - July 1983

UCB/EERC-83/16 "System Identification of Structures with Joint Rotation," by J. S. Dimsdale and H. D. McNiven - July 1983

UCB/EERC-83/17 "Construction of Inelastic Response Spectra for Single-Degree-of-Freedom Systems," by S. Mahin and J. Lin - July 1983

UCB/EERC-83/18 "Interactive Computer Analysis Methods for Predicting the Inelastic Cyclic Behavior of Structural Sections," by S. Kaba and S. Mahin - July 1983